

DYSREGULATED FGF AND P38 MAPK SIGNALING  
UNDERLIES LOSS OF STEM CELL SELF-RENEWAL IN  
AGING SKELETAL MUSCLE

by

Jennifer Delaney Bernet  
B.S., Wake Forest University, 2005

A thesis submitted to the Faculty of the Graduate School of the University of Colorado in  
partial fulfillment of the requirement for the degree of Doctor of Philosophy  
Department of Molecular, Cellular, and Developmental Biology  
2013

This thesis entitled:  
Dysregulated FGF and P38 MAPK Signaling Underlies Loss of  
Stem Cell Self-Renewal in Aging Skeletal Muscle  
written by Jennifer Delaney Bernet  
has been approved for the Department of Molecular, Cellular and Developmental Biology.

---

Dr. Kenneth Krauter  
(Committee Chair)

---

Dr. Bradley B. Olwin  
(Thesis Advisor)

Date \_\_\_\_\_

The final copy of this thesis has been examined by the signatories, and we  
Find that both the content and the form meet acceptable presentation standards  
Of scholarly work in the above mentioned discipline.

Bernet, Jennifer Delaney (Ph.D., Molecular, Cellular and Developmental Biology)

Dysregulated FGF and P38 MAPK Signaling Underlies Loss of Stem Cell Self-Renewal in  
Aging Skeletal Muscle

Thesis directed by Professor Bradley Bruce Olwin

Sarcopenia is a geriatric syndrome characterized by loss of skeletal muscle mass, skeletal muscle function and decreased regenerative capacity. A number of skeletal muscle-specific physiological decrements may contribute to sarcopenia; among these is an age-related impairment of satellite cells, the skeletal muscle stem cells required for muscle regeneration. I find that cell-autonomous deficits underlie a loss of self-renewal in aging satellite cells. The decline in self-renewal implicates altered p38 $\alpha\beta$  mitogen-activated protein kinase (MAPK) activity, which is activated by fibroblast growth factor (FGF) signaling and involved in satellite cell activation, differentiation and self-renewal in young satellite cells. Asymmetric activation of active p38 $\alpha\beta$  MAPK produces one daughter cell committed to myogenesis and one quiescent daughter cell. In old satellite cells, elevated levels of phosphorylated p38 $\alpha\beta$  MAPK inhibit asymmetric distribution of active p38 $\alpha\beta$  MAPK thereby preventing self-renewal through asymmetric division. Partial inhibition of p38 $\alpha\beta$  MAPK rescues asymmetric distribution of active p38 $\alpha\beta$  MAPK and self-renewal in aging satellite cells. Attenuated FGF signal transduction fails to stimulate further p38 $\alpha\beta$  MAPK phosphorylation and contributes to reduced self-renewal in aging satellite cells. Constitutive activation of FGF Receptor 1 rescues the reduced FGF signaling in old satellite cells to increase Pax7 expression and self-renewal. Signaling through the FGF/p38 $\alpha\beta$  MAPK axis regulates satellite cell self-renewal and suggest therapeutic targets

for treatment of age-related muscle wasting. While Wnt, Notch and now FGF signaling regulate self-renewal in the satellite cell niche, the specific molecular mechanisms driving asymmetric and symmetric division remain unclear. I develop degradable, 4-arm (poly)ethylene glycol (PEG) hydrogels as an artificial satellite cell niche to study the molecular interactions driving self-renewal. I identify heparin sequences and extracellular matrix proteins that promote satellite cell self-renewal in hydrogel culture, and I demonstrate that 4-arm PEG hydrogels are good candidates for future use in regenerative medicine.

## **Acknowledgments**

I would like to thank Dr. Brad Olwin for his mentorship and support as well as the past and present members of the Olwin laboratory. I would like to thank Tanner McClure and Thomas Carter for their assistance with image analysis. I would like to thank the MCDB Light Microscopy facility for allowing access to microscopes. I would especially like to thank my friends and family for all of their support through the years.

The work presented in Chapter 3 was performed in collaboration with the laboratories of Krisi Anseth (University of Colorado-Boulder) and Jeremy Turnbull (University of Liverpool). I would like to thank Dr. Anseth and Dr. Turnbull as well as the members of their laboratories, especially April Kloxin and Melissa Pope.

## Table of Contents

<b>Chapter 1: Introduction</b>	<b>1</b>
<b>Chapter 2: P38 MAPK signaling underlies a cell autonomous loss of stem cell self-renewal in aged skeletal muscle</b>	<b>25</b>
I.    Introduction	26
II.   Results	28
III.  Discussion	54
IV.  Methods	58
<b>Chapter 3: Developing an artificial niche in culture to promote satellite self-renewal</b>	<b>64</b>
I.    Introduction	65
II.   Results	67
III.  Discussion	96
IV.  Methods	101
<b>Chapter 4: Discussion</b>	<b>108</b>
<b>References</b>	<b>119</b>
<b>Appendix 1</b>	<b>152</b>
<b>Appendix 2</b>	<b>157</b>

## Tables

### Chapter 2

Table 2.1	IPA pathway analysis of transcripts changing >4-fold between young and old satellite cells	47
Table 2.2	IPA pathway analysis of transcripts changing >6-fold between young and old satellite cells	48

### Chapter 3

Table 3.1	Proteoglycan transcript levels change throughout satellite cell activation and proliferation	89
Table 3.2	Transcript levels of glycosaminoglycan biosynthesis enzymes change throughout satellite cell activation and proliferation	90

## Figures

### Chapter 1

- Figure 1.1 Myogenic transcription factors regulate satellite cell progression through myogenesis 4
- Figure 1.2 Satellite cells can self-renew through both asymmetric and symmetric divisions 15

### Chapter 2

- Figure 2.1 Old satellite cell explants exhibit reduced proliferation and decreased Pax7 expression 30
- Figure 2.2 Old myofiber-associated satellite cells exhibit reduced proliferation and increased differentiation 31
- Figure 2.3 Heterochronic transplantation of old satellite cells to local or systemic young environment fails to rescue age-associated phenotypes 32
- Figure 2.4 Aged satellite cells exhibit elevated p38 $\alpha\beta$  MAPK signaling and altered FGFR1 signaling 35
- Figure 2.5 FGF maintains self-renewal and expansion of young cells but not aged cells in culture and *in vivo* 39
- Figure 2.6 The self-renewing population is lost in aged satellite cell culture 41
- Figure 2.7 Loss of self-renewal in aged satellite cells correlates with loss of asymmetric phospho-p38 and can be rescued by partial inhibition of p38 $\alpha\beta$  MAPK signaling 44
- Figure 2.8 Transcripts related to inhibition of differentiation are decreased in old satellite cells 45
- Figure 2.9 Transcripts related to self-renewal and p38 $\alpha\beta$  MAPK/FGF signaling are decreased in old satellite cells 46
- Figure 2.10 Partial inhibition of p38 $\alpha\beta$  MAPK rescues self-renewal in aged satellite cells 50

Figure 2.11	Constitutive FGFR1 signaling partially rescues cell autonomous self-renewal defect in aged satellite cells	52
Figure 2.12	Model for cell autonomous loss of aged satellite cell self-renewal	55
<b>Chapter 3</b>		
Figure 3.1	The glycosaminoglycan heparin is composed of variably sulfated, repeating disaccharide units	69
Figure 3.2	Heparin fragment length regulates FGF signaling in MM14 cells	71
Figure 3.3	Addition of longer heparin fragments increases self-renewal and decreases differentiation in MM14 cells	73
Figure 3.4	Specific heparin sulfation patterns drive FGF signaling in MM14 cells	75
Figure 3.5	FGF-2 and heparan sulfate are concentrated at myofiber-associated satellite cells	76
Figure 3.6	PEG hydrogels promote satellite cell self-renewal <i>in vitro</i>	78
Figure 3.7	Satellite cells form myosphere-like structures in 2D and 3D hydrogel culture	79
Figure 3.8	Satellite cells proliferate after adhering to hydrogels	82
Figure 3.9	Integrin-binding peptide sequences promote Pax7 retention in 2D hydrogel culture	83
Figure 3.10	Laminin increases the proportion of self-renewing cells in 2D hydrogel culture	85
Figure 3.11	Laminin concentration affects satellite cell self-renewal and proliferation	86
Figure 3.12	FGF-2 addition to culture media increases self-renewal	88
Figure 3.13	Encapsulating heparin in hydrogels increases proliferation but not self-renewal	92
Figure 3.14	Satellite cells survive encapsulation into 3D hydrogels	95

- Figure 3.15 Satellite cells in 3D hydrogels proliferate from small clones to form myosphere-like structures 98
- Figure 3.16 Heparin fragments direct satellite cell activity in 3D hydrogel cultures 100

# **Chapter 1: Introduction**

## **Frailty is a major cause of disability and mortality in the elderly population**

Aging is a gradual deterioration of physiological systems that leads to disability and death. The number of people older than 65 years is expected to grow from 461 million (2004) to 2 billion by 2050 which will increase government healthcare expenditures and strain social services (Janssen et al., 2004; Fuchs et al., 2004). Many of the elderly will be diagnosed as clinically frail, a poorly defined syndrome marked by exhaustion, tissue wasting and decreased mobility. A diagnosis of clinical frailty identifies elderly individuals with a need for long-term care and increased risk of disability and mortality (Fried et al., 2001; Walston et al., 2006; Song et al., 2010; Young et al., 1990).

## **The age-related decline of skeletal muscle is a major component of clinical frailty**

Sarcopenia is a major component of disability and clinical frailty in the elderly (Roubenoff, 2000). Sarcopenia is a geriatric syndrome characterized by a progressive loss of skeletal muscle mass and function which first becomes evident in middle age (Evans and Campbell, 1993; Baumgartner et al., 1998; Roubenoff, 2000; Bischoff, 1990; Landi et al., 2013). In humans, up to 50% of muscle mass is lost from middle age to old age (Metter et al., 1997). Loss of muscle mass is due to a decline in both the size and number of myofibers that are the contractile, multinucleate muscle cells. Sarcopenic skeletal muscle regenerates poorly after myotrauma (Brooks and Faulkner, 1990; Grounds, 1998; Karakelides and Nair, 2005; Day et al., 2010) while detrimental adipogenic and fibrotic tissue infiltrate and further weaken the skeletal muscle (Evans and Lexell, 1995). The underlying causes of sarcopenia are unknown but may include increased inflammation and apoptosis, mitochondrial abnormalities, loss of

neuromuscular junctions, altered hormone and growth factor levels, and reduced stem cell activity (Walston, 2012).

While sarcopenia is a key component of frailty, clinical frailty can result from the concurrent deterioration of many tissues, including the neural, endocrine, immune, respiratory, cardiovascular, and renal systems (Chaves et al., 2005; Kirkwood, 2005; Afilalo et al., 2009). Of the alterations observed in aging muscle, some commonalities that appear in the aging of most tissues are a decline or senescence of stem cell populations, altered levels of hormones and growth factors present in tissues, and an altered response of stem cells to these signals (Miller, 1996; Lamberts, 2002; Leng et al., 2004; Cunningham et al., 2005; Streit, 2006; Cawthon et al., 2009; Hubbard et al., 2009; Bishop et al., 2010). Thus, loss of stem cell function may be a general underlying cause of tissue aging driven by cumulative molecular and cellular damage, cellular aging, and telomere loss (López-Otín et al., 2013).

Skeletal muscle has a remarkable capacity for regeneration, which restores tissue homeostasis after myotrauma (Tatsumi et al., 2006) but is lost with aging (Brooks and Faulkner, 1990; Grounds, 1998; Karakelides and Nair, 2005; Day et al., 2010). The nuclei of myofibers are terminally differentiated, incapable of entry into the cell cycle, and unable to repair muscle (Bintliff and Walker, 1960). Instead, the satellite cell, the adult muscle stem cell, is responsible for the robust regeneration of young muscle (Mauro, 1961; Sambasivan et al., 2011; Lepper et al., 2011; Murphy et al., 2011) (Figure 1.1). While satellite cells from both young and old animals can adopt a myogenic fate in culture (Konigsberg, 1961; Konigsberg, 1960; Allen et al., 1980), old satellite cells exhibit decreased participation in myogenesis (muscle formation), including decreased proliferation, aberrant differentiation, and decreased stem cell self-renewal

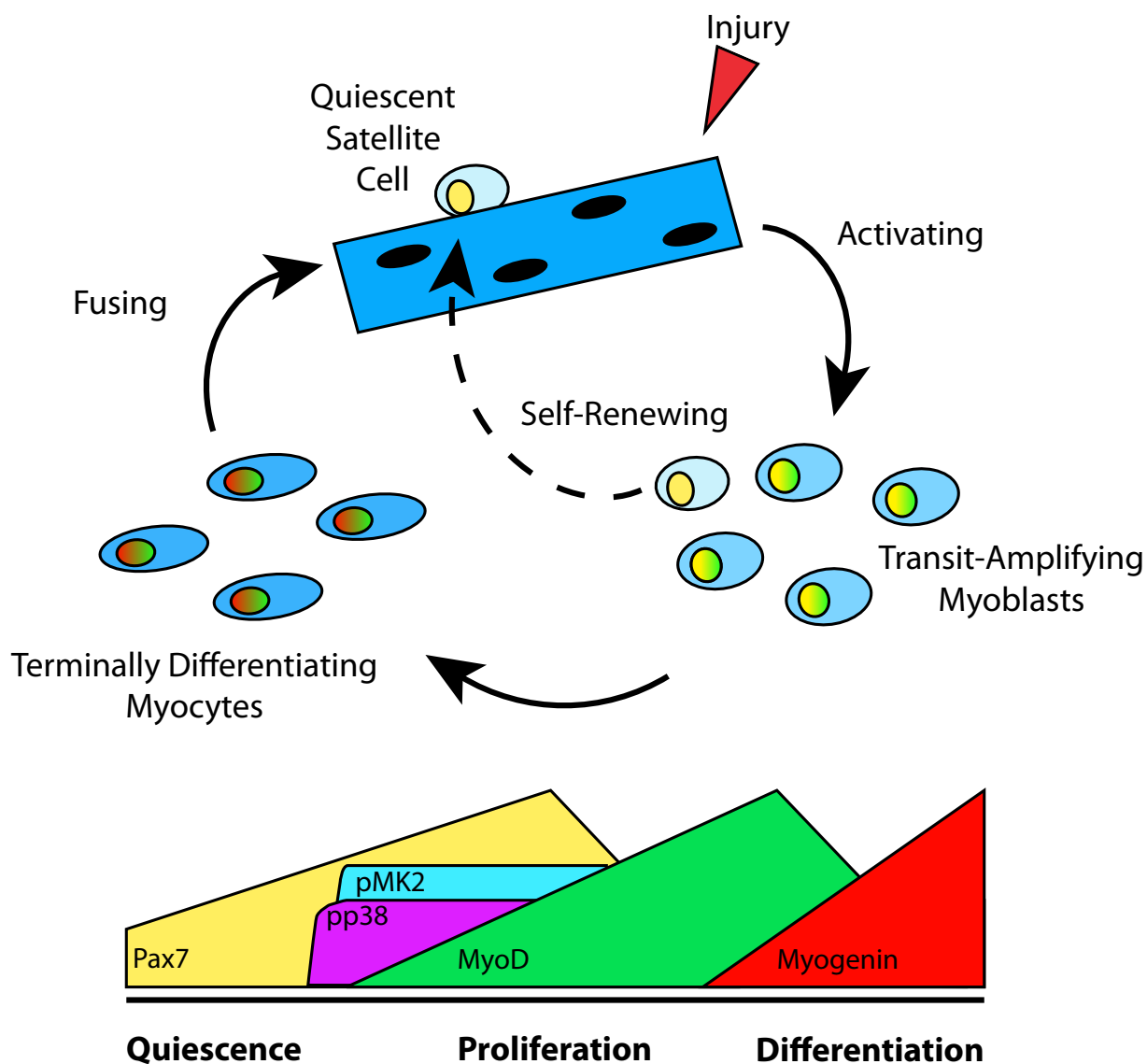


**Figure 1.1: Myogenic transcription factors regulate satellite cell progression through myogenesis.** The upper panel is a model of myogenesis. Quiescent satellite cells reside on the myofiber in skeletal muscle. Upon injury, satellite cells proliferate and differentiate to fuse into damaged myofibers or form *de novo* myofibers. A subset of proliferating satellite cells self-renew (dotted line) to repopulate the quiescent satellite cell pool. Myogenesis is driven in part by the regulated expression of the transcription factors Pax7 (yellow), MyoD (green), and Myogenin (red) (nuclei color represents which transcription factors are expressed in cells at the different stages of myogenesis). In the lower panel, the height of the shape corresponding to each transcription factor indicates the expression level of the transcription factor at different stages of myogenesis. The satellite cell transition from quiescence to proliferation is marked by the phosphorylation of both p38 $\alpha\beta$  MAP Kinase (phospho-p38 $\alpha\beta$ , purple) and its target, MAPKAPK2 (pMK2, cyan).

(Schultz and Lipton, 1982; Decary et al., 1997; Roth et al., 2000; Tapscott et al., 1988; Shefer et al., 2006; Collins et al., 2007; Day et al., 2010). Additionally, there is a reported decline in the number of old satellite cells, which varies between the specific muscles and species studied (Snow, 1977; Gibson and Schultz, 1983; Conboy et al., 2003; Sajko et al., 2004; Brack et al., 2005; Shefer et al., 2006; Chakkalakal et al., 2012). Thus, reduced muscle stem cell activity may contribute to sarcopenia leading to reduced regeneration and decreased muscle mass.

### **Alterations to both the aging muscle environment and the satellite cell impair satellite cell activity in sarcopenic muscle**

The muscle environment regulates satellite cell activity in young cells and may prevent the activity of old satellite cells. Heterochronic transplantation of extensor digitorum longus (EDL) muscles between young and old rats reveals that muscle age affects the efficiency of regeneration in muscle grafts. Transplantation of an old EDL to a young host increases recovery of muscle mass and strength while EDL transplantation to an old host decreases muscle mass and strength regardless of the age of the muscle graft (Rantanen et al., 1995). Heterochronic parabiosis studies, which surgically combine the circulatory systems of young and old mice, reveal that systemic factors that change with age modulate satellite cell activity. Exposing old muscle to a young circulatory system rescues satellite cell proliferation and myofiber formation whereas parabiosis of two old mice has no effect on muscle regeneration (Conboy et al., 2005; Brack et al., 2007). Age-related changes in the muscle environment appear to inhibit satellite cell function and muscle regeneration while signals in the young environment rescue old satellite cell activity.

There are many age-related changes in skeletal muscle that could reduce satellite cell activity. Macrophages, responsible for phagocytic clearance of debris and release of signaling molecules, decreases in old muscle after injury (Zacks and Sheff, 1982; Grounds, 1998). Old muscle contains more fibrotic tissue (Marshall et al., 1989), an altered extracellular matrix (ECM) composition (Young et al., 1990; Oliver et al., 2005) and a thickening myofiber basement membrane (Snow, 1977; Goldspink et al., 1994; Evans and Lexell, 1995; Grounds, 1998), which change both structural and biochemical cues to the satellite cells. Testosterone (McIntire and Hoffman, 2011) and insulin growth factor-1 (IGF-1) (Whitney et al., 2001) protein levels decline in aging muscle decreasing muscle mass and altering satellite cell fate. Increased levels of Wnt3a and transforming growth factor-beta (TGF $\beta$ ) proteins, which promote cell fate determination, are present in aging blood and muscle while decreased Delta ligand reduces Notch activation, which promotes stem cell maintenance and proliferation, in satellite cells (Conboy et al., 2003; Brack et al., 2007). These altered signals may shift aging satellite cells towards differentiation, which diminishes the self-renewing satellite cell population (Conboy and Rando, 2002; Brack et al., 2008; Carlson et al., 2008). Exposing old satellite cells to a young environment restores “young” levels of signaling factors to rescue differentiation, stem cell maintenance and muscle homeostasis in old skeletal muscle (Conboy et al., 2005; Brack et al., 2007).

The heterochronic transplantation and parabiosis experiments suggest that the aging muscle environment, rather than intrinsic changes, inhibit satellite cell activity. Transplantation of young and old myofiber-associated satellite cells to muscle of young, dystrophic, nude mice, results in equivalent levels of engraftment into the host muscle (Collins et al., 2007) providing

further evidence that a young environment can overcome any intrinsic deficits in old cells. However, fibroblast growth factor-2 (FGF-2) treatment before myofiber transplantation drives a permanent, cell-autonomous change in donor satellite cells that overcomes inhibitory signals from the old environment (Hall et al., 2010). FGF-2-treated satellite cells robustly engraft into the host muscle's satellite cell niche and myofibers, which increases the strength and mass of host muscle, and effectively prevent sarcopenia as the host muscle ages (Megency et al., 1996). Heterochronic transplantation of satellite cells to wildtype host mice reveals that young donor satellite cells produce 2-fold more donor-derived satellite cell and myofiber engraftment in young host muscle than old donor satellite cells (Chakkalakal et al., 2012). Young endogenous satellite cells in wildtype mice may outcompete old donor cells for niche occupancy in contrast to impaired, endogenous satellite cells present in the immunocompromised and dystrophic host mice used in previous transplantation experiments. Decreased engraftment from old donor satellite cells demonstrates that intrinsic alterations in old satellite cells do impair satellite cell activity as well as a refractory, aging muscle environment.

Alterations in aged old satellite cells that may underlie age-related satellite cell impairment, include altered signaling pathways, increased molecular damage, and changes gene expression. Old satellite cells are less responsive to growth factor stimulation and exhibit delayed activation after injury (Schultz and Lipton, 1982; Mezzogiorno et al., 1993). Decreased responsive to signals may result from altered levels of glycosaminoglycan (GAG) proteoglycan co-receptors of growth factor-receptor complexes in satellite cells (Watanabe et al., 1986; Young et al., 1990; Oliver et al., 2005). Old satellite cells exhibit telomere shortening (in human cells) (Decary et al., 1997; Zhu et al., 2007; O'Connor et al., 2009), increased apoptosis (Collins et al.,

2007; Lees et al., 2009) and increased oxidative stress (Beccafico et al., 2007; Pietrangelo et al., 2009), but not increased DNA damage (Cousin et al., 2013). Global gene expression changes as satellite cells age although it is unknown if these gene expression changes in result from altered signal transduction or from epigenetic effects (Bortoli et al., 2003). It remains unclear if these intrinsic changes underlie old satellite cell impairment or which of the age-related changes are rescued by exposure to a young muscle environment.

### **The satellite cell as the primary muscle stem cell**

Several cell populations present in young and old skeletal muscle exhibit a capacity to form muscle, but the satellite cell is the primary skeletal muscle stem cell (Relaix and Zammit, 2012). Ablation of satellite cells during development and adult muscle regeneration *in vivo* demonstrates that satellite cells are required for myogenesis (Lepper et al., 2011; Murphy et al., 2011; Sambasivan et al., 2011). After muscle injury, satellite cells participate in myogenesis by proliferating and differentiating to fuse into damaged myofibers or form *de novo* myofibers. A subset of proliferating cells self-renews to reform the quiescent satellite cell pool for future tissue maintenance and repair.

#### *The quiescent satellite cell in uninjured skeletal muscle*

Satellite cells reside in a mitotically quiescent state until stimulated to participate in myogenesis (Figure 1.1). Quiescent satellite cells do not incorporate labeled nucleotides (Reznik, 1969) and contain nuclei with tightly packed heterochromatin (Mauro, 1961). Surprisingly, microarray analysis of quiescent and activated satellite cells reveals that quiescence is an actively maintained state since as many mRNA transcripts are down regulated upon satellite cell activation as are up regulated (Farina et al., 2012). Quiescent satellite cells express

transcripts whose proteins induce myogenesis, but which are suppressed by an RNA-destabilizing protein (Melissa Hausburg, Thesis). Thus, quiescent satellite cells are poised to contribute to myogenesis when myotrauma induces a release of signals from the muscle environment.

Quiescent satellite cells express the transcription factor Pax7 (Olguin and Olwin, 2004), which maintains quiescence, and growth factor receptors, which poise the cells to respond to activating signals from the muscle environment. Pax7, a paired-box transcription factor, is required for the establishment of a long-term satellite cell population, as Pax7 helps maintain satellite cell quiescence (Olguin and Olwin, 2004). In Pax7 null mice, the adult satellite cell population is lost as myogenic cells present at birth apoptose before the quiescent satellite cell pool forms (Seale et al., 2000; Oustanina et al., 2004). Some satellite cells also express Myf5 (Crist et al., 2012) and MyoD (Hausburg, Thesis) transcripts, two of the four myogenic regulatory transcription factors that promote expression of the myogenic gene program. Myf5 and MyoD transcripts are translationally inhibited until satellite cells activate, which suggests quiescent satellite cells are primed for myogenesis. Along with these transcription factors, quiescent satellite cells express receptors to signals that will be released upon muscle injury. These receptors include receptor tyrosine kinases for Hepatocyte Growth Factor (c-Met receptor) (Allen et al., 1995), FGF Receptor 1 and FGF Receptor 4 (Cornelison and Wold, 1997) as well as the GAG proteoglycan co-receptors (Cornelison et al., 2001) such as Syndecan-3 (facilitates Notch processing) (Pisconti et al., 2010) and Syndecan-4 (a co-receptor for FGF-FGF Receptor binding) (Rapraeger et al., 1991).

*Satellite cells in myogenesis*

Upon myofiber injury, signals released from the muscle environment cause satellite cells to activate, enter into the cell cycle, proliferate and differentiate to repair muscle (Figure 1.1) (Schultz, 1984; Schultz et al., 1994; Schiaffino and Partridge, 2008). In satellite cell cultures, all myofiber-associated satellite cells activate and enter the cell cycle (Troy et al., 2012). The sequential expression of myogenic regulatory factors drives activated satellite cells through proliferation and to terminally differentiate. Myogenic regulatory factors are basic helix loop helix transcription factors that induce transcription of genes required for muscle formation that include Myf5, MyoD, Myogenin and MRF4 (Schiaffino and Partridge, 2008). Self-renewing satellite cells inhibit translation of myogenic regulatory factors to prevent differentiation and return to quiescence.

#### *Activation of quiescent satellite cells*

Myofiber injury and necrosis releases growth factors from the muscle environment to activate satellite cells. Injured myofibers synthesize nitric oxide (NO) which promotes hepatocyte growth factor (HGF) release from the ECM. HGF binds to the c-Met receptor present on quiescent satellite cells causing receptor dimerization and HGF signal transduction to activate the satellite cell (Tatsumi et al., 1998; Anderson and Pilipowicz, 2002; Tatsumi et al., 2002; Tatsumi et al., 2006). Intraperitoneal injection of tumor necrosis factor-alpha (TNF- $\alpha$ ), an inflammatory cytokine, also activates satellite cells in uninjured muscle, and TNF- $\alpha$  signaling is required for normal muscle regeneration (Li, 2003; Chen et al., 2007). Injured muscle releases FGF-2 (Hannon et al., 1996; Kastner et al., 2000) that does not directly act as a mitogen but instead functions to repress myogenesis (Clegg et al., 1987; Olwin and Rapraeger, 1992) and promote self-renewal (Andrew Troy, Thesis). FGF-2 likely prevents differentiation, permitting

cell cycle entry following activation by HGF and TNF- $\alpha$  as FGF signaling is required for satellite cell entry into the cell cycle (Olwin and Hauschka, 1986). Satellite cells from Syndecan-4 (a FGFR co-receptor) null mice can neither activate nor signal via FGF receptor 1 (Cornelison et al., 2004). Other growth factors (IGF, TGF $\beta$ , and Platelet-Derived Growth Factor (PDGF)) are released soon after muscle injury but are unable to stimulate activation and entry into the cell cycle (Johnson and Allen, 1995).

The first molecular marker of satellite cell activation is the phosphorylation of p38 alpha/beta MAP Kinase (p38 $\alpha\beta$  MAPK), which promotes cell cycle entry through MyoD translation. Within 40 minutes of myofiber isolation, ~40% of satellite cells are immunoreactive for phosphorylated p38 $\alpha\beta$  MAPK (phospho-p38 $\alpha\beta$ ) (Jones et al., 2005). Activation of the p38 $\alpha\beta$  MAPK pathway is required for activation as inhibiting p38 $\alpha\beta$  MAPK maintains satellite cells in a quiescent state (Jones et al., 2005) (Hausburg, Thesis). Active, phospho-p38 $\alpha\beta$  phosphorylates and inhibits the activity of Tristetraprolin (TTP), a protein that destabilizes MyoD transcript in quiescent satellite cells (Hausburg, Thesis). Inhibition of TTP in activated satellite cells allows translation of MyoD, the 'master' myogenic regulatory factor (Tapscott et al., 1988; Tapscott, 2005), within 3h to 12h after activation (Cooper et al., 1999; Dhawan and Rando, 2005). MyoD induction promotes entry into S-phase within 12h to 18h after activation, then MyoD<sup>+</sup> cells proliferate as transit-amplifying cells commonly called myoblasts (Blais et al., 2005; Dhawan and Rando, 2005; Jenniskens et al., 2000).

#### *Proliferation and differentiation of satellite cells*

The first myoblast divisions occur within 48h of muscle injury (Cornelison et al., 2001) then myoblasts undergo rounds of rapid division to expand the population of cells that can

contribute to muscle repair. Proliferating myoblasts eventually exit the cell cycle and terminally differentiate to a muscle-specific lineage (myocytes). Differentiated myocytes fuse to damage myofibers or fuse to form *de novo* myofibers to repair the damaged skeletal muscle (Schultz et al., 1994; Hawke and Garry, 2001).

The levels of Pax7 and myogenic regulatory factor proteins regulate progression through myogenesis. Following activation, Pax7 protein levels rise and repress MyoD translation as Pax7 promotes MyoD transcript and protein degradation. Repressing accumulation of MyoD protein drives a myoblast proliferation (Zammit et al., 2002; Olguin and Olwin, 2004; Olguin et al., 2007; Troy et al., 2012). As cells continue to proliferate, Pax7 levels decrease, which alleviates MyoD repression. MyoD is necessary for progression through myogenesis as satellite cells from MyoD null mice exhibit impaired proliferation and differentiation (Megency et al., 1996; Le Grand et al., 2009). MyoD commits the cells to terminal differentiation through induction of Myogenin. Myogenin is a myogenic transcription factor that commits cells to terminal differentiation (Lassar et al., 1989; Montarras et al., 1989; Clegg et al., 1987; de la Serna et al., 2005; Hall et al., 2010; Zammit et al., 2004; Olguin et al., 2007) by inducing transcription of the myogenic gene program. Transcription of myogenic genes causes myocytes to fuse into myofibers and express the contractile proteins generating force in myofibers (Prody and Merlie, 1991; Seale et al., 2004; Christov et al., 2007).

#### *Self-renewal of a subpopulation of satellite cells during myogenesis*

A subset of satellite cells self-renew during myogenesis to repopulate the satellite cell pool both *in vivo* and in culture. The quiescent satellite cell population reappears in skeletal muscle several weeks after severe myotrauma, (Schultz, 1984) while in culture, a mitotically

quiescent, Pax7+/MyoD- ‘reserve’ population forms alongside differentiated myocytes (Yoshida et al., 1998; Zammit et al., 2006; Olguin and Olwin, 2004; Olguin et al., 2007). Both the *in vitro* and *in vivo* populations contribute to further myogenesis after additional passages in culture or after serial injury and transplantation (Yoshida et al., 1998; Hall et al., 2010). Thus, satellite cells demonstrate a capacity for long-term maintenance and self-renewal that characterize other adult stem cells (Scadden, 2006).

### **Potential mechanisms driving satellite cell self-renewal**

#### *A satellite cell stem cell subpopulation*

Heterogeneity in the satellite cell pool may predispose some satellite cells to self-renew to repopulate the quiescent satellite cell pool. As in other stem cell populations, a subpopulation of satellite cells express the stem cell markers Sca-1 (Holmes and Stanford, 2007) and Abcg2 (Tanaka et al., 2009; Ding et al., 2010), which suggests that a stem cell subpopulation may exist within the larger satellite cell population (Esko and Selleck, 2002). Some Abcg2+ satellite cells comprise a ‘side population’, which efflux Hoechst dye, within the Syndecan-4+ satellite cell population (Tanaka et al., 2009; Ding et al., 2010). Another example of satellite cell heterogeneity is in Myf5 expression where a subset of quiescent Pax7+ cells never express Myf5 as determined by lineage tracing from the Myf5 locus (Kuang et al., 2007). Both the satellite cell ‘side population’ and Myf5- cells exhibit increased self-renewal after transplantation to injured muscle (Kuang et al., 2007; Tanaka et al., 2009) supporting the hypothesis that the satellite cell population contains a stem cell subpopulation.

#### *Asymmetric and symmetric divisions produce self-renewal in satellite cells*

Self-renewing stem cells arise from either asymmetric or symmetric divisions, but determining which mechanism drives self-renewal in a given tissue is difficult. For example, intestinal crypt stem cells appear to divide asymmetrically, but lineage tracing reveals intestinal crypt stem cells instead undergo daily symmetric divisions to clonally expand the stem cell population (Snippert et al., 2010; Edgar, 2012). In satellite cell cultures, both symmetric and asymmetric divisions produce self-renewing, quiescent satellite cells have been reported (Kuang et al., 2007; Le Grand et al., 2009; Troy et al., 2012) (Figure 1.2). Symmetric divisions, promoted by *Wnt7a* through the non-canonical Wnt pathway, produce two Pax7<sup>+</sup>/MyoD<sup>-</sup> daughter cells to clonally expand the quiescent satellite cell population (Le Grand et al., 2009). Asymmetric satellite cell division produces a daughter cell that joins the transit-amplifying population and a daughter cell that retains a stem cell fate (Kuang et al., 2007; Troy et al., 2012). Asymmetric division of satellite cells has been examined during the first satellite cell division following injury, where a Pax7<sup>+</sup>/MyoD<sup>-</sup> daughter cells and a MyoD<sup>+</sup> daughter cell are produced, suggesting that a quiescent subpopulation is generated with a transit amplifying myoblast. The quiescent Pax7<sup>+</sup>/MyoD<sup>-</sup> satellite cell can then be stimulated to reenter the cell cycle generating additional transit-amplifying population and undergoing self-renewal, thereby demonstrating that the quiescent daughter cells retain stem cell function (Troy et al., 2012).

The mechanisms regulating satellite cell self-renewal are just beginning to be understood, and, as in many stem cells, the satellite cell niche likely plays a critical role in asymmetric division (Knoblich, 2008). A key player in this process, the Par complex comprises the core proteins Partitioning Defective 3 (Par-3), Partitioning Defective 6, (Par-6) and atypical Protein Kinase C (Suzuki and Ohno, 2006). A membrane anchor, such as a Junctional Adhesion

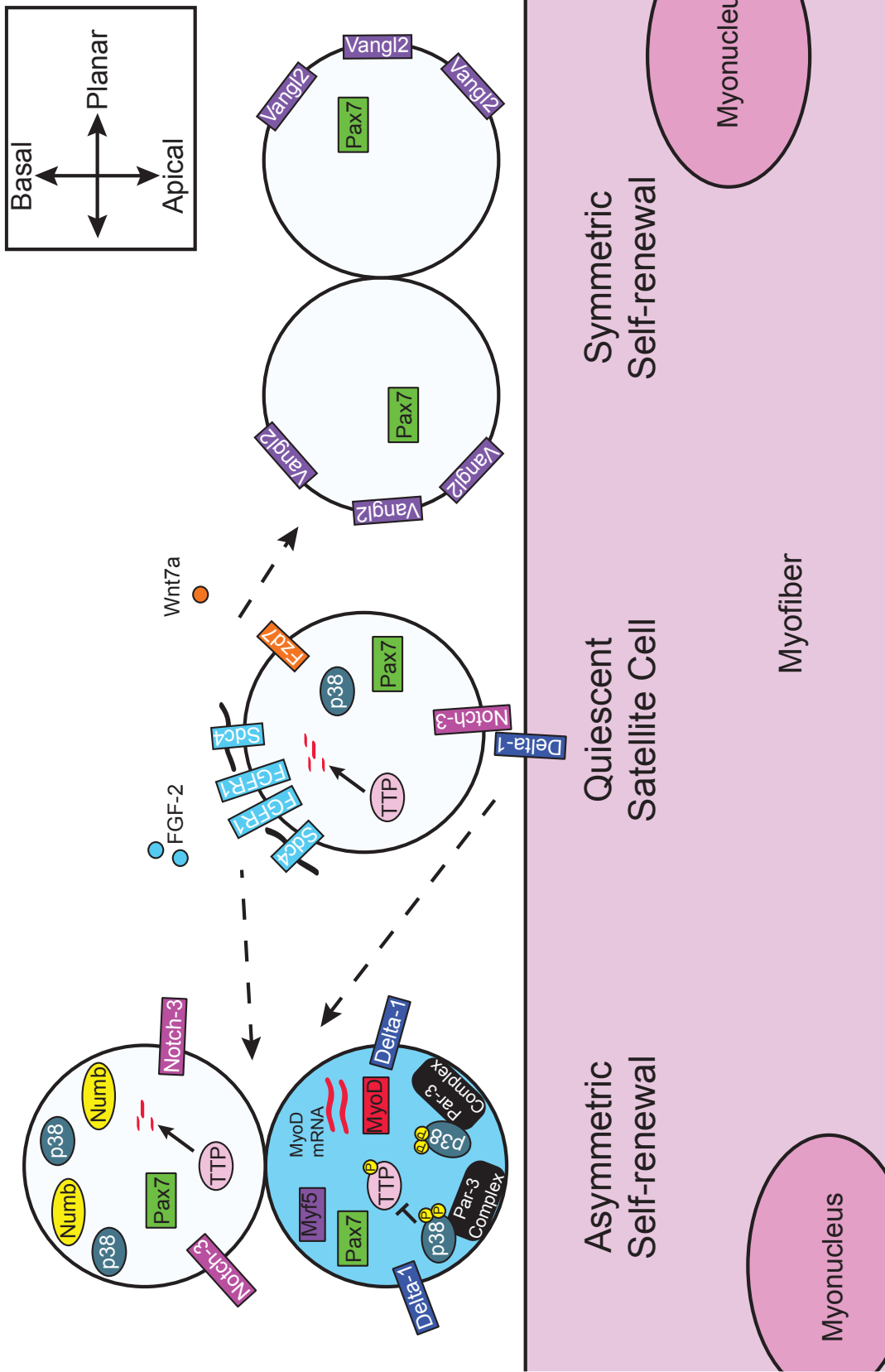


**Figure 1.2: Satellite cells can self-renew through both asymmetric and symmetric divisions.** Quiescent satellite cells reside on the myofiber (pink) underneath the basal lamina (not shown). The quiescent satellite cell expresses Pax7, Notch receptor and the receptors Notch3, Frizzled7 (Fzd7), FGFR1, c-met (not shown) and FGFR4 (not shown). In the quiescent cell, TTP degrades MyoD transcripts to prevent translation of MyoD protein and entry into the cell cycle. After muscle injury, signals released from the satellite cell niche induce a symmetric or an asymmetric division in a subset satellite cells. Wnt7a stimulates a planar division along the myofiber which produces two Pax7<sup>+</sup>/Myf5<sup>-</sup> daughter cells that distribute Vangl2, a Planar Cell Polarity pathway component, in a parallel pattern (Le Grand et al., 2009). FGF and Notch signaling induce a basal-apical-oriented division which produces a quiescent Pax7<sup>+</sup>/MyoD<sup>-</sup>/Myf5<sup>-</sup> satellite cell (white) and a Pax7<sup>+</sup>/MyoD<sup>+</sup>/Myf5<sup>+</sup> myoblast (blue). One mechanism for asymmetric division is the polar segregation of the Par-3/p38αβ MAPK complex, which inhibits TTP to upregulate MyoD protein in the myoblast daughter cell. Par-3 segregation also inhibits Numb, an inhibitor of Notch signaling, in the myoblast daughter cell. The quiescent daughter cell expresses Notch receptor and remains in contact with the basal lamina (not shown). The myoblast daughter cell expresses Delta, a Notch ligand, and remains in contact with the myofiber.

Molecule (Jam) (Ebnet et al., 2001), localizes the complex to one region of a dividing cell to segregate opposite cell fates to the daughter cells. In activated satellite cells, the Par-3 complex asymmetrically segregates p38 $\alpha$  $\beta$  MAPK to one membrane region which permits asymmetric activation of p38 $\alpha$  $\beta$  MAPK in one daughter cell during cell division (Figure 1.2). Active p38 $\alpha$  $\beta$  MAPK inhibits TTP in one daughter cell (Troy et al., 2012), de-repressing MyoD translation and promoting cell cycle entry (Hausberg, Thesis). The lack of p38 $\alpha$  $\beta$  MAPK activity in the other daughter cell de-represses TTP to inhibit MyoD translation promoting re-acquisition of a quiescent state (Troy et al., 2012). Interestingly, asymmetric segregation of mRNA transcripts during cell division generates *Drosophila* oocytes. Mago Nashi, Tsunagi/Y14, and Ranshi proteins form a complex on spliced mRNA that restricts transcripts to the developing oocyte cell within a 16-cell cyst (Lewandowski et al., 2010). Thus, regulation of asymmetric division by post-translational regulation of mRNA transcripts may function as a common mechanism to drive asymmetry in dividing stem cells.

#### *Signals from the environment regulate satellite cell self-renewal*

Extracellular signals appear to play a role in initiating and regulating asymmetric division. Two of these signals, Notch and FGF appear to regulate self-renewal of satellite cells. Persistent activation of the Notch pathway *in vivo* promotes expansion of the satellite cell pool at the expense of transit amplifying myoblasts, reducing the amount of skeletal muscle (Bröhl et al., 2012; Mourikis et al., 2012). FGFR1 signals promote asymmetric p38 $\alpha$  $\beta$  MAPK activation (Bernet, unpublished) and loss of FGFR1 from satellite cells eliminates self-renewal, abrogating skeletal muscle regeneration following an induced injury (Troy, Thesis).

Activation of Notch signaling by cleavage of Notch intracellular domain influences satellite cell self-renewal in culture (Kuang et al., 2007) (Figure 1.2). Notch, a transmembrane receptor, binds the membrane-bound Delta on adjacent myofibers or myoblasts. Delta binding induces proteolytic cleavage of Notch to release an intracellular domain that enters the nucleus and influences gene expression to regulate satellite cell activity (Buas and Kadesch, 2010). Notch-1 promotes proliferation and inhibits differentiation by inhibiting transcription of cell cycle inhibitors and by reducing p38 $\alpha$  MAPK activation (Conboy et al., 2003; Kondoh et al., 2007; Carlson et al., 2008). Notch activation promotes self-renewal as overexpression of Notch-1 intracellular domain upregulates Pax7 to expand the satellite cell population (Wen et al., 2012) while inhibition of Notch signaling eliminates satellite cell self-renewal in muscle (Bjornson et al., 2012). Thus, Notch signaling not only promotes self-renewal but may also regulate asymmetric cell fate.

FGF signaling prevents satellite cell differentiation and may have a role in satellite cell self-renewal (Figure 1.2). Satellite cells express FGF Receptor (FGFR) (Cornelison and Wold, 1997) and the ligands FGF-1 (alpha), FGF-2 (beta), FGF-4, FGF-6 and FGF-9 ligands (Olwin et al., 1994; Sheehan and Allen, 1999). FGF signaling requires complex formation between heparan sulfate proteoglycans (HSPGs) and FGFRs to form high affinity FGF ligand binding sites. FGF-FGFR-HSPG complex formation activates the FGFR tyrosine kinase domains that induce downstream signal transduction of multiple pathways including MAPK pathways (Campbell et al., 1995; Mohammadi et al., 1997; Eswarakumar et al., 2005; Mohammadi et al., 2005). FGF signaling represses satellite cell differentiation to promote proliferation, promotes myogenic cell survival and maintains stem cell plasticity in other stem cells (Clegg et al., 1987; Allen and

Boxhorn, 1989; Conti et al., 2005; Durcova-Hills et al., 2006; Hill et al., 2006; Iwata et al., 2006; Shefer et al., 2006; Cosgrove et al., 2009). FGFR4 null mice do not exhibit detectable defects in satellite cell self-renewal (John Hall, Thesis). However, satellite cells derived from FGFR1 null mice differentiate without forming a Pax7<sup>+</sup>/MyoD<sup>-</sup> reserve cells, which implies that the self-renewing population is lost (Hall, Thesis; Troy, Thesis). Consistent with this observation is the failure of FGFR1 null muscle to regenerate following an induced injury (Troy, Thesis).

Importantly, constitutive activation of an FGFR1 intracellular domain upregulates Pax7 in a satellite cell line to form a quiescent cell population in culture (Whitney et al., 2001), and FGF-2 pretreatment before myofiber transplantation massively expands the quiescent satellite cell population generated from donor satellite cells (Hall et al., 2010). As FGF signaling activates p38 $\alpha\beta$  MAPK, the FGF signal transduction could influence satellite cell self-renewal by regulating asymmetric activation of p38 $\alpha\beta$  MAPK.

Notch and FGF signaling may act in concert to promote self-renewal by asymmetric division. The Par-3/p38 $\alpha\beta$  MAPK complex interacts with the Notch pathway. The Par-3 complex inhibits Numb, an inhibitor of Notch, resulting in localization of active Numb to the daughter cell forming opposite the Par-3 complex (Smith et al., 2007). The FGF co-receptor, Syndecan-4, often localizes with phospho-p38 $\alpha\beta$  in satellite cells (Rapraeger et al., 1991; De Cristofaro et al., 1998; Troy et al., 2012), and Syndecan-4 regulates Rac1, a member of the Par-3/p38 $\alpha\beta$  MAPK complex, signaling in other cell types (Tkachenko et al., 2004). Syndecan-4 can act independently of satellite cells but may be acting with FGF and Notch to regulate asymmetric division in satellite cells.

**Satellite cells reside in a polar satellite cell niche that may regulate asymmetric division**

The interaction of the satellite cell with the satellite cell niche likely regulates self-renewal and asymmetric division. Satellite cells reside on myofibers in a polar niche where the basal membrane of the satellite cell contacts the basal lamina, an extracellular matrix sheet surrounding the myofiber, and the apical membrane contacts the myofiber plasma membrane (Mauro, 1961). Similar polar environments direct asymmetric division in other stem cell populations to produce a self-renewing stem cell and a daughter cell that will leave the niche and differentiate (Fuchs et al., 2004). Asymmetric distribution of signals within the satellite cell niche may direct the orientation of asymmetric division to protect quiescent daughter cells from the signals released by regenerating myofibers (Kuang et al., 2007). Additionally, asymmetric distribution of signals along regions of the basal lamina or myofiber could produce the satellite cell heterogeneity that may mark a stem cell population within the satellite cell population.

#### *The role of the basal lamina in the myofiber niche*

The myofiber basal lamina forms extracellular matrix sheets around individual myofibers and their associated satellite cells (Sanes, 2003). The basal lamina comprises extracellular matrix proteins, linear GAG (sugar) chains on proteoglycans, and soluble signaling factors (Sanes, 2003; Kjaer et al., 2006; Schiaffino and Partridge, 2008). These components provide structural and biochemical cues to satellite cells that promote or inhibit satellite cell activity, including self-renewal and asymmetric division.

The dominant structural proteins in the basal lamina are laminin and collagen isoforms while fibronectin, the major component of basement membranes in other stem cell niches, is not present in the myofiber basal lamina (Sanes, 2003). Laminin and collagen form supramolecular aggregates with perlecan (Grounds et al., 2005) and nidogen/entactin that create the scaffold of

the extracellular matrix. Laminin and collagen also convey mechanical cues to the myofiber and satellite cell through cell surface integrins (Ingber, 2006; Kjaer et al., 2006). Laminin  $\alpha 2$  chains are the major component of basal lamina, but  $\alpha 4$  and  $\alpha 5$  chains appear in regenerating muscle (Sorokin et al., 2000; Grounds et al., 2005), which suggests different laminin isoforms may affect satellite cell behavior. Several collagen isoforms are present in the basal lamina where collagen IV forms the matrix scaffold and collagen VI anchors the basal lamina to interstitial connective tissue (Zou et al., 2008). Interestingly, collagen VI is expressed in quiescent satellite cells, and collagen VI null mice exhibit decreased numbers of satellite cells after injury (Urciuolo et al., 2013), suggesting that structural proteins may affect satellite cell behavior.

Proteoglycans, core proteins with GAG chains, are important components of the basal lamina that help form the matrix scaffold and regulate growth factor signaling (Sanes, 2003). Proteoglycans are secreted by cells in the niche or are enzymatically cleaved from cell membranes to the matrix. Many types of proteoglycans are present in skeletal muscle, but heparan sulfate proteoglycans are the most prevalent in the basal lamina. These highly sulfated heparan sulfate GAG chains have a high negative charge that promotes binding to many soluble molecules in the matrix. Variation in GAG sequence and sulfation are likely to establish domains for specific growth factors as differences in sulfation affect the specificity of FGF interactions with their cognate receptors (Esko and Selleck, 2002). Heparan sulfate GAG composition can change during regeneration and may function to present or to sequester signals with spatial and temporal specificity from satellite cells during muscle regeneration (Sanes et al., 1986; Coombe and Kett, 2005; Bishop et al., 2007).

The basal lamina contains signaling factors secreted from systemic (interstitial cells, nerve and vascular networks (Bortoluzzi et al., 2006; Kragstrup et al., 2011)) and local (satellite cell and myofiber) sources. The basal lamina forms a repository of these signals that poises the niche to direct satellite cell activity (Olwin and Rapraeger, 1992; Cornelison et al., 2001; Jenniskens et al., 2006; Langsdorf et al., 2007). Muscle injury causes expression of matrix metalloproteinases (MMP) 2 and 9, which degrade the basal lamina to release growth factors to bind to satellite cell proteoglycans and growth factor receptors cells (Sanes, 2003). The most common receptor ligands in basal lamina include proteoglycan-binding HGF, Epidermal Growth Factor (EGF), Wnts, FGF-2, IGF-1 and collagen-binding TGF $\beta$  (J. DiMario et al., 1989; Tatsumi et al., 1998; Gelse et al., 2003; Machida and Booth, 2004; Brack et al., 2008; Le Grand et al., 2009; Chakkalakal et al., 2012). As many of these signals affect satellite cell behavior in culture, it remains unclear how these signals cumulatively regulate satellite cell self-renewal and progression through myogenesis.

#### *The role of the myofiber in the satellite cell niche*

Quiescent satellite cells likely reside in a discrete niche on myofibers rather than localizing randomly across myofibers. Satellite cell frequency on myofibers is higher in ‘slow’ muscles than in ‘fast’ muscles (Aloisi et al., 1973) and satellite cells often associated with the neuromuscular junctions (Kelly, 1978) and capillaries (Christov et al., 2007). These regions may contain unique localized membrane environments compared to the majority of the myofiber. Integrin  $\alpha 3\beta 1$  (in *Xenopus*) (Cohen et al., 2000) and distinct laminin isoform levels increase at the neuromuscular junction, suggesting that the interaction of the myofiber with the nerve terminal alters the local basal lamina composition (Jenniskens et al., 2006). Distribution of

ligands in discrete regions of the myofiber may establish satellite cell domains that form the niche within the larger myofiber environment.

Myofibers secrete ligands to the satellite cells that direct satellite cell activity. Signals from the myofiber can inhibit satellite cell activity as Marcaine-treated myofibers, which undergo necrosis leaving the basal lamina and satellite cells intact, contain more proliferating satellite cells than untreated myofibers (Bischoff, 1990). Myofibers secrete SDF-1 which binds to CXCR4 receptor on satellite cells to promote migration (Ratajczak et al., 2003; Sherwood et al., 2004). Additionally, myofibers express the Notch ligand Delta-1, which interacts with Notch on satellite cells (Conboy et al., 2003). These signals are not present in the basal lamina and may provide mechanisms for regulation of satellite cell asymmetric division.

In summary, the presence of unique and variable environments within the basal lamina and myofiber plasma membrane may provide an environment directed toward regulating satellite cell self-renewal and thereby regulating satellite cell numbers, a satellite cell niche. This niche may serve to promote either symmetric or asymmetric satellite cell division depending on the needs of the skeletal muscle for maintenance, growth or repair. Further studies are needed to delineate the separate roles the basal lamina and the myofiber may play in regulating satellite cell behavior.

Here, I present my thesis work characterizing a loss self-renewal in satellite cells from old mice. I have found cell intrinsic impairments in the old satellite cell cannot be rescued by a young muscle environment, contradicting a popular model presented for satellite cell aging, which postulates that the old environment is primarily responsible for inhibiting satellite cell function. I present evidence that aberrant activation of p38 $\alpha$  $\beta$  MAPK and decreased FGF

signaling underlie impaired self-renewal in aged satellite cells and that heterochronic transplantation to a young environment fails to rescue self-renewal. I propose a novel role for the involvement of FGF signaling in regulating asymmetric satellite cell division by influencing asymmetric activation of p38 $\alpha\beta$  MAPK. As part of a collaborative effort, I present 2D and 3D hydrogels as tunable, artificial satellite cell niches and characterize the effect of components added to the hydrogels on satellite cell self-renewal in culture.

**Chapter 2: P38 MAPK signaling underlies a cell autonomous loss of stem cell self-renewal in aged skeletal muscle**

## INTRODUCTION

Sarcopenia, defined as an irrevocable loss of skeletal muscle mass and strength in the aged (Evans and Campbell, 1993; Baumgartner, et al., 1998), results in frailty and a high risk of mortality (Roubenoff, 2000; Landi et al., 2013), thus greatly increasing government healthcare expenditures in the face of a rapidly expanding elderly population (Janssen et al., 2004). The mechanisms involved in the development of sarcopenia are poorly understood but include diverse changes in skeletal muscle metabolism (Karakelides and Nair, 2005) and compromised regeneration (Brooks and Faulkner, 1990; Grounds, 1998; Day et al., 2010). Widely regarded as critical to the regeneration process, satellite cells reside between the basal lamina and the myofiber plasma membrane of young skeletal muscle (Mauro, 1961). Indeed, ablation experiments demonstrate that satellite cells are bona-fide muscle stem cells as they exhibit remarkable regenerative and self-renewing properties (Sambasivan et al., 2011; Lepper et al., 2011; Murphy et al., 2011).

Functional deficits in the satellite cell population (Conboy et al., 2003; Collins et al., 2007) are thought to be responsible for the poor regenerative capacities of sarcopenic muscle (Brooks and Faulkner, 1990; Grounds, 1998; Day et al., 2010; Sadeh, 1988; McGeachie and Grounds, 1995; Marsh et al., 1997), where age-related changes in satellite cells include an impaired response to injury (Collins et al., 2007; Allen et al., 1980; Decary et al., 1997; Shefer et al., 2006), and although controversial, a reduction in satellite cells that could contribute to reduced progenitor expansion (Day et al., 2010; Conboy et al., 2003; Shefer et al., 2006; Roth et al., 2000). Additionally, systemic cues within the aged environment are reported to impair satellite cell activity while exposure to a young environment improves regeneration of aged

muscle and satellite cell differentiation (Conboy et al., 2003; Collins et al., 2007; Carlson and Faulkner, 1989; Carlson and Faulkner 1996; Conoby et al., 2005; Brack and Rando, 2007). Interestingly, recent data suggest that the aged environment can be overcome as transplantation of young myofibers with their attached satellite cells prevented age-associated loss of muscle mass and strength (Hall et al., 2010). Thus, while the aged environment appears inhibitory, these data demonstrate the existence of cell-autonomous behaviors not subject to repressive extrinsic cues.

FGFR tyrosine kinases play important roles in coordinating extracellular signals with internal satellite cell regulatory networks. While FGFRs indirectly promote proliferation by repressing myoblast differentiation, they do not directly function as mitogens (Hannon et al., 1996). Satellite cells express FGFR1 and FGFR4 (Sheehan and Allen 1999; Kastner et al., 2000) where FGFR4 plays a role in cell fate determination during embryonic muscle development (Lagha et al., 2008) and FGFR1 prevents terminal differentiation (Kudla et al., 1998; Flanagan-Steele et al., 2000). Intracellular signals activated by FGFR1 include both ERK and p38 $\alpha$  MAPK pathways, which regulate satellite cell proliferation and asymmetric division, respectively (Jones et al., 2001; Jones et al. 2005).

Members of the MAPK family play diverse and complicated roles in the maintenance, proliferation, asymmetric division and differentiation of satellite cells. ERK is necessary but not sufficient for myoblast proliferation (Jones et al., 2001; Chakkalakal et al., 2012) and does not regulate differentiation (Kudla et al., 1998; Jones et al., 2001), but is implicated in age-related losses of satellite cell proliferative capacity (Chakkalakal et al., 2012). Regulation of ERK signaling by Sprouty affects satellite cell numbers, where Sprouty null mice exhibit regenerative

deficits associated with aging (Chakkalakal et al., 2012). Since Sprouty regulates multiple signaling pathways, it is unclear which growth factors are involved in mediating Sprouty effects on satellite cells (Guy et al., 2009). The p38 MAPK family comprises four members, two closely related (p38 $\alpha\beta$  MAPKs), p38 $\delta$  MAPK and p38 $\gamma$  MAPK. Signaling by p38 $\alpha\beta$  MAPK is involved in the exit of satellite cells from quiescence (Jones et al., 2005; Troy et al., 2012), asymmetric division of satellite cells (Troy et al., 2012), and for p38 $\alpha$ , maintenance of satellite cell numbers *in vivo* (Brien et al., 2013). The p38 $\alpha\beta$  MAPKs and p38 $\gamma$  MAPK play roles in myogenic differentiation (Kang et al., 2008; Gillespie et al., 2009). Because of the diverse roles the MAPK family plays in regulating satellite cell function, their relative activities are likely spatially and temporally context dependent.

Here I show that aged satellite cells possess a cell-autonomous defect in self-renewal that cannot be rescued by exposure to a young environment. Importantly, this impairment of self-renewal in aged satellite cells may explain the poor regenerative capacity of aged muscle. I demonstrate that these functional deficits arise from an impaired response to FGF ligands and elevated p38 $\alpha\beta$  MAPK activity, which when corrected, rescues self-renewal of aged satellite cells. Thus, my data identify cell autonomous FGF/p38 $\alpha\beta$  MAPK signaling as a critical pathway deregulated in aged satellite cells and highlight a novel therapeutic opportunity for clinical management of age-associated sarcopenia.

## **RESULTS**

### **A young local environment does not rescue age-associated self-renewal defects**

Substantial evidence from our group and others shows that aged satellite cells fail to expand as efficiently as young satellite cells cultured *in vitro* (Figures 2.1, 2.2, Appendix 1)

(Collins et al., 2007; Shefer et al., 2006). Since parabiosis and transplantation experiments show that a young environment can restore some aspects of aged satellite cell function (Collins et al., 2007; Conboy et al., 2005; Brack and Rando, 2007) we developed a heterochronic culture assay (Figure 2.3a) to specifically assess whether a young local environment (intact myofibers) could restore aged satellite cell expansion. Satellite cells isolated from young or aged mice constitutively expressing GFP ( $\beta ActGFP$ ) were seeded onto unlabeled myofibers from a young mouse (Figure 2.3a) and fixed for analysis at 24h (Figure 2.3b) and 72h post-transplantation (Figure 2.3c). Quantification of endogenous host satellite cells marked by Syndecan-4 (Cornelison, et al., 2001) (\*, Figure 2.3b) and donor GFP+ satellite cells ( $\wedge$ , Figure 2.3b, c) revealed equivalent young and old donor satellite cell attachment at 24h (Figure 2.3d). Strikingly, we observed 3-fold fewer aged donor cells compared to young donor cells at 72h (Figure 2.3e) indicating impaired aged satellite cell expansion and suggesting that a young local environment is not sufficient to restore aged satellite cell function.

### ***In vivo* transplantation of aged satellite cells to a young muscle environment reveals cell-autonomous self-renewal defects**

As *in vitro* transplantation of aged satellite cells onto young myofibers failed to rescue aged satellite cell expansion, I reasoned that a young global environment, including circulating factors, may be necessary to rescue aged satellite cell self-renewal and subsequent expansion. Therefore, I performed *in vivo* transplantation experiments where young and aged  $\beta ActGFP$  myofiber-associated satellite cells were engrafted into young wild type hosts concurrent with  $BaCl_2$  injury (Hall et al., 2010) (Figure 2.3f). Although young and aged satellite cells fused into

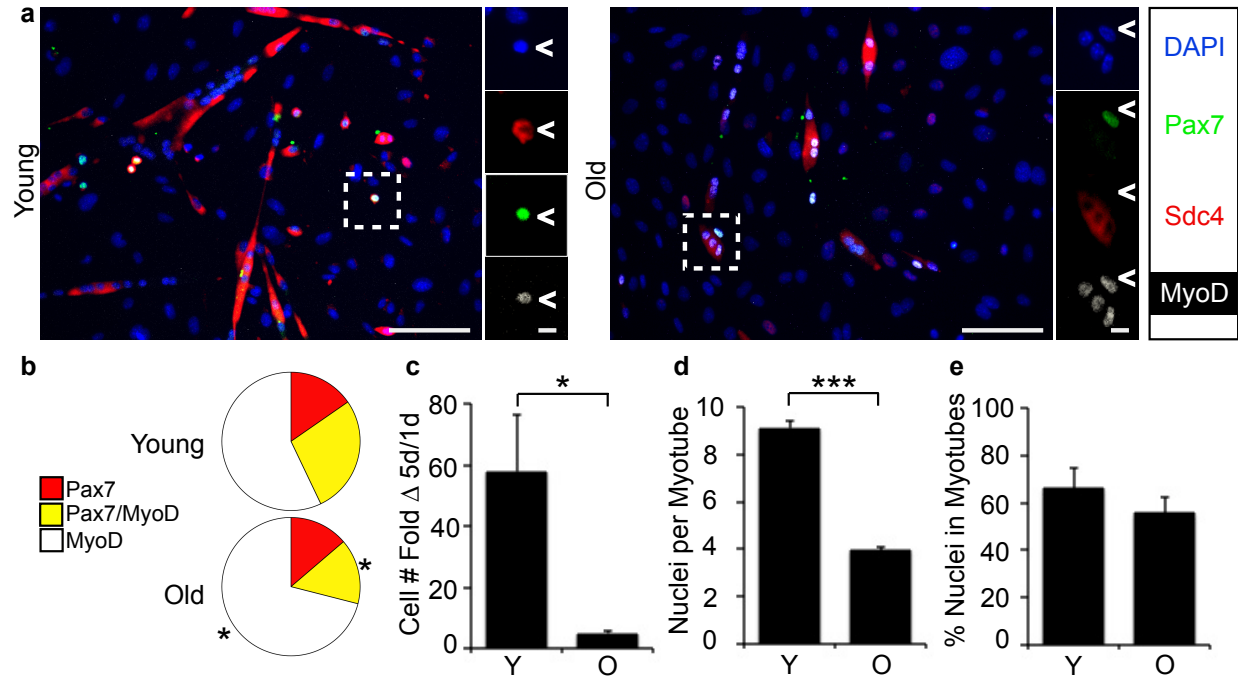


**FIGURE 2.1. Old satellite cell explants exhibit reduced proliferation and decreased Pax7 expression.** (a) Satellite cells explanted from young (Y) and old (O) mice were cultured and fixed at five days in culture, immunostained for Syndecan-4, Pax7 and MyoD (white) and (b) scored for the numbers of Syndecan-4+ (Sdc4) cells that were Pax7+/MyoD- reserve (self-renewed) cells (■), Pax7+/MyoD+ myoblasts (■), and Pax7-/MyoD+ differentiating myocytes (□). Pie charts comprise the percentages of Syndecan-4+ satellite cells that are Pax7+/MyoD-, Pax7+/MyoD+ and Pax7-/MyoD+. Inset (^) shows Pax7+/MyoD+ satellite cell. Scale bars, 50  $\mu$ m (10  $\mu$ m). Young cells (c) proliferated more and (d) formed larger myotubes (myofiber-like structures) than old cultures, despite similar (e) percentages of total cellular differentiation (% of Syndecan-4+ nuclei in myotubes). (Syndecan-4-, mononuclear cells are contaminating fibroblasts). Mean  $\pm$  s.e.m. n=3 independent experiments. \* $P < 0.05$  \*\*\* $P < 0.0001$  by one-way ANOVA with Tukey's test. 30d post-transplantation compared to young donor-derived satellite cells (Fig. 1h). By 60d, I detected virtually no aged donor-derived satellite cells (Fig. 1h), whereas young donor-derived cells declined but were readily detectable (Fig. 1h). Collectively, these data demonstrate that the young environment permits but fails to maintain aged satellite cell engraftment.

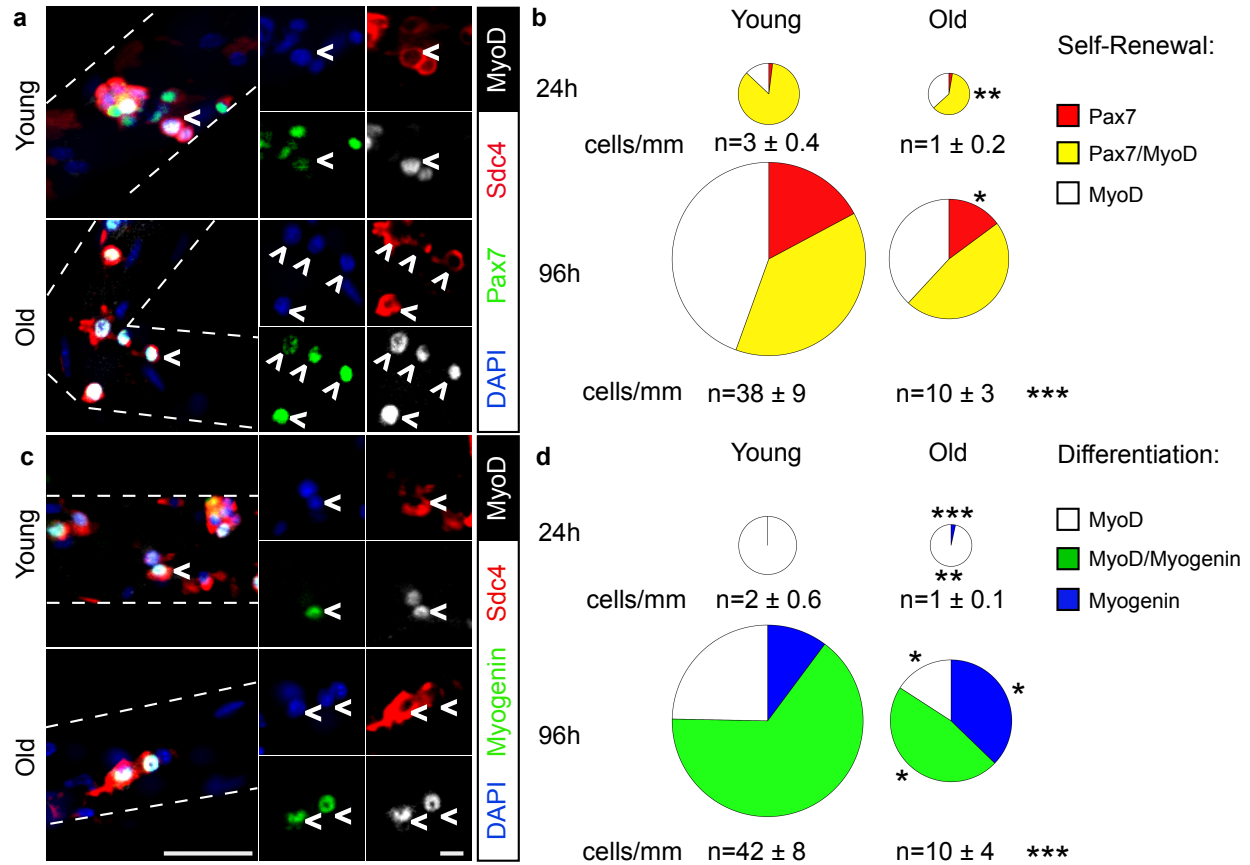


**FIGURE 2.2. Old myofiber-associated satellite cells exhibit reduced proliferation and increased differentiation.** (a,c) Young and old myofiber-associated satellite cells were scored after 24h or 96h for Syndecan-4+ (red) cells that were (b) Pax7+/MyoD- reserve cells (■, ^), Pax7+/MyoD+ myoblasts (■), and Pax7-/MyoD+ myocytes (□)-or (d) for MyoD+ myoblasts (□), MyoD+/Myogenin+ committed myocytes (■), or Myogenin+ terminally differentiated cells (■). Pie charts comprise the percentages of Syndecan-4+ satellite cells that are Pax7+/MyoD-, Pax7+/MyoD+ and Pax7-/MyoD+ or are MyoD+/Myogenin-, MyoD+/Myogenin+ and MyoD-/Myogenin+. Pie chart size is directly (1:1) scaled to the number of Syndecan-4+ cells/myofiber (mm). Insets depict (^) Pax7+/MyoD+ satellite cells. Scale bars, 50  $\mu$ m (10  $\mu$ m). Pie chart areas represent Syndecan-4+ cells/mm, revealing no significant difference in the number of young and old satellite cells at 24h. Young satellite cells proliferated and retained Pax7 more than old satellite cells. A subset of old satellite cells was Myogenin+ at isolation, and by 96h more old satellite cells were terminally differentiated. Mean  $\pm$  s.e.m.  $n=3$  independent experiments. \* $P < 0.05$ , \*\* $P < 0.001$ , \*\*\* $P < 0.0001$  by unpaired, two-way Student's t-test (marker profiles) or one-way ANOVA with Tukey's test (mean Syndecan-4+ cells/mm). Significance is measured across age, not across culture time.

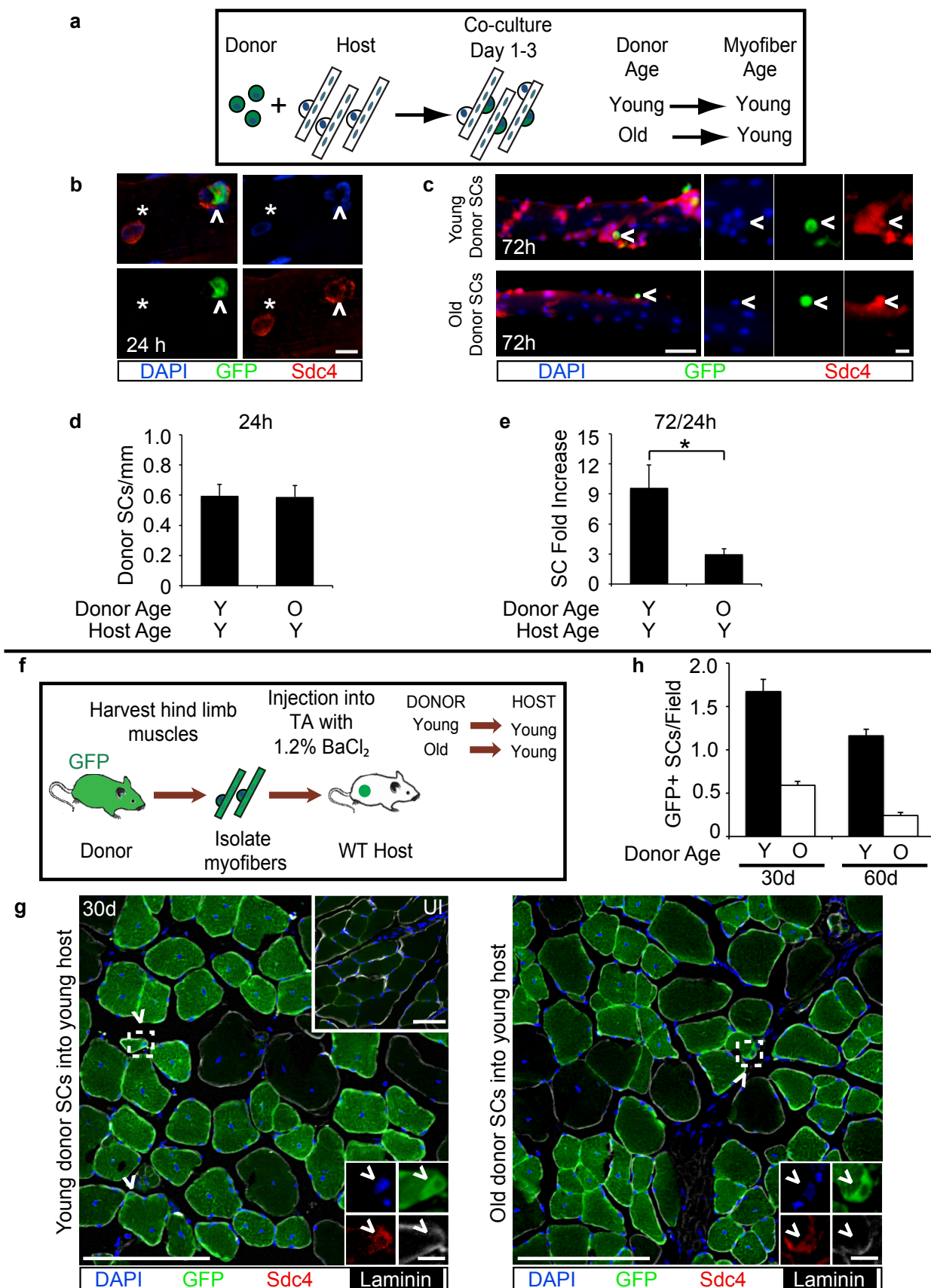


**FIGURE 2.3. Heterochronic transplantation of old satellite cells to local or systemic young environment fails to rescue age-associated phenotypes. (a-e)** (a) Donor satellite cells (SCs) from young (Y) or old (O)  *$\beta$ ActGFP* mice (green) were transplanted onto young myofibers. Donor satellite cells, ( $\wedge$  GFP+/Syndecan-4+ (Sdc4)) attached to host myofibers possessing endogenous satellite cells (\* GFP-/Sdc4+), were visualized after (b) 24h or (c) 72h in culture. (Insets, donor satellite cells; scale bar=50  $\mu$ m or 10  $\mu$ m, inset). Quantification of myofiber-associated donor satellite cells, normalized to myofiber length, at (d) 24h or (e) at 72h, plotted as fold-change from 72h/24h. (Mean $\pm$ s.e.m., n=3,  $\geq$  20 myofibers scored per condition. \* $P$  < 0.05,  $t$  test). (f-h) (f) Donor myofiber-associated satellite cells from young or old  *$\beta$ ActGFP* mice (green) were transplanted into young host TA muscles. (g) TA muscles were harvested at (g) 30d or (not shown) 60d post-transplantation and processed to visualize GFP, Sdc4 and Laminin where sections show GFP+ and GFP- myofibers. ( $\wedge$  marks all GFP+/Sdc4+ satellite cells). Dotted line indicates magnified insets (boxes) of representative young donor-derived satellite cell or old donor-derived satellite cell. The solid boxed area is a section from contralateral uninjured (UI) TA muscle. (Scale bars=50  $\mu$ m or 10  $\mu$ m, insets). (h) The numbers of donor-derived satellite cells per field were quantified and plotted for 30d and 60d post-transplantation. (A minimum of 10 fields were scored for n=3-5 transplant recipients. Mean $\pm$ s.e.m;  $P$  < 0.05 for Young 30d vs. 60d, Old 30d vs. 60d, by one-way ANOVA).

host myofibers (Figure 2.3g), I detected 3-fold fewer aged donor-derived cells in the satellite cell position 30d post-transplantation compared to young donor-derived SCs (Figure 2.3h). By 60d, we detected virtually no aged donor-derived SCs (Figure 2.3h), whereas young donor-derived cells declined but were readily detectable (Figure 2.3h). Collectively, these data demonstrate that the young environment permits but fails to maintain aged SC engraftment.

### **Aged satellite cells exhibit elevated p38 $\alpha$ $\beta$ MAPK signaling and altered FGF signaling**

One explanation for the poor engraftment of aged satellite cells is that the cells fail to properly activate. Given the prominent role of p38 $\alpha$  $\beta$  MAPK signaling in regulating satellite cell activation (Jones et al., 2005) and asymmetric division (Troy et al., 2012), I systematically interrogated the integrity of this signal transduction cascade in aged satellite cells. Young myofiber-associated satellite cells activate within 30 min of injury or explantation as measured by p38 $\alpha$  $\beta$  MAPK phosphorylation (Jones et al., 2005). Surprisingly, I found enhanced p38 $\alpha$  $\beta$  MAPK phosphorylation in aged myofiber-associated satellite cells compared to young satellite cells analyzed 1h post-isolation (Figure 2.4a, b) and that 3-fold more aged satellite cells than young satellite cells were positive for phosphorylated MK2 (pMK2), a direct target of p38 $\alpha$  $\beta$  MAPK (Figure 2.4a, b). This suggests a possible defect in the activation of aged satellite cells that may lead to inappropriate cycling of satellite cells in resting muscle as previously reported (Chakkalakal et al., 2012). Interestingly, by 24h, the number of phosphorylated p38 $\alpha$  $\beta$  MAPK+ (phospho-p38) cells was higher in young satellite cells than in aged satellite cells (Figure 2.4c, d), indicating a failure by aged satellite cells to appropriately advance through the cell cycle.

Since FGF is a known upstream activator of p38 $\alpha$  $\beta$  MAPK, I next investigated FGFR1 activation in aged versus young satellite cells. Immunostaining revealed that phospho-FGFR1+

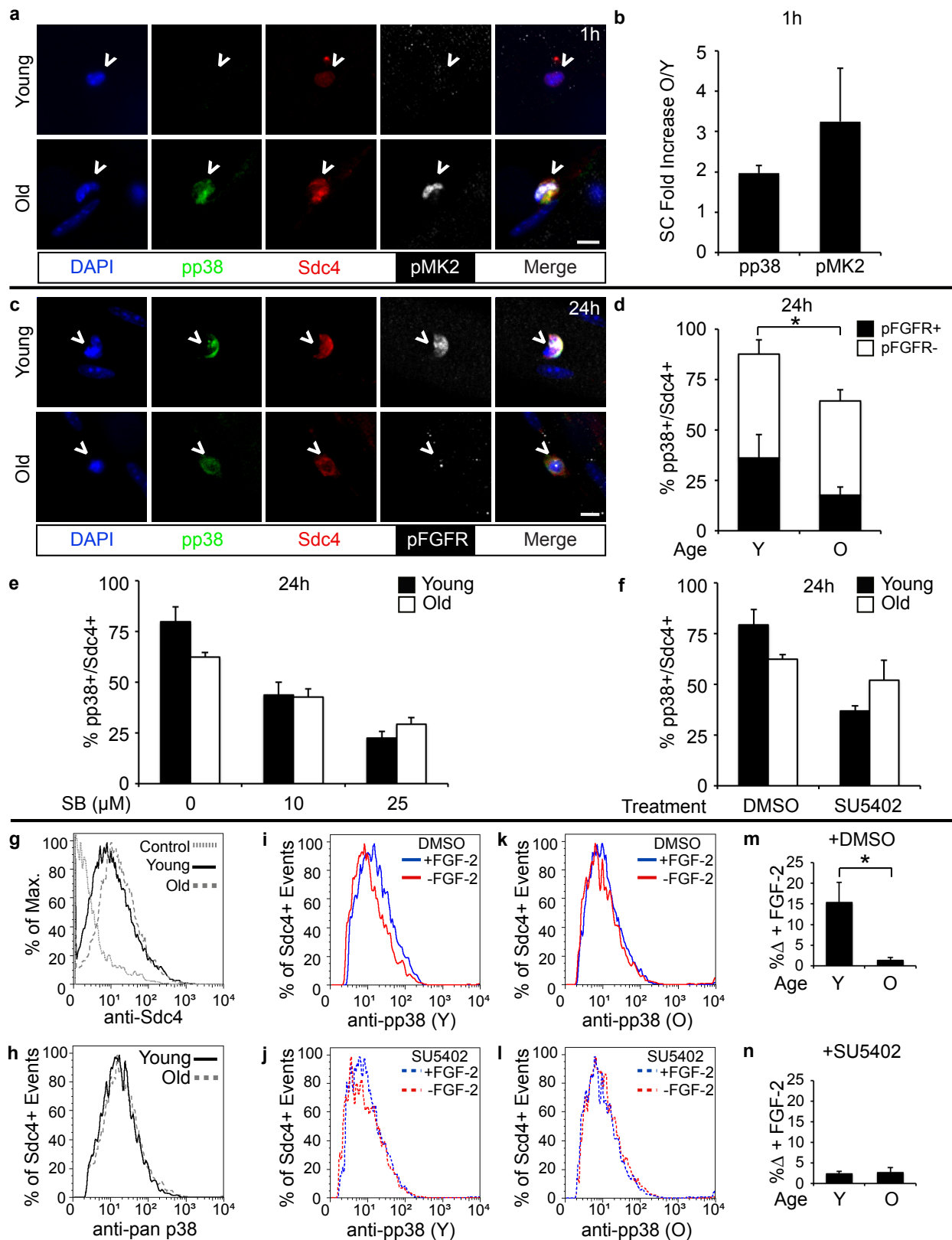


**FIGURE 2.4. Aged satellite cells exhibit elevated p38 $\alpha$  $\beta$  MAPK signaling and altered FGFR1 signaling.** (a) Young (Y) and old (O) myofiber-associated satellite cells (SCs) ( $\wedge$ ) were fixed and stained for Syndecan-4 (Sdc4), phospho-p38 (pp38) and phospho-MK2 (pMK2) at 1h post-dissection ( $\wedge$  marks pp38+/pMK2+ satellite cells; scale bar=10  $\mu$ m). Sdc4+ satellite cells were quantified and (b) plotted for the fold increase for pp38 and pMK2 in old vs. young satellite cells. (c) Myofibers from young and old mice were cultured for 24h, stained as described for 1h except that phospho-FGFR1 (pFGFR) immunostaining replaced pMK2 immunostaining ( $\wedge$  marks pp38+/pFGFR1+ satellite cells; scale bar=10  $\mu$ m). Sdc4+ satellite cells were quantified and (d) the % of pp38+/pFGFR1+ SCs and pp38+/pFGFR1- satellite cells were normalized to the total number of Sdc4+ satellite cells. (e) Young and old myofibers were cultured for 24h with increasing SB203580 (SB), fixed and stained for Sdc4 and pp38, scored and plotted as the % Sdc4+ cells that were pp38+ (\* $P$  < 0.05 for (d) Young vs. Old total pp38 and for (e,f) Young vs Old at 0  $\mu$ M SB and for Young 0 $\mu$ M SB vs Young 10 $\mu$ M SB;  $P$  < 0.0001 for Young and Old 0 $\mu$ M SB vs. 25  $\mu$ M SB by one-way ANOVA. Mean $\pm$ s.e.m., n=3 experiments,  $\geq$  20 myofibers scored per condition). (g-n) Young and aged satellite cells isolated from equivalent muscle masses were cultured for 16h and then assayed for FGF-stimulated phosphorylation of p38 $\alpha$  $\beta$  MAPK by flow cytometry. (g-l) Histograms for young and old satellite cell cultures of (g) Sdc4+ cells and (h) p38 $\alpha$  $\beta$  MAPK+ cells. Histograms for pp38+ cells following a 5 min FGF-stimulation in (i) young cells and (k) aged cells in DMSO or for (j) young cells and (l) old cells in 25  $\mu$ M SU5402. (m-n) A plot of the % population shifts (Overton subtraction) for FGF-stimulated pp38+ immunoreactivity in young vs. old cells, (m) DMSO carrier and (n) 25  $\mu$ M SU5402 (n=3 experiments. \* $P$  < 0.05 by  $t$  test).

(pFGFR1)/phospho-p38<sup>+</sup> satellite cell numbers were reduced in aged cultures at 24h post-isolation (Figure 2.4d). I then scored phospho-p38<sup>+</sup> cells in the presence of SB203580, a p38 $\alpha\beta$  MAPK inhibitor, and found that both young and aged satellite cells were sensitive to SB203580 (Figure 2.4e). To assess whether the elevated phospho-p38 levels in aged cells were FGF-dependent, I tested the FGFR inhibitor SU5402 on myofiber-associated satellite cells.

Unexpectedly, I found that p38 $\alpha\beta$  MAPK signaling was abrogated by FGFR inhibition only in young satellite cells, suggesting that the FGFR-p38 $\alpha\beta$  MAPK signaling pathway is specifically altered in aged satellite cells (Figure 2.4f). Single cell analyses of p38 $\alpha\beta$  MAPK phosphorylation by FGF-2 revealed essentially identical numbers of young and aged Syndecan-4<sup>+</sup> (Figure 2.4g) and p38 $\alpha\beta$  MAPK<sup>+</sup> (Figure 2.4h) satellite cells from equivalent muscle masses. Upon FGF-2 stimulation, young satellite cells exhibited marked p38 $\alpha\beta$  MAPK phosphorylation (Figure 2.4i, m) whereas p38 $\alpha\beta$  MAPK phosphorylation in aged satellite cells was refractory to FGF-2 (Figure 2.4k, m). Importantly, inhibition of FGF signaling with SU5402 eliminated FGF-stimulated phosphorylation of p38 $\alpha\beta$  MAPK in young satellite cells (Figure 2.4j, n) but had no effect on aged satellite cells (Figure 2.4l, n), highlighting the FGF insensitivity of p38 $\alpha\beta$  MAPK in aged satellite cells.

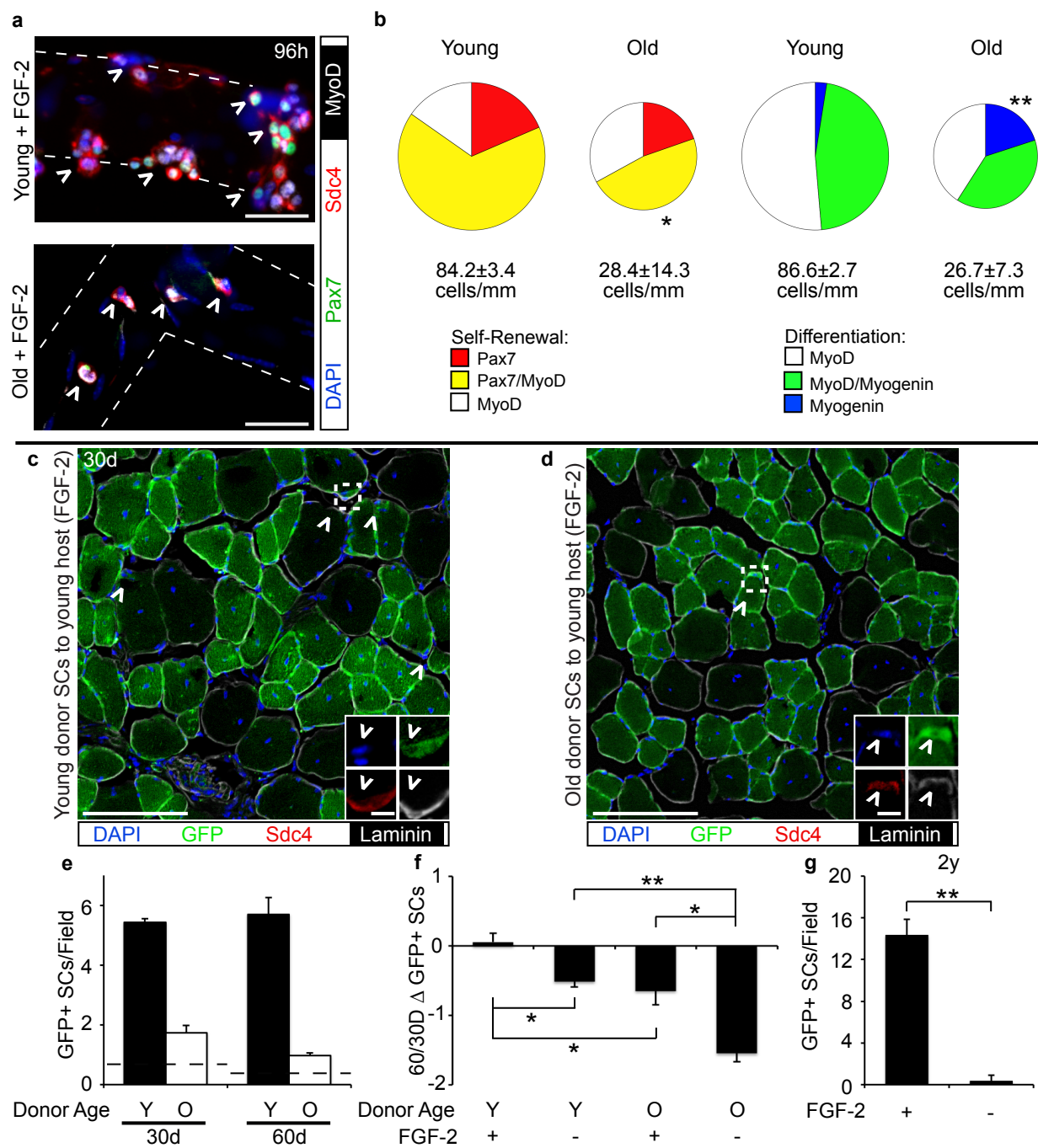
### **FGF-2 enhances self-renewal of young but not aged satellite cells**

Aged donor-derived satellite cells cannot be maintained when transplanted into young host mice (Figure 2.3), despite similar percentages of Pax7<sup>+</sup>/MyoD<sup>-</sup> reserve cells in cultures (Figures 2.1, 2.2). Since aged satellite cells are inappropriately activating (Figure 2.4), this could affect both self-renewal and expansion in host tissue post-transplantation. Therefore, I asked if FGF-2, which enhances self-renewal in other stem cells (Coutu and Galipeau, 2011), would

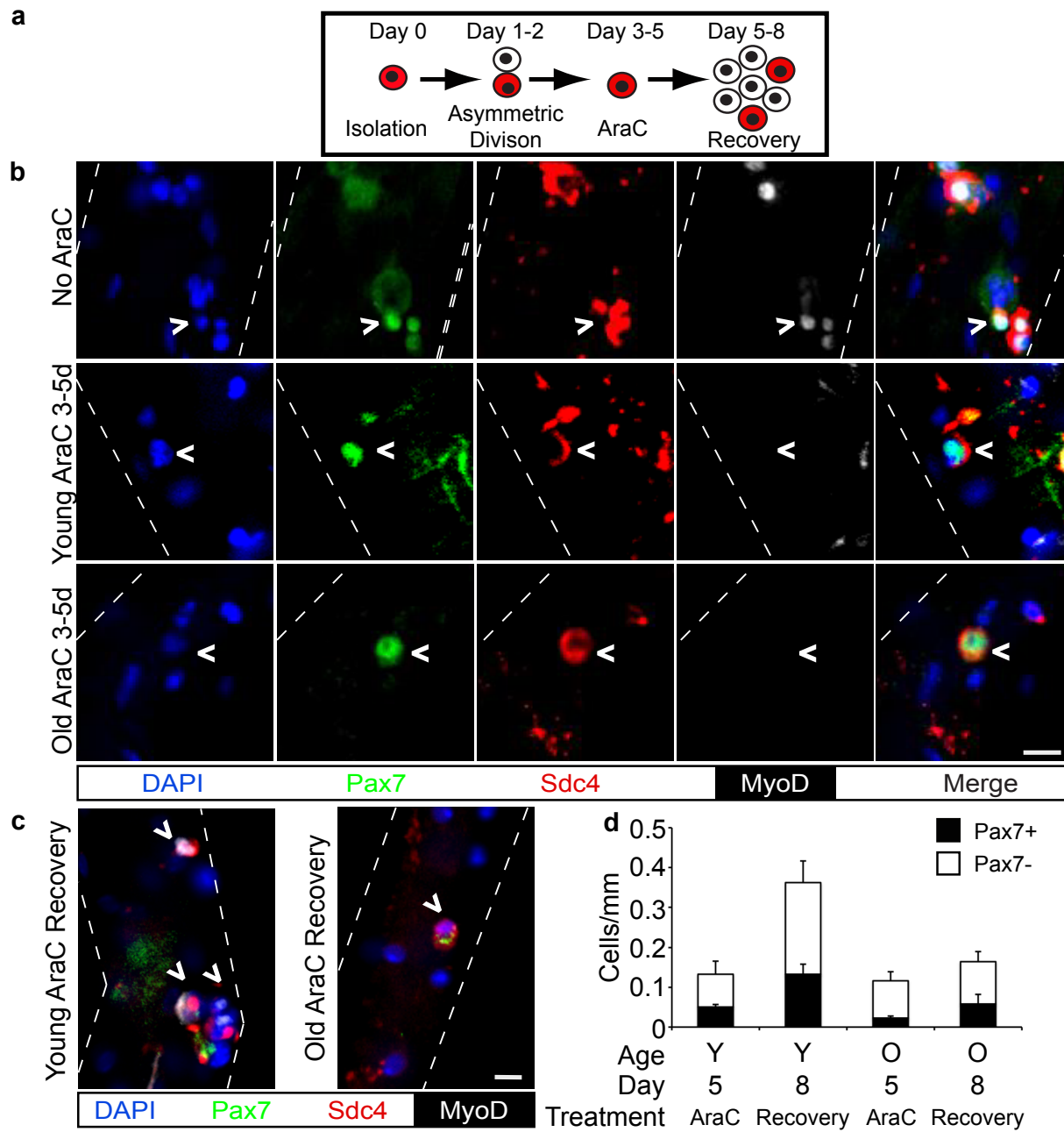
affect satellite cell self-renewal. FGF-2 addition dramatically increased the numbers of young Pax7<sup>+</sup> myofiber-associated satellite cells (Figure 2.5a, b, Appendix 1) and reduced the proportion of terminally differentiated young cells (Figures 2.5b, 2.2). In contrast, FGF-2 addition to aged satellite cells had no effect on the generation of reserve Pax7<sup>+</sup> cells but reduced terminal differentiation. When young myofiber-associated satellite cells were pre-treated with FGF-2 prior to transplantation into injured host muscles, satellite cell engraftment was enhanced (Figure 2.5c) by 3-fold compared to no FGF-2 pretreatment (Figures 2.5e, 2.3h) and donor satellite cells were maintained in the host tissue between 30d and 60d post-transplantation (Figure 2.5e, f). FGF-2 pretreatment of aged myofiber-associated satellite cells (Figure 2.5d) similarly enhanced engraftment (Figure 2.5e) but aged satellite cell numbers were not maintained as evidenced by a 2-fold decline in aged donor-derived satellite cells between 30d and 60d post-transplantation (Figure 2.5f). Interestingly, FGF-2 pretreatment of young satellite cells is necessary to maintain self-renewal of donor cells for the lifetime of the mouse (Figure 2.5g) (Hall et al., 2010). Taken together, these data highlight a role for FGF signaling in promoting survival and self-renewal in young satellite cells that is not maintained as satellite cells age.

### **Generation of quiescent daughter cells and asymmetric phospho-p38 is impaired in aged satellite cells.**

Our data indicate that maintenance and self-renewal of aged satellite cells cannot be rescued by transplantation into a young host environment even with FGF-2 pretreatment. Therefore, I assayed the ability of aged satellite cells to generate quiescent daughter cells (Figure 2.6a) (Troy et al., 2012). When myofiber-associated satellite cells were treated with the mitotoxin 1 $\beta$ -arabinofuranosylcytosine (AraC) for 3-5d post-isolation, I observed similar



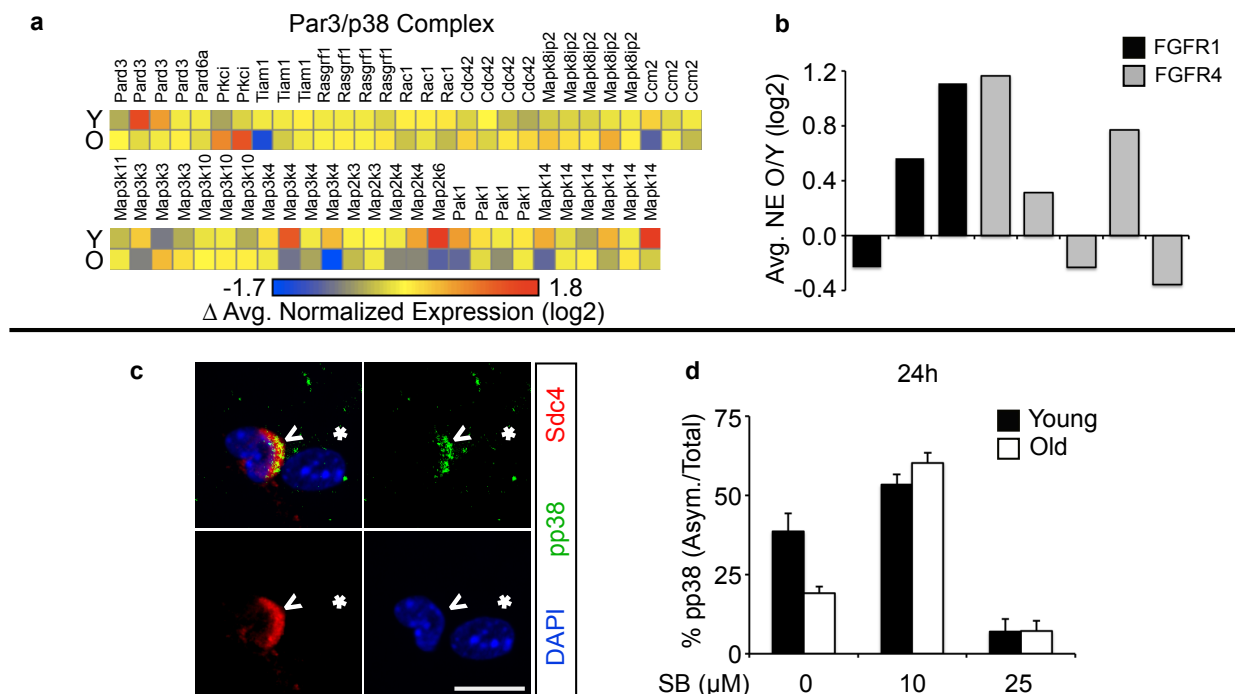
**FIGURE 2.5. FGF maintains self-renewal and expansion of young cells but not aged cells in culture and *in vivo*.** (a) Myofiber-associated satellite cells (SCs) were cultured in FGF-2 for 96h and stained for (a) Syndecan-4 (Sdc4), Pax7, MyoD and DAPI, or (not shown) Syndecan-4, MyoD, and Myogenin (Scale bar=50  $\mu$ m). (b) Pie charts representing percentages of Sdc4+ cells that are Pax7+/MyoD- self-renewed satellite cells (■), Pax7+/MyoD+ myoblasts (■), and Pax7-/MyoD+ myocytes (□) or for MyoD+ myoblasts (□), MyoD+/Myogenin+ committed myocytes (■), and Myogenin+ differentiated cells (■), where chart area is directly scaled to the number of Sdc4+ cells per myofiber length at 96h. (Mean $\pm$ s.e.m., n=3 experiments,  $\geq$  20 myofibers per condition. \* $P$ <0.05, 96h Young vs. Old Pax7+/MyoD+, \*\* $P$ <0.001 96h Young vs. Old Myogenin+, by one-way ANOVA.) (c-f) Donor myofibers from  $\beta$ ActGFP (c) young (Y) or (d) aged (O) mice were treated with 1.5 nM FGF-2 and transplanted into host TA muscles ( $\wedge$  marks all donor-derived satellite cells; scale bar=50  $\mu$ m). Dotted box indicates magnified inset area of a (c) young donor-derived satellite cell and (d) an old donor-derived satellite cell (Scale bar=10  $\mu$ m). (e) FGF-2-pre-treated donor (GFP+/Syndecan-4+) satellite cells were scored and plotted per field of view (Dotted line marks donor cell numbers without FGF-2 pretreatment.  $P$ <0.05 for Old 30d-60d, by one-way ANOVA). (f) Plot of log<sub>2</sub> fold change in donor satellite cell number comparing 60d to 30d post-transplantation. (Mean  $\pm$ s.e.m., n=3-5 recipient mice/condition. \* $P$ <0.05, \*\* $P$ <0.001 by one-way ANOVA.) (g) A plot of donor-derived satellite cells per field pretreated with or without FGF-2 from a young donor  $\beta$ ActGFP mouse harvested 21 mo. post-transplantation (\*\* $P$ <0.001,  $t$  test).



**FIGURE 2.6. The self-renewing population is lost in aged satellite cell culture. (a)** A schematic of AraC treatment shows survival of quiescent satellite cell daughter cells derived from asymmetric divisions (red) that recover upon AraC removal functioning as stem cells to self-renew (red) and generate committed myoblast progenitors (white). Myofibers isolated from young and aged mice were cultured for 72h then **(b)** treated for 48h with or without AraC, fixed and stained for Syndecan-4 (Sdc4), Pax7, MyoD and DAPI ( $\wedge$ , marks Sdc4<sup>+</sup> satellite cell clones in no AraC and quiescent Sdc4<sup>+</sup>/Pax7<sup>+</sup>/MyoD<sup>-</sup> satellite cell daughters in AraC-treated cultures; scale bar=10 $\mu$ m). **(c)** After 48h in AraC, AraC was removed, and myofibers were cultured for an additional 72h and stained as for AraC-treated myofiber cultures (Recovery where  $\wedge$  marks Sdc4<sup>+</sup> clones (Y) and a Sdc4<sup>+</sup>/Pax7<sup>+</sup>/MyoD<sup>low</sup> satellite cell (O); scale bars=10  $\mu$ m).. **(d)** Myofiber-associated AraC-resistant cells and cells following AraC recovery were quantified and plotted as self-renewed daughter cells (■ Pax7<sup>+</sup>) and committed myogenic progenitors (□ Pax7<sup>-</sup>), where  $P < 0.05$  for Young Pax7 AraC vs Recovery and for Young total cells AraC vs. Recovery, by one-way ANOVA; .mean  $\pm$ s.e.m., n=3 experiments, with  $\geq 20$  myofibers scored per condition).

numbers of surviving quiescent daughters in young and aged cultures (Figure 2.6b, d). To test for continued stem cell function, the AraC was washed out and cultures were maintained for an additional 4d to assess myoblast expansion and self-renewal of satellite cells as previously described (Troy et al., 2012). In contrast to young cultures, aged myofiber-associated satellite cells were incapable of further expansion and continued self-renewal upon AraC removal (Figure 2.6c, d).

To investigate the molecular basis of this self-renewal defect, I collected RNA from FACS-isolated young and aged satellite cells pooled from multiple animals for an unbiased gene expression analysis to query gene ontology (GO) terms and molecular pathways that changed significantly between young and old satellite cells. I identified a general reduction of gene expression associated with asymmetric division (Troy et al., 2012) (Figure 2.7a, Appendix 2) and cell growth and differentiation (Figures 2.8, 2.9, Appendix 2, Tables 2.1, 2.2). In contrast, expression of FGFR1 and FGFR4 transcripts were elevated in aged satellite cells compared to young satellite cells (Figure 2.7b). Together, these data and the observation that aged myofibers express high levels of FGF-2 (Chakkalakal et al., 2012) suggest that aged SC FGF signaling is impaired and may result in altered p38 $\alpha\beta$  MAPK pathway activation. Since satellite cells undergo self-renewal by asymmetric division (Troy et al., 2012; Kuang et al., 2007) driven by the asymmetric activation of p38 $\alpha\beta$  MAPK (Troy et al., 2012), I expected a reduction in asymmetric phospho-p38 to accompany the impaired self-renewal in aged satellite cells. To test this, I scored Syndecan-4+ myofiber-associated satellite cells for asymmetrically distributed phospho-p38 (Figure 2.7c) and observed a 2-fold reduction in the number of aged satellite cells with asymmetric phospho-p38 compared to young satellite cells (Figure 2.7d). Inhibition of

p38 $\alpha\beta$  MAPK signaling with

**FIGURE 2.7. Loss of self-renewal in aged satellite cells correlates with loss of asymmetric phospho-p38 and can be rescued by partial inhibition of p38 $\alpha\beta$  MAPK signaling.** (a) Heatmaps of normalized expression (see Methods) for probsets in the Par-3/p38 $\alpha\beta$  MAPK complex for young (Y) and old (O) satellite cells where blue is low expression and red high expression, respectively. (b) A plot of old versus young normalized expression of FGFR1 and FGFR4 probesets. (c) Young and old myofiber-associated satellite cells were cultured with or without SB203580 (SB) for 24h, fixed and stained for Syndecan-4 (Sdc4), phospho-p38 $\alpha\beta$  (pp38) and DAPI ( $\wedge$  marks a Sdc4 $^{+}$ /asymmetric pp38 $^{+}$  satellite cell and \* marks a Sdc4 $^{-}$  myonucleus.; scale bar=10  $\mu$ m). (d) The asymmetric pp38 $^{+}$ /Sdc4 $^{+}$  satellite cells were scored and plotted as a percentage of pp38 $^{+}$ /Sdc4 $^{+}$  satellite cells for myofiber-associated satellite cells derived from young and old mice cultured in the presence or absence of the indicated SB203580 concentrations added at isolation for 24h ( $P < 0.05$  for Young vs. Old 0  $\mu$ M SB;  $P < 0.0001$  for Young 0  $\mu$ M vs. 25  $\mu$ M SB and for Old 0  $\mu$ M SB vs. 10  $\mu$ M SB, by two-way ANOVA. Mean  $\pm$  s.e.m.,  $n = 3$  experiments, for  $\geq 20$  myofibers scored per condition).

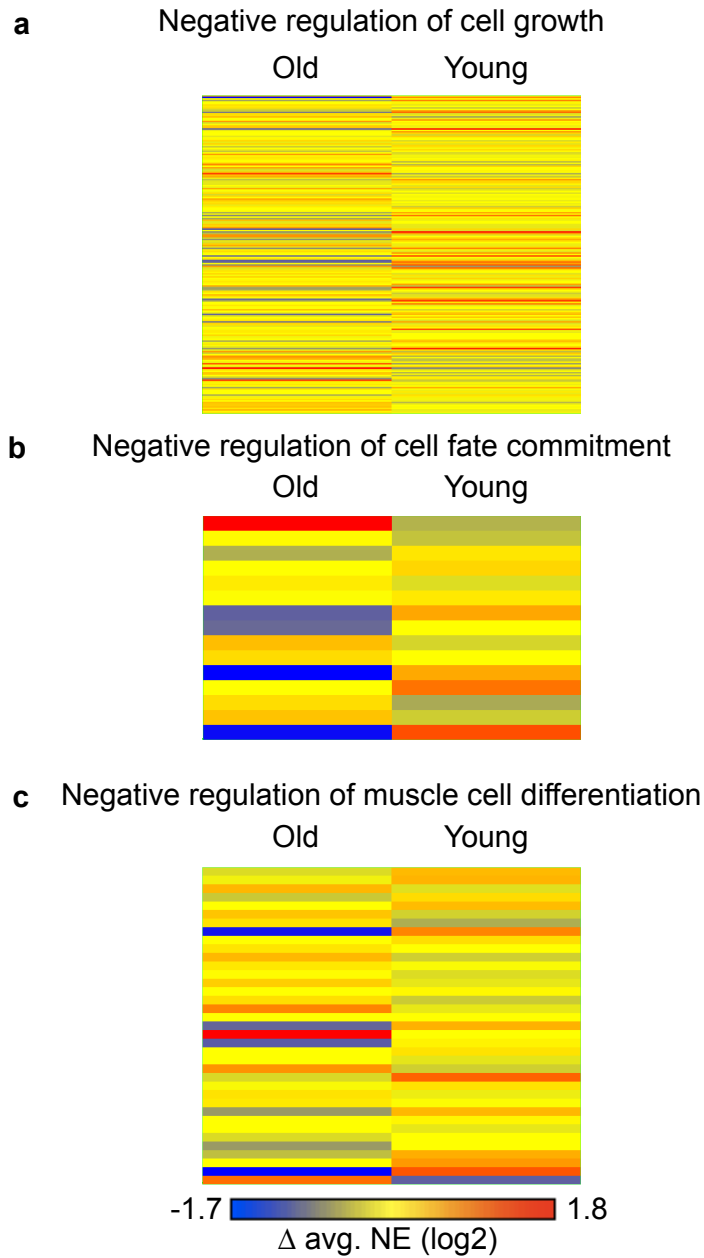


**FIGURE 2.8. Transcripts related to inhibition of differentiation are decreased in old satellite cells.** Heat maps of transcripts from young and old microarrays included in the GO Terms: GO:0030308 Negative regulation of cell growth, GO:0010454 Negative regulation of cell fate commitment, and GO: 0051148 Negative Regulation of muscle cell differentiation. Red indicates increased expression and blue indicates decreased expression.

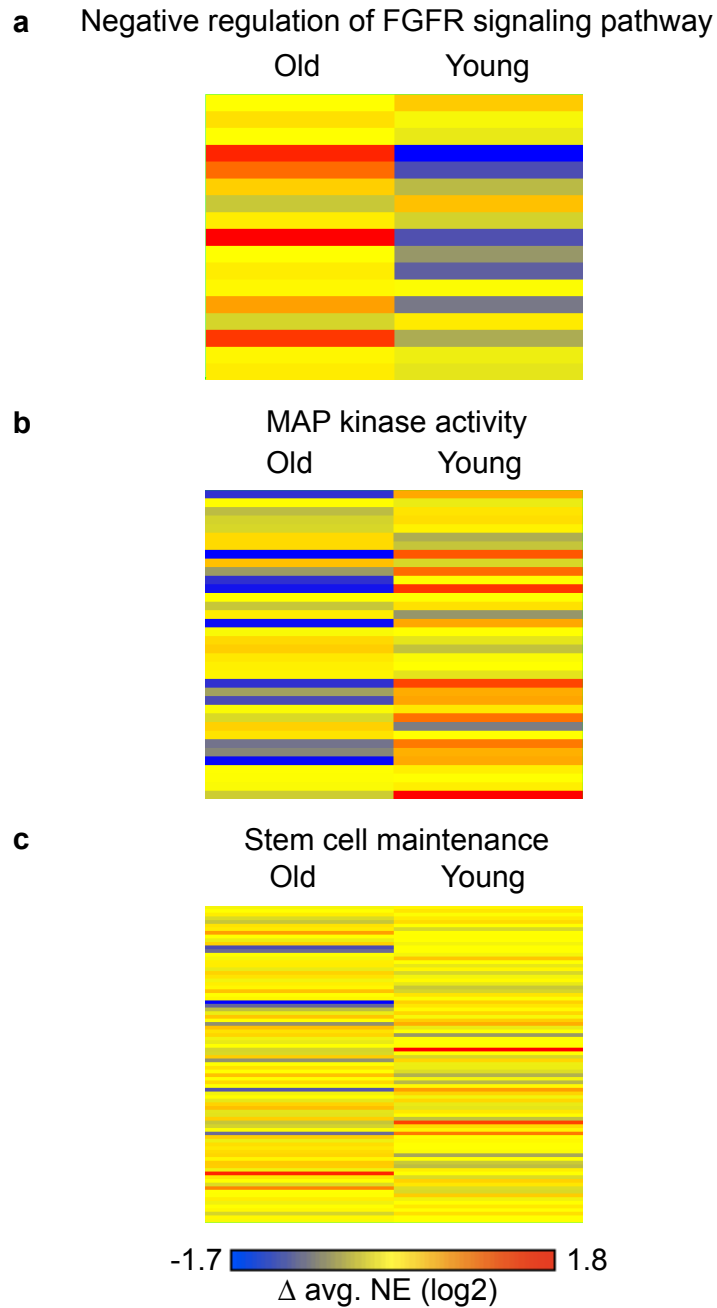


**FIGURE 2.9. Transcripts related to self-renewal and p38 $\alpha$  $\beta$  MAPK/FGF signaling are decreased in old satellite cells.** Heat maps of transcripts from young and old microarrays included in the GO Terms: GO: 0040037 Negative regulation of FGFR signaling pathway, GO: 0004707 MAP kinase activity, and GO: 0019827 Stem cell maintenance. Red indicates increased expression and blue indicates decreased expression.

**TABLE 2.1. IPA pathway analysis of transcripts changing >4-fold between young and old satellite cells.**

<b>Top Networks for transcripts changing &gt;4-fold Young/Old</b>
1-DNA Replication, Recombination, and Repair, Cellular Response to Therapeutics, Cancer
2-Organ Morphology, Skeletal and Muscular System Development and Function, Carbohydrate Metabolism
3- Embryonic Development, Tissue Development, Organismal Survival
4-Organ Morphology, Skeletal and Muscular System Development and Function, Cellular Assembly and Organization
5-Gene Expression, Tissue Development, Cellular Development

<b>Top Canonical Pathways</b>	<b>p-value</b>
Mitochondrial Dysfunction	2.38E-06
Glycolysis I	1.12E-05
Gluconeogenesis I	1.50E-05
Calcium Signaling	3.60E-04
ILK Signaling	5.88E-04

<b>Top Bio Functions-Molecular and Cellular Functions</b>	<b>p-value</b>
Cell Cycle	8.27E-06 - 3.86E-02
Post-Translational Modification	2.48E-04 - 4.71E-02
Cell Death and Survival	6.52E-04 - 4.41E-02
Molecular Transport	7.30E-04 - 4.41E-02
Cell Morphology	8.67E-04 - 4.38E-02

**TABLE 2.2. IPA pathway analysis of transcripts changing >6-fold between young and old satellite cells.**

<b>Top Networks for transcripts changing &gt;6-fold Young/Old</b>
1-Cancer, Gastrointestinal Disease, Hepatic System Disease
2-Cardiovascular Disease, Cardiovascular System Development and Function, Organ Morphology
3-Carbohydrate Metabolism, Skeletal and Muscular System Development and Function, Organ Morphology
4-Inflammatory Response, Humoral Immune Response, Protein Synthesis
5-Connective Tissue Disorders, Hematological Disease, Infectious Disease

<b>Top Canonical Pathways</b>	<b>p-value</b>
Calcium Signaling	6.37E-06
Glycolysis I	3.51E-05
Gluconeogenesis I	4.70E-04
Glycerol-3-phosphate Shuttle	2.87E-03
NRF2-mediated Oxidative Stress Response	3.38E-03

<b>Top Bio Functions-Molecular and Cellular Functions</b>	<b>p-value</b>
Carbohydrate Metabolism	4.70E-04 - 4.15E-02
Cell Cycle	5.89E-04 - 3.73E-02
Cellular Assembly and Organization	5.89E-04 - 4.31E-02
Cell Death and Survival	1.41E-03 - 4.31E-02
Molecular Transport	1.41E-03 - 4.31E-02

25 $\mu$ M SB203580 virtually eliminated asymmetric phospho-p38<sup>+</sup> young and phospho-p38<sup>+</sup> aged satellite cells (Figure 2.7d). Unexpectedly, partial inhibition of p38 $\alpha\beta$  MAPK signaling with 10 $\mu$ M SB203580 dramatically enhanced asymmetric phospho-p38 in aged satellite cells but not young satellite cells (Figure 2.7d), suggesting that excessive activation of p38 $\alpha\beta$  MAPK in aged satellite cells interferes with asymmetric p38 $\alpha\beta$  MAPK activation.

### **Partial inhibition of p38 $\alpha\beta$ MAPK signaling restores aged satellite cell self-renewal.**

The restoration of asymmetric phospho-p38 by partial inhibition of p38 $\alpha\beta$  MAPK suggests that self-renewal in aged satellite cells may be similarly rescued. I employed a dye retention assay we have previously used (Troy et al., 2012) to test this hypothesis whereby cell permeable carboxyfluorescein diacetate, succinimidyl ester (CFDA-SE) is acquired by all cells but is retained only in quiescent or differentiated non-cycling cells (Figure 2.10a). Quiescent Pax7<sup>+</sup>satellite cells that retained CFDA-SE were present in young and aged cultures (Figure 2.10b). Compared to young satellite cells, there was a 4-fold reduction in aged quiescent CFDA<sup>+</sup>/Pax7<sup>+</sup> satellite cells (Figure 2.10c). This reduction was rescued by partial p38 $\alpha\beta$  MAPK inhibition and exacerbated by complete inhibition of p38 $\alpha\beta$  MAPK signaling (Figure 2.10c). Consistent with a role for FGF signaling in asymmetric division of satellite cells, addition of SU5402 nearly eliminated generation of quiescent daughters in young satellite cells, reducing self-renewal to the low levels observed in aged cultures (Figure 2.10d). Together, our data indicate that FGF signaling via p38 $\alpha\beta$  MAPK plays a critical role in satellite cell self-renewal by promoting asymmetric division of satellite cells to generate quiescent daughter cells.

### **Constitutive FGFR1 signaling rescues self-renewal in aged satellite cells**

Our observations that aged satellite cells exhibit FGF-2 insensitivity (Figure 2.4g-n), and

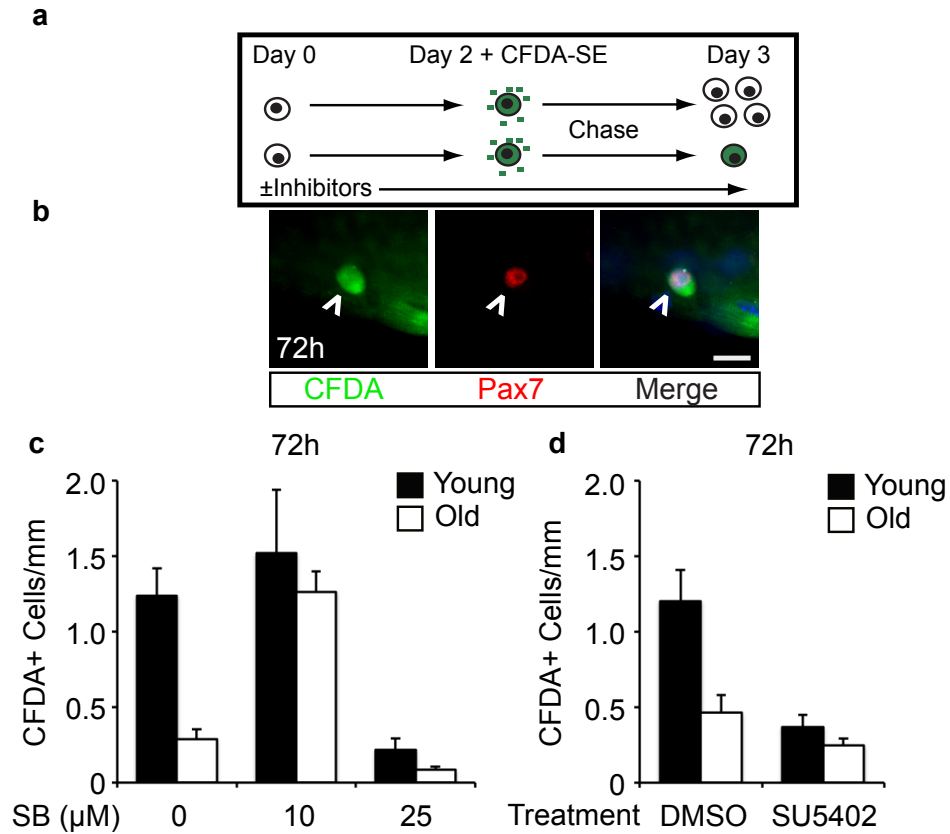


**FIGURE 2.10. Partial inhibition of p38 $\alpha\beta$  MAPK rescues self-renewal in aged satellite cells.** (a) CFDA-SE retention schematic shows CFDA-SE label is acquired by all cells (green) but following a chase is retained only in non-dividing cells (green). (b) CFDA-SE was added at 24h to myofiber cultures from young and old mice for 15 min, washed out and myofibers maintained in the presence or absence of either SB203580 (SB) or SU5402 for 72h, fixed and visualized (b) for CFDA retention, Pax7+ immunoreactivity and DAPI ( $\wedge$  marks a young CFDA+/Pax7+ untreated satellite cell; scale bar=10  $\mu\text{m}$ ). After 72h treatment with (c) 0-25  $\mu\text{M}$  SB203580 or (d) SU5402 CFDA-SE+/Pax7+ satellite cells were quantified, and plotted normalized to myofiber length. ( $P < 0.05$  for Young vs. Old in 0  $\mu\text{M}$  SB, for Young vs. Old in DMSO, for Young 0 $\mu\text{M}$  SB vs. 25  $\mu\text{M}$  SB, for Old 0 $\mu\text{M}$  SB vs. 10  $\mu\text{M}$  SB, and for Young DMSO vs. SU5402, all by two-way ANOVA).

elevated activity of the p38 $\alpha\beta$  MAPK pathway coupled with prior studies documenting the upregulation of FGF-2 in aged muscle (Chakkalakal et al., 2012), all suggest that aged satellite cells are compensating for an attenuation of FGFR1 signaling. Therefore, I asked if enhancing FGFR1 activity could increase self-renewal of aged satellite cells. I utilized an inducible, constitutively active FGFR1 (iFR1) (Whitney et al., 2001; Stevens et al., 2007) to provide ligand-independent FGFR1 signaling via small molecule-induced dimerization (Whitney et al., 2001). Upon isolation, myofiber-associated satellite cells were transfected with iFR1 expression vectors, treated with Dimerizer B/B to activate iFR1 (Whitney et al., 2001; Stevens et al., 2007) and harvested at 72h for immunofluorescence analysis (Figure 2.11a). The iFR1<sup>+</sup> satellite cells were scored for Pax7 and Myogenin to determine if ligand-independent activation of FGFR1 signaling altered self-renewal (Figure 2.11b). In the absence of iFR1 dimerization, fewer Pax7<sup>+</sup> and more Myogenin<sup>+</sup> cells were present in aged satellite cells than in young controls (Figure 2.11c). Activation of iFR1 dramatically increased Pax7<sup>+</sup> cells at the expense of Myogenin<sup>+</sup> cells in both aged and young cultures to similar levels (Figure 2.11c). I then assayed for enhanced self-renewal by CFDA-SE dye retention assay in aged satellite cell cultures (Figure 2.11d). To distinguish terminally differentiated cells from quiescent cells, CFDA-SE<sup>+</sup> myofiber-associated cells were stained and scored for iFR1 and Pax7 (Figure 2.11e). Addition of either Dimerizer B/B or FGF-2 yielded similar numbers of CFDA-SE<sup>+</sup> label-retaining cells in young cultures, indicating equivalent young satellite cell self-renewal from ectopic iFR1 signaling or FGF-2 addition (Figure 2.11f). In contrast, FGF-2 treatment elicited no response in aged SCs but iFR1 activation increased the aged CFDA-SE<sup>+</sup>/Pax7<sup>+</sup> satellite cells nearly 4-fold (Figure 2.11f, g). That aged satellite cell self-renewal can be rescued by intracellular FGFR1 signaling and is

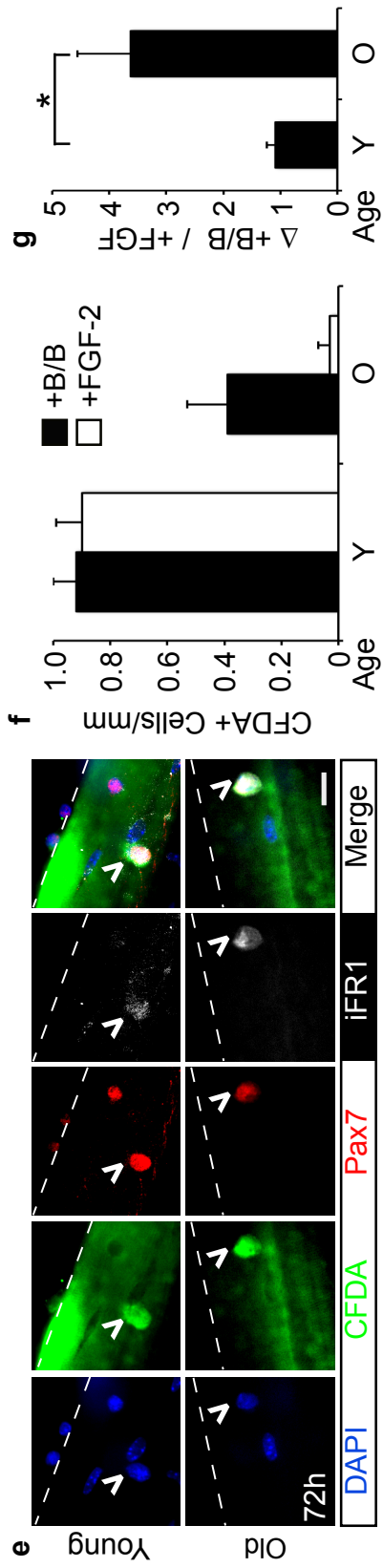
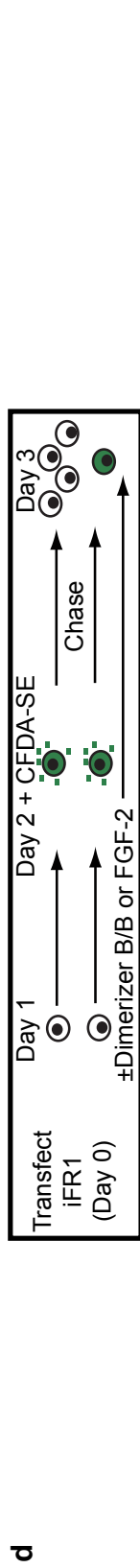
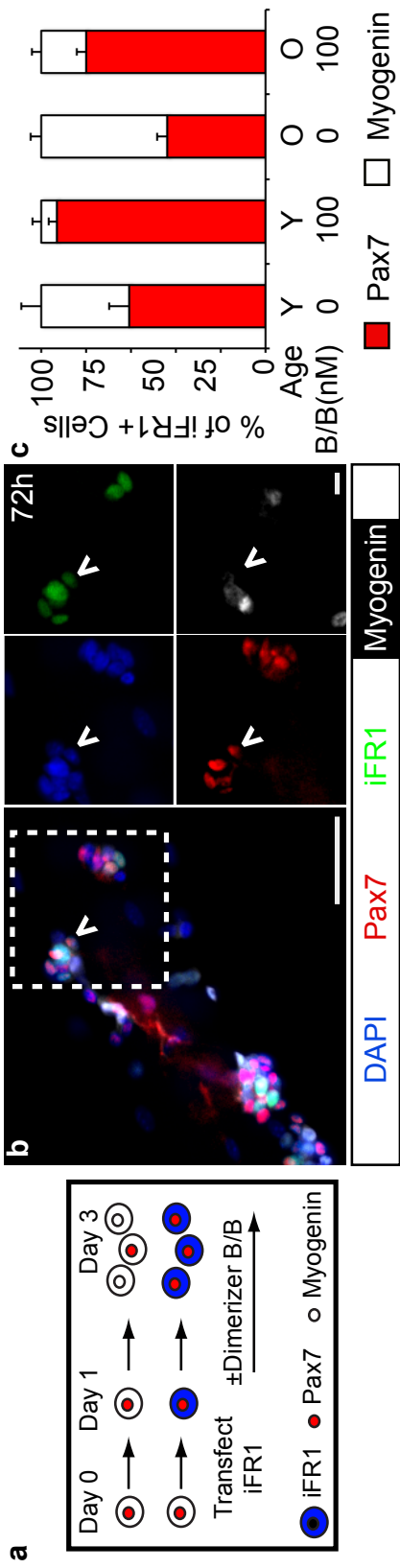


**FIGURE 2.11. Constitutive FGFR1 signaling partially rescues cell autonomous self-renewal defect in aged satellite cells.** (a) A schematic depicting transfection of myofiber-associated satellite cells upon isolation and treatment with Dimerizer B/B at 24h followed by scoring at 3d for Pax7+(red nuclei), Myogenin+ (white nuclei) and iFR1 (blue). (b) Myofiber-associated satellite cells from young and old mice satellite cells transfected and treated as in (a), fixed and stained for Pax7, iFR1 and Myogenin ( $\wedge$ , marks a clone of Pax7+/iFR1+ satellite cells). The dotted box denotes the magnified insets of the Pax7+/iFR1+ clone (Scale bars=50  $\mu$ m or 10  $\mu$ m, inset). (c) Satellite cells from (b) were scored and the percent of iFR1+ cells that were Pax7+ or Myogenin+ plotted for young and old cultures treated in the presence or absence of Dimerizer B/B (B/B;  $P < 0.05$  for both Young and Old 0nM vs. 100 nM B/B, by one-way ANOVA). (d) A schematic depicting myofiber-associated satellite cells transfected with iFR1 as in (a), treated with Dimerizer B/B or FGF-2 at 24h, and pulsed with CFDA-SE at 48h to assess if iFR1 rescues self-renewal. CFDA-SE label is acquired by all cells (green) but following a chase is retained only in non-dividing cells (green). (e) At 72h, young and old satellite cells were fixed and imaged to quantify iFR1+ young and old myofiber-associated satellite cells that were CFDA+/Pax7+ ( $\wedge$ ). (f) The CFDA+/Pax7+ young and old satellite cells were quantified and normalized per myofiber length ( $P < 0.05$ , for Young vs. Old B/B, Young vs. Old FGF-2, Old B/B vs. FGF-2, by two-way ANOVA). (g) The fold change in Pax7+/CFDA+ myofiber-associated satellite cells was calculated and plotted as a ratio of Dimerizer B/B-treated/FGF-2-treated dye-retaining satellite cells ( $P < 0.05$  by  $t$  test; scale bar=10  $\mu$ m; mean $\pm$ s.e.m.,  $n=3$  experiments with  $\geq 20$  myofibers scored).

sensitive to the levels of phospho-p38 (Figure 2.10a-d) reinforces the notion that the FGF/p38 $\alpha\beta$  MAPK signaling axis is a critical cell autonomous regulator of satellite cell function. Disruptions of this core signaling network contribute to age-associated deficits in satellite cell proliferation and self-renewal (Figure 2.12).

## **DISCUSSION**

Skeletal muscle function and mass decline with age beginning around 40y in men (Faulkner et al., 2007). Sarcopenia, a more severe loss of muscle mass and function, leads to frailty, increased morbidity and increased health care costs (Baumgartner et al., 1998; Landi et al., 2013; Janssen et al., 2004). The mechanisms involved in sarcopenia are only beginning to be understood but clearly involve major metabolic changes in muscle tissue (Ruegg and Glass, 2011) and reductions in skeletal muscle regeneration (Brooks and Faulkner, 1990; Grounds, 1998; Day et al., 2010). Previous work suggested that an altered global environment in aged mice inhibited satellite cell function and that aged satellite cells could be rescued by exposure to a young environment (Collins et al., 2007; Carlson and Faulkner, 1989; Carlson and Faulkner, 1996; Conboy et al., 2005; Brack and Rando, 2007). The present study aimed to address two major unresolved issues: 1) whether aged satellite cells exhibit cell intrinsic alterations in self-renewal and 2) the long-term behavior of aged satellite cells transplanted to a young environment. I performed an in-depth analysis of satellite cell self-renewal finding that aged satellite cells fail to robustly self-renew. I then asked if transplantation of aged satellite cells onto young myofibers or into young host muscle could rescue the reductions in aged satellite cell self-renewal. The failure of the young environment to rescue aged satellite cell self-renewal identified cell-autonomous deficits in aged satellite cell self-renewal where alterations in an

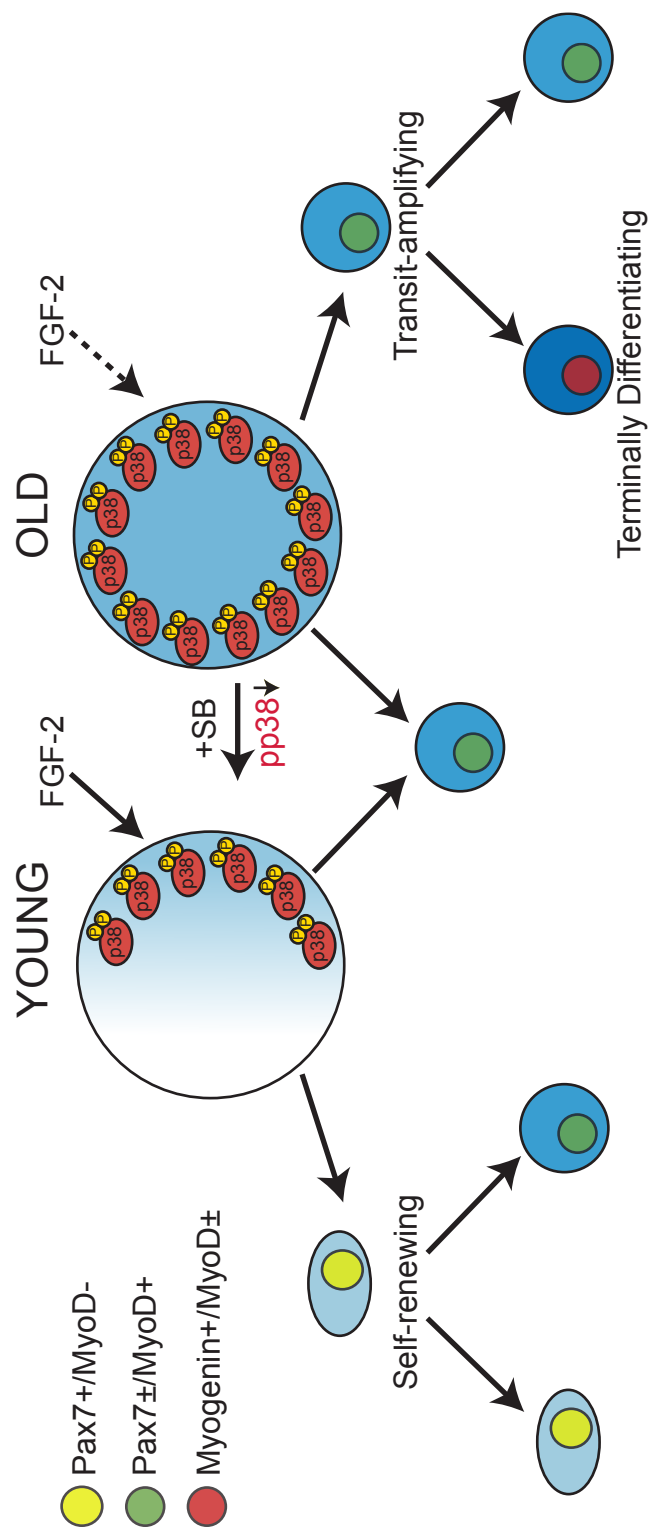


**FIGURE 2.12. Model for cell autonomous loss of aged satellite cell self-renewal.** Aged satellite cells exhibit attenuated FGF-R1 signaling and elevated p38 $\alpha$  $\beta$  MAPK activity, preventing asymmetric p38 $\alpha$  $\beta$  MAPK activation, generating committed transit-amplifying myoblast daughters. Partial inhibition of p38 $\alpha$  $\beta$  MAPK promotes a young cell phenotype whereby asymmetric p38 $\alpha$  $\beta$  MAPK permits generation of a quiescent daughter stem cell and committed transit-amplifying myoblast from an asymmetric division.

FGF/p38 $\alpha\beta$  MAPK signaling axis appear at the core of these age-associated deficits.

Elevated p38 $\alpha\beta$  MAPK activity is present in freshly isolated aged satellite cells when compared to young satellite cells. Accompanying the elevated p38 $\alpha\beta$  MAPK signaling is an attenuation of FGFR1 activity upon ligand binding. I propose that the elevated p38 $\alpha\beta$  MAPK activity is a compensatory response to the loss of FGF sensitivity, and furthermore, hyperactive p38 $\alpha\beta$  MAPK prevents asymmetric p38 $\alpha\beta$  MAPK signaling, thus disrupting asymmetric division and the generation of quiescent daughter cells (Figure 2.12). The observation that partial inhibition of p38 $\alpha\beta$  MAPK signaling restores (i) generation of Pax7<sup>+</sup> cells, (ii) asymmetric phospho-p38 $\alpha\beta$  MAPK, (iii) and generation of quiescent dye-retaining daughter cells in aged satellite cells, to levels comparable to young satellite cells, strongly supports this model. Moreover, near complete inhibition of p38 $\alpha\beta$  MAPK virtually eliminates self-renewal demonstrating that p38 $\alpha\beta$  MAPK is required for satellite cell maintenance. Other published work demonstrates that elevated p38 $\alpha\beta$  MAPK signaling promotes myoblast differentiation (Stevens et al., 2007; Faulkner et al., 2007) which may exacerbate the failure of aged satellite cells to expand irrespective of the surrounding environment. Together, these data support a critical role for p38 $\alpha\beta$  MAPK in satellite cell self-renewal, suggesting that the subcellular localization, duration of signaling, and timing of p38 $\alpha\beta$  MAPK activation are highly regulated to permit asymmetric division and satellite cell self-renewal.

While the role of FGFR1 in regulating satellite cell self-renewal is less clear, observations that loss of FGFR1 signaling *in vivo* reduces skeletal muscle mass during development (Flanagan-Steet et al., 2000), that FGFR1 is expressed in freshly isolated satellite cells (Cornelison et al., 2001), and that FGFR1 signaling represses myogenesis in satellite cell

lines (Kudla et al., 1998), together suggest that FGFR1 signaling plays an important role in regulating satellite cell function. Consistent with these are observations that (i) FGFR1 signaling is disrupted in Syndecan-4 null mice (Cornelison et al., 2004), (ii) Syndecan-4 null satellite cells fail to engraft and expand when transplanted into wild type muscle (Hall et al., 2010), (iii) . FGF-2 pretreatment of young donor satellite cells prior to transplantation maintains lifelong satellite cell self-renewal, (iv) FGFR1 signaling is attenuated in aged satellite cells, and (v) aged satellite cell self renewal is rescued by ligand-independent, ectopic FGFR1 stimulation. As FGF stimulation of FGFR1 activates p38 $\alpha\beta$  MAPK in satellite cells (Jones et al., 2005; Cornelison et al., 2004) and ectopic FGFR1 signaling rescues self-renewal it seems likely that FGFR1 signaling is involved in asymmetric p38 $\alpha\beta$  activation and asymmetric satellite cell division. The attenuation of FGFR1 activation by FGF-2 in aged satellite cells could arise from changes in either FGFR1 interactions with other cell surface proteins or from altered heparan sulfate since FGF binding and signaling from FGFR1 requires a ternary complex comprising heparan sulfate, FGFR1 and the FGF ligand (Yayon et al., 1991; Rapraeger et al., 2000; Schlessinger et al., 2000). Thus, alterations in either FGFR1 or heparan sulfate, observed in other aging tissues (Huynh et al., 2012; Williamson et al., 2013), could contribute to the decline in signal transduction efficiency and cell autonomous loss of satellite cell self-renewal.

between FGFR1 signaling, p38 $\alpha\beta$  MAPK activation, and satellite cell asymmetric division and self-renewal that is deregulated in aged satellite cells and reduces self-renewal while promoting terminal differentiation. While the precise mechanism of FGFR1 involvement in asymmetric activation of p38 $\alpha\beta$  MAPK is unclear, it is an area primed for future investigation. Interestingly, recently published data demonstrate that satellite cell-specific loss of p38 $\alpha$  MAPK

promotes satellite cell expansion, reduces muscle mass and myofiber area (Brien et al., 2013). Thus, FGF/p38 $\alpha$  $\beta$  MAPK signaling is a potentially new therapeutic target for manipulation of skeletal muscle regeneration.

## **METHODS**

### **Animal Studies**

Animal experiments in this study were performed in accordance with protocols approved by the Institutional Animal Care and Use Committee at the University of Colorado. Female C57BL/6 mice (Jackson Labs and the National Institutes on Aging) were used for all *ex vivo* experiments. Transplant recipients were female C57Bl/6xDBA2 mice (Jackson Labs) while donor tissue was isolated from female,  $\beta$ -actin GFP (FVB.Cg-Tg(CAG-EGFP)B5Nagy/J; Jackson Labs) mice referred to as  $\beta ActGFP$ , (Hall et al., 2012) with sample size determined by power analysis of previous transplantation studies. Mice were used at 3-6 months of age (Young, median 4 months) or 20-25 months of age (Aged/Old, median 23 months).  $\beta ActGFP$  mice were aged in our facilities for transplantation assays.

### **Cell Isolation, Culture and Transfection**

SCs were isolated by enzymatic digestion of whole hindlimb skeletal muscle and preplated on uncoated plates overnight at 6% O<sub>2</sub>. Cells were then cultured on gelatin-coated 6-well plates (~10,000 cells/well) in growth medium (F12-C + 15% horse serum)  $\pm$  1.5 nM FGF-2 at 6% O<sub>2</sub> for 1-5d.

Myofibers with associated SCs were isolated as previously described (Troy et al., 2012). For all experiments, myofibers were cultured in growth medium, F12-C (Life Science Products) + 15% horse serum  $\pm$  1.5 nM FGF-2 at 6% O<sub>2</sub> with daily medium and reagent changes. AraC

(Sigma Aldrich) was used at 100  $\mu$ M, CFDA-SE (Invitrogen) at 10  $\mu$ M, SU5402 (Tocris) at 25  $\mu$ M, SB203580 (Tocris) at 10 and 25  $\mu$ M, sodium orthovanadate at 2mM (Sigma Aldrich), and Dimerizer B/B at 100  $\mu$ M (B/B Homodimerizer, previously AP20187, Clontech).

For transfection experiments, we purchased the plasmid pSH1/M-FGFR1-Fv-FV12-E containing the inducible iFGFR1 construct from Addgene (Addgene plasmid 15285) (Welm et al., 2002). I transfected the iFGFR1 construct or performed a mock transfection into myofiber-associated SCs with Lipofectamine 2000 (Invitrogen) 8h post-isolation. Dimerizer B/B was added 24h post-transfection, and added with daily media changes until fixation at 72h.

For CFDA-SE retention assay, myofiber-associated cells were transfected as above and treated with Dimerizer B/B or FGF-2 after 24h. At 48h, CFDA-SE in Dulbecco's PBS was added for 15 min then myofibers were washed three times with growth media to remove excess CFDA. For each experiment, a subset of myofibers was fixed 30 min post-CFDA-SE treatment to verify CFDA uptake by all Syndecan-4+ SCs. The remaining myofibers were transferred to growth media with FGF-2 or Dimerizer B/B and fixed at 72h.

### **Myofiber Transplantation**

For heterochronic local transplantation assays, satellite cells from  $\beta$ *ActGFP* were isolated alongside myofibers from wild type mice. Cells were preplated (2-3h) on an uncoated plate during myofiber isolation. A total of  $2 \times 10^4$  cells were mixed with 50 myofibers in a 0.2 mL microcentrifuge tube in 0.2 mL warm growth media containing 1.5 nM FGF-2. The mixture was rotated slowly at 37°C for 3.5h then myofibers were gently transferred to individual tissue culture plates for three successive washes with fresh growth media to remove unattached cells, and cultured for 24 or 72h as described above.

Transplantation of myofiber-associated satellite cells to host *tibialis anterior* muscle was performed as previously described (Hall et al., 2010) except that myofibers were pretreated for 5h with or without 1.5 nM FGF-2 prior to injection. Recipients were randomly selected from a group of young C57BL/6 mice ~4 months of age. TA muscles were harvested and sections processed as previously described in that protocol. To count the number of donor satellite cells, I scored ~10 fields across at least four serial 10  $\mu$ m sections from mid-muscle. Fields scored were 750  $\mu$ m x 750  $\mu$ m. Range in reported sample size due to attrition between injury and harvest.

### **Flow cytometry and analysis**

For phosphorylation analysis, SCs were isolated and cultured in growth media with 25  $\mu$ M SU5402 (Tocris) or dimethyl sulfoxide (DMSO) on uncoated plates for 16h (starved of FGF-2). Additional SU5402 or DMSO and 2mM sodium orthovanadate were added 1h before FGF-2 stimulation. Cells were pulsed with or without FGF-2 in Bovine Serum Albumin (BSA) for 5 min then fixed in 4% paraformaldehyde at 4°C, remaining at 4°C through flow analysis. Sodium orthovanadate (Sigma Aldrich) was added to all reagents through primary antibody staining. Cells were permeabilized with 0.1% Triton X-100 then washed and blocked in 2% Fetal Bovine Serum (FBS). Cells were stained with 1:1000 chicken anti-Syndecan-4 and 1:50 mouse anti-phospho-p38 MAPK (Cell Signaling 9216S) or no primary control for 1h in 2% FBS in PBS, then 30 min for secondary antibodies (anti-chick AlexaFluor 647 and anti-mouse AlexaFluor 488), and stained before analysis with 4',6-diamidino-2-phenylindole (DAPI). Cells were analyzed by flow cytometry (CyAN ADP Analyzer) and data was analyzed in FlowJo 9.6. A gate was set to exclude small debris based off previous analysis of freshly isolated SCs in the Olwin lab. Population shifts in Syndecan-4+/phospho-p38+ cells were quantified by population

comparison (Overton subtraction) in FlowJo.

### **Immunofluorescence**

All cells and tissues were fixed in 4% paraformaldehyde and permeabilized as necessary with 0.1% Triton X-100. Muscle sections were prepared as previously described (Hall et al., Cornelison et al., 2001). All slides were blocked in 3% bovine serum albumin (BSA) 1h at RT and stained in 1% BSA. Primary antibodies were incubated at 4°C overnight, and secondary antibodies incubated 1h at RT. Nuclei were stained with 4',6-diamidino-2-phenylindole (DAPI). The following primary antibodies were used: chicken Syndecan-4 (1:500) (Cornelison et al., 2001), chicken Syndecan-3 (1:50) (Cornelison et al., 2001), mouse Pax7 (Developmental Hybridoma Bank at Iowa University, 1:5), rabbit MyoD (C-20, Santa Cruz Biotechnology, sc-304, 1:400), mouse Myogenin (5FD, Developmental Hybridoma Bank at Iowa University, straight), rabbit p38 MAPK (C-20, Santa Cruz Biotechnology, sc-535, 1:50), mouse phospho-p38 MAPK (Cell Signaling, 9216S, 1:50), rabbit phospho-FGFR (Cell Signaling, 3471S, 1:50), rat HA tag (used to image iFGFR1 transfected cells) (Roche, 11867423001, 1:200), rat Laminin (Sigma, L0663, 1:200). AlexaFluor 488-, 555-, and 647-conjugated secondary antibodies (Invitrogen) were used at 1:500.

### **Microscopy and Image Processing**

A Leica TCS SP2 AOBS confocal microscope with Leica software, using an HC Plan Apochromat 20x/0.70 IMM CORR CS lens was used to image muscle sections or a HCX Plan-Apochromat 40x/1.25-0.75 NA was used to image the local transplantation assay (24h representative image). Micrographs of local transplantation assays for scoring were captured with a Nikon Eclipse E800 equipped with a Sensicam (Cooke) digital camera and Slidebook v4.1

(3i) software with a PlanFluor 20x/NA 0.50 PH1 DLL (Nikon) lens.. All other myofiber experiments were imaged with a Leica DM RXA Spinning Disk confocal microscope with EM-CCD digital camera (Hamamatsu) with Metamorph software (Molecular Devices), using HC Plan APO 20x/0.70 or HCX PL APO 40x/0.85 CORR lenses. A Nikon TE2000-U spinning disk confocal (Yokogawa) microscope equipped with a Cascade II CCD camera (Photometrics) using a Nikon 40x/0.75 DIC MN2 lens captured images for 3D reconstruction. All digital microscopic images were acquired at room temperature. The mounting medium for cells and sections was Vectashield Mounting Medium (Vector). Images were processed then scored with blinding in ImageJ64. As necessary, the brightness and contrast were adjusted linearly for the entire image and adjusted equivalently across the experimental image set. Muscle section images are averaged Z-stacks with Tikhonov-Miller deconvolution (ImageJ64) of the Syndecan-4 and Laminin channels.

### **Microarray and Analysis**

SCs from 6-8 young or old mice were isolated, pooled, and sorted for Syndecan-4 expression as previously described (Tanaka et al., 2009). RNA was isolated followed by two rounds of linear T7-based amplification (RiboAmp HA kit, Arcturus). Labeled RNA (5 $\mu$ g) was hybridized to Affymetrix 430 v.2 mouse microarrays and processed as recommended by the supplier. A total of two chips, each representing a separate pool of mice, were used for each age. Raw data were pre-processed using Genespring software (Agilent) and analyzed for differential gene expression changes occurring over time. For selected heatmaps, individual probeset expression ( $\log_2$ ) from young and old microarray datasets was normalized to the mean relative expression ( $\log_2$ ) from probesets against transcripts of one gene, where multiple probesets are

described for one gene to cover variant transcripts. Pathway analyses were conducted using Ingenuity Pathway Analysis (IPA) software on lists of transcripts changing either 4- or 6- fold between young and old datasets.

### **Statistical analysis**

All values represent the mean  $\pm$  s.e.m. of at least three biological replicates except microarray data, which represent biological replicates from SCs isolated from multiple animals. Statistical differences between groups were determined by unpaired, two-tailed Student's *t*-test, one-way ANOVA with Tukey's post-hoc test or two-way ANOVA with Tukey's post-hoc test using Graph-Pad Prism 6.  $P < 0.05$  was determined to be significant for all experiments. *P* values for signaling networks were determined by IPA software. Actual *P* values and specific statistical tests are listed in each figure legend.

## **Chapter 3: Developing an artificial niche in culture to promote satellite self-renewal**

## **INTRODUCTION**

### **Satellite cells self-renew to maintain the quiescent satellite cell population**

Satellite cells persist in skeletal muscle by self-renewal, which produces quiescent satellite cells to maintain the muscle stem cell population. Both asymmetric and symmetric divisions yield self-renewing satellite cells in culture, but asymmetric division, which produces a quiescent satellite cell and a myoblast, appears to be the dominant mechanism of satellite cell self-renewal (Conboy and Rando, 2002; Shinin et al., 2006; Kuang et al., 2007; Le Grand et al., 2009; Troy et al., 2012). Several molecular mechanisms promote asymmetric division in culture, including Notch-Delta signaling, FGF signaling and asymmetric activation of phosphorylated p38 $\alpha\beta$  MAPK (Kuang et al., 2007; Troy et al., 2012). The satellite cell niche may regulate the activation of these pathways by polar distribution of signaling ligands within the niche, which could restrict Notch or FGF receptor activation to one region of the dividing satellite cell (Mauro, 1961; Kuang et al., 2008; Cosgrove et al., 2009).

### **Maintaining satellite cells in their niche prevents loss of self-renewal**

The local satellite cell niche, a polar environment comprising the basal lamina and the myofiber (Mauro, 1961), maintains satellite cell self-renewal. Culturing satellite cells that have been removed from the niche eliminates the cells' capacity for self-renewal as transplantation of cultured satellite cells produces little engraftment into host skeletal muscle (Montarras et al., 2005). However, transplanting a small number of myofiber-associated satellite cells, either immediately after isolation or after 48h in culture (Bernet, unpublished), enhances self-renewal and results in engraftment throughout the host muscle (Hall et al., 2010). The mechanisms by which satellite cell-myofiber interactions promote self-renewal remain poorly understood and are

difficult to study in myofiber culture. Developing an artificial satellite niche could reduce the complexity present in the myofiber niche and allow us to identify the specific signals that influence satellite cell self-renewal.

### **Hydrogels serve as an artificial satellite cell niche**

Hydrogels, three-dimensional (3D) cross-linked scaffolds, are being developed to recapitulate aspects of tissue microenvironments for cell culture (Tibbitt and Anseth, 2009). Both natural and synthetic materials can form hydrogels, but material from natural tissue sources is poorly defined and exhibits batch-to-batch variability. Synthetic hydrogels, such as those made of (poly)ethylene glycol (PEG), are biocompatible and tunable scaffolds that better serve as artificial stem cell niches. Synthetic hydrogels are highly reproducible and provide a minimalistic approach to cell culture. However, synthetic hydrogels require the addition of molecular signals to direct cell behavior (Slaughter et al., 2009; Tibbitt and Anseth, 2009). Synthetic, PEG hydrogel that are modified to contain proteins found in the myofiber change cell fate in culture to increase satellite cell self-renewal and enhance engraftment after transplantation (Gilbert et al., 2010). These results demonstrate that PEG hydrogels can act as artificial satellite cell niches.

PEG hydrogels can be further optimized to allow for study of the mechanisms underlying satellite cell self-renewal. 4-arm PEG norbornene hydrogels are photopolymerizable, which enables cells to be grown on (2D) or encapsulated within the scaffold to study how niche polarity influences self-renewal. PEG hydrogels are degradable, which allows cells to remodel their environment in culture as cells appear to do *in vivo* (Bryant and Anseth, 2003; Daley et al., 2008; Tibbitt and Anseth, 2009). Additionally, PEG hydrogels may be modified to contain signals

found in a stem cell niche to attempt to regulate self-renewal in culture (Huang et al., 2012; Ding et al., 2013). Thus, these characteristics make PEG hydrogels a minimalist, artificial microenvironment in which to probe the role of the niche in satellite cell self-renewal.

Identifying and screening components of the myofiber niche in PEG hydrogels may help to elucidate the satellite cell-niche interactions that underlie self-renewal. The niche contains structural and biochemical cues to satellite cells that can be incorporated into hydrogels. For example, extracellular matrix (ECM) proteins enable satellite cells to adhere to the niche and signal to satellite cells through cell surface integrins (Giancotti and Ruoslahti, 1999; Sanes, 2003; Weber et al., 2008; Cosgrove et al., 2009). ECM proteins may promote self-renewal by helping stem cells home to the niche and by establishing polarity during asymmetric division (Kim et al., 2011; Chen et al., 2013). Adding ECM proteins present in the satellite cell niche to hydrogels should increase satellite cell self-renewal in culture.

Other important cues in the satellite cell niche that influence self-renewal are growth factors and cell surface and ECM-bound proteoglycans. Heparan sulfate glycosaminoglycan (GAG) chains, which are often linked to proteoglycans, bind heparin-binding growth factors to sequester signals from satellite cells and facilitate growth factor receptor activation in satellite cells. Several growth factors that are present in muscle increase self-renewal in cultured cells (Rapraeger et al., 1991; Olwin and Rapraeger, 1992; Bernfield et al., 1999; Gallagher, 2001; Coutu and Galipeau, 2011; Kraushaar et al., 2013), so incorporating these growth factors into hydrogels should increase self-renewal. However, the specific composition and spatio-temporal distribution of heparan sulfate GAGs in the satellite cell niche are unknown (Jenniskens et al., 2000; Jenniskens et al., 2002; Bink et al., 2003), so the GAG sequences that promote satellite

cell self-renewal must be empirically determined. As heparan sulfate composition may be quite variable, libraries of enzymatically modified heparin, a highly sulfated, but structurally similar GAG to heparan sulfate (Sasisekharan and Venkataraman, 2000), will be used in place of heparan sulfate to reveal GAG sequences that affect satellite cell self-renewal in hydrogel cultures (Puvirajesinghe et al., 2012; Rudd et al., 2011). Thereby, adding both growth factors and heparan sulfate GAG chains to hydrogels will establish which signals regulate satellite cell self-renewal and promote asymmetric division.

In this chapter, I develop degradable, 4-arm PEG hydrogels as an attempt to create an artificial satellite cell niche. I screen putative niche components, including heparin sequences, growth factors, and ECM proteins for the ability to promote satellite cell self-renewal. I find that heparin length and sulfation pattern affect satellite cell activity and that, among the ECM proteins tested, the presence of laminin most successfully increases satellite cell self-renewal. I demonstrate that the distribution of signals in hydrogels affects self-renewal, which supports the model that the polarity found in the niche helps establish asymmetric divisions.

## **RESULTS**

### **Hydrogels are versatile and can be designed to mimic the SC niche**

The mechanisms by which the myofiber niche (Figure 3.1a) promotes self-renewal remain unclear and are difficult to study in myofiber culture. I propose that tunable, degradable 4-arm PEG norbornene hydrogels can serve as an artificial satellite cell niche in culture as these hydrogels can mimic the elasticity and polarity of the myofiber (Figure 3.1c, d). The concentration of PEG (6%wt PEG) in these hydrogels (Figure 3.1e, f) is optimized to produce scaffolds with the elasticity of muscle tissue (Young's modulus ~12 kPa) rather than the stiff

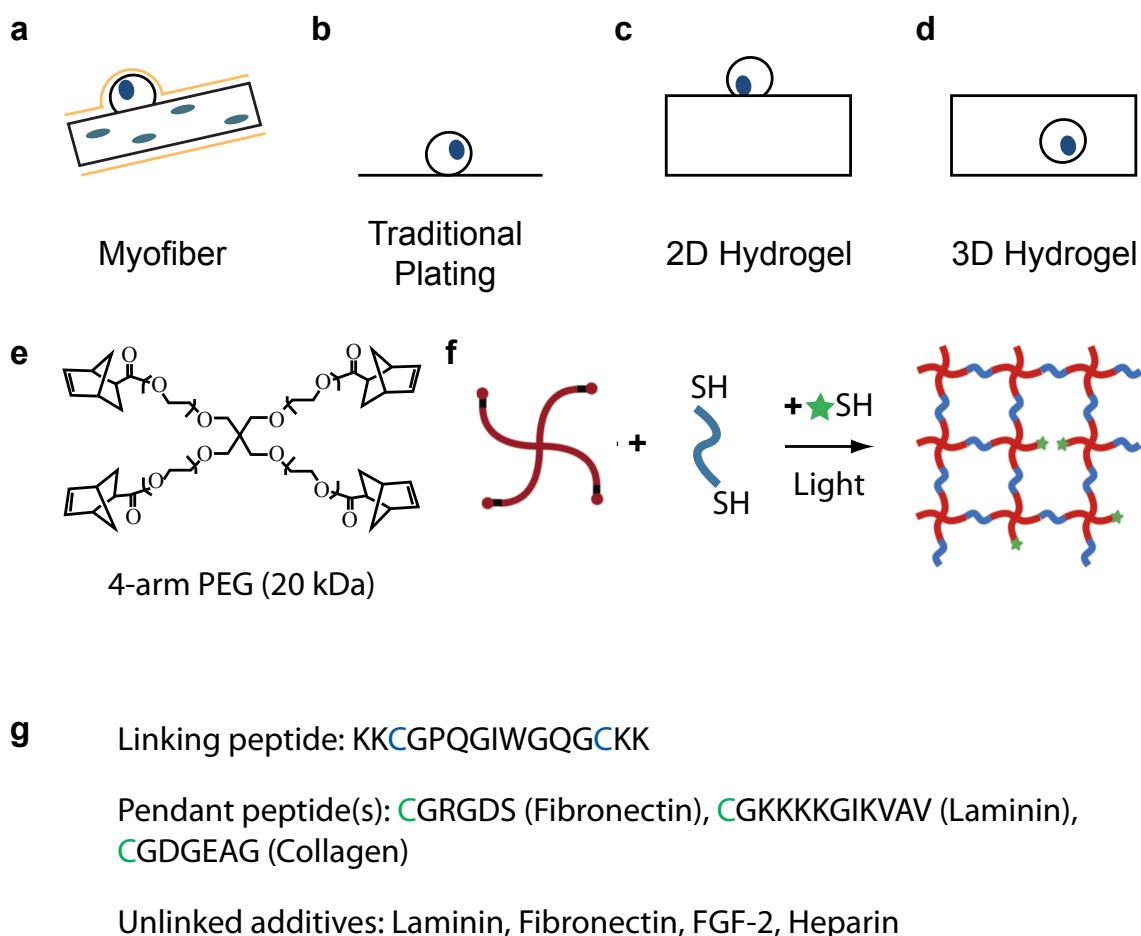


**Figure 3.1: PEG hydrogels serve as a satellite cell niche *in vitro*.** (a) Satellite cells reside on myofibers *in vivo* where satellite cell-myofiber interactions drive satellite cell fate and maintain the quiescent satellite cell pool. (b) Satellite cells are normally cultured on gelatin-coated plastic plates that are both very rigid and that form a polar environment between the plate and the media. After a short time in culture on coated plates, satellite cells lose the ability to engraft into muscle after transplantation. (c,d) Hydrogels better mimic the myofiber niche as rigidity, molecular composition and polarity can be altered to maintain self-renewing satellite cells. In the experiments described in this chapter, satellite cells are cultured on (c) 2D degradable hydrogels or (d) encapsulated in 3D degradable hydrogels. To form these hydrogels, monomer solutions of (e) 4-arm PEG norbornene are mixed with (f) MMP-cleavable linking peptides. (g) Pendant peptides (green) containing integrin-binding sequences from ECM proteins can be covalently incorporated into the matrix or macromolecules can be physically constrained within the gel matrix. For 3D experiments, satellite cells are added to the monomer solution before photopolymerization. Upon exposure to UV radiation, the hydrogel solution polymerizes to form the hydrogel scaffold which is then cultured in growth media.

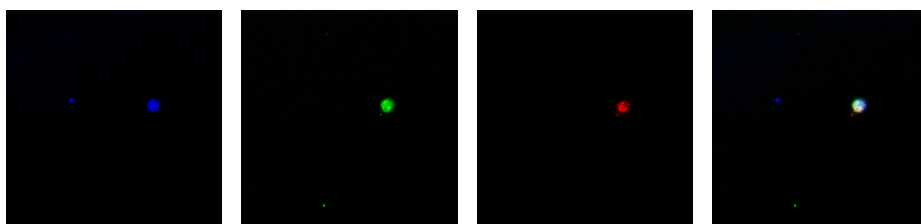
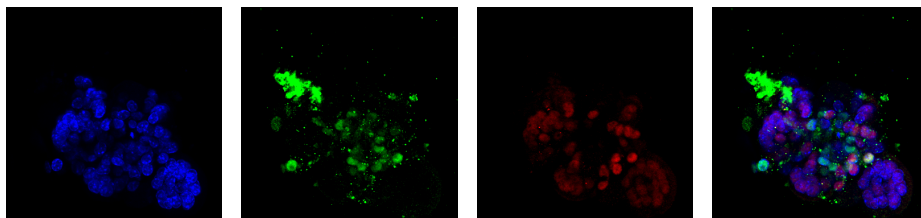
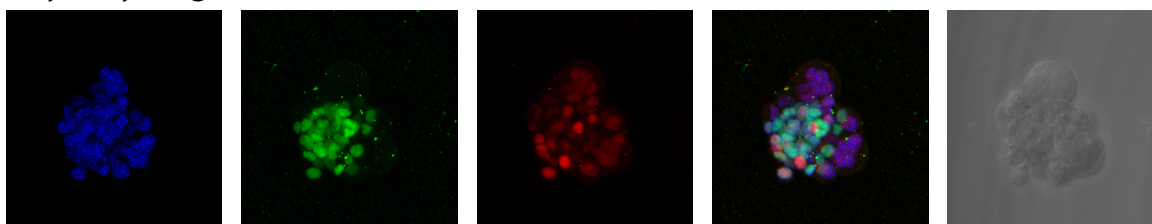
surface of polystyrene plastic plates (Young's modulus  $\sim 3$  GPa) (Figure 3.1b) (Engler et al., 2004; Callister and Rethwisch, 2013; Gilbert et al., 2010). Additionally, these hydrogels provide tools to study polarity in the satellite cell niche as satellite cells can be grown on top of (Figure 3.1c) or encapsulated within hydrogels (Figure 3.1d). By altering the presentation of signals within the hydrogels (polar-2D versus nonpolar-3D), I can ask whether signal distribution in the niche affects satellite cell self-renewal.

### **Optimization of hydrogels for SC attachment and growth**

I first determined whether satellite cells would survive and grow on 2D hydrogels by culturing satellite cells on 6 wt% PEG hydrogels from 0d - 6d (Figure 3.2a, b), then scoring cells for myogenic markers (Figure 3.3a) and proliferation (Figure 3.3b). Satellite cells adhered to hydrogels within 4h of plating (Figure 3.2a) and then entered the cell cycle as indicated by the increase in MyoD immunoreactivity by 24h post-plating (Figure 3.3). By 6d, satellite cells proliferated to form myospheres (clusters of muscle stem cells that resist differentiation in culture (Sarig et al., 2006; Wei et al., 2012)) that consisted of reserve cells (Pax7+/MyoD- cells) and myoblasts (MyoD+ cells) (Figure 3.2, 3.3). The myospheres contained almost no terminally differentiated, Myogenin+ cells, which was unexpected as other types of hydrogels promote myogenic differentiation (Gilbert et al., 2010; Boonen et al., 2009). Thus, I found that 2D, 4-arm PEG norbornene hydrogels were permissive for satellite cell attachment and survival but not for terminal differentiation.

### **ECM molecules increase self-renewal of satellite cells cultured on hydrogels**

I next incorporated ECM proteins into hydrogels to begin to determine which cues in the satellite cell niche affected self-renewal. The most common ECM proteins in the satellite cell

**a** Day 1 Hydrogel**b** Day 6 Hydrogel (2D)**c** Day 6 Hydrogels (3D)**d**

DAPI

Pax7

MyoD

Merge

B.F.

**Figure 3.2: Satellite cells form myspheres in 2D and 3D hydrogel culture.** Satellite cells were cultured on 6 wt% hydrogels with RGDS (2D) or encapsulated within hydrogels (3D), by resuspending satellite cells in 6 wt% 4-arm PEG norbornene monomer solution followed by photo-polymerization with UV light. Hydrogels were fixed then stained and visualized for DAPI (blue), Pax7 (green) or MyoD (red) and by brightfield. **(a)** After 1d, Pax7+/MyoD+ satellite cells were in single cell suspension and sparsely dispersed throughout the 3D hydrogel. By 6d, large, spherical cell clusters formed in both **(b)** 2D and **(c)** 3D culture. The myspheres comprised Pax7+ reserve cells, Pax7+/MyoD+ myoblasts and MyoD+ myocytes, but terminally differentiated Myogenin+ cells were not present. **(d)** Contaminating, nonmyogenic cells formed large, branching structures that were negative for Pax7, MyoD and Myogenin.(Figure 3.3a). By 6d in culture, proliferating (~15-fold increase in cells) satellite cells formed large clusters similar to myspheres (Sarig et al., 2006) (Figures 3.2b, 3.3b) but did not terminally differentiate as no Myogenin+ cells or myotubes were observed (Figure 3.3a). Nonmyogenic cells also adhered to hydrogels and proliferated by 120h (Figure 3.3b), which could be improved by more selective satellite cell isolation. This experiment established that 4-arm PEG norbornene hydrogels with degradable peptides could act as an artificial satellite cell niche.

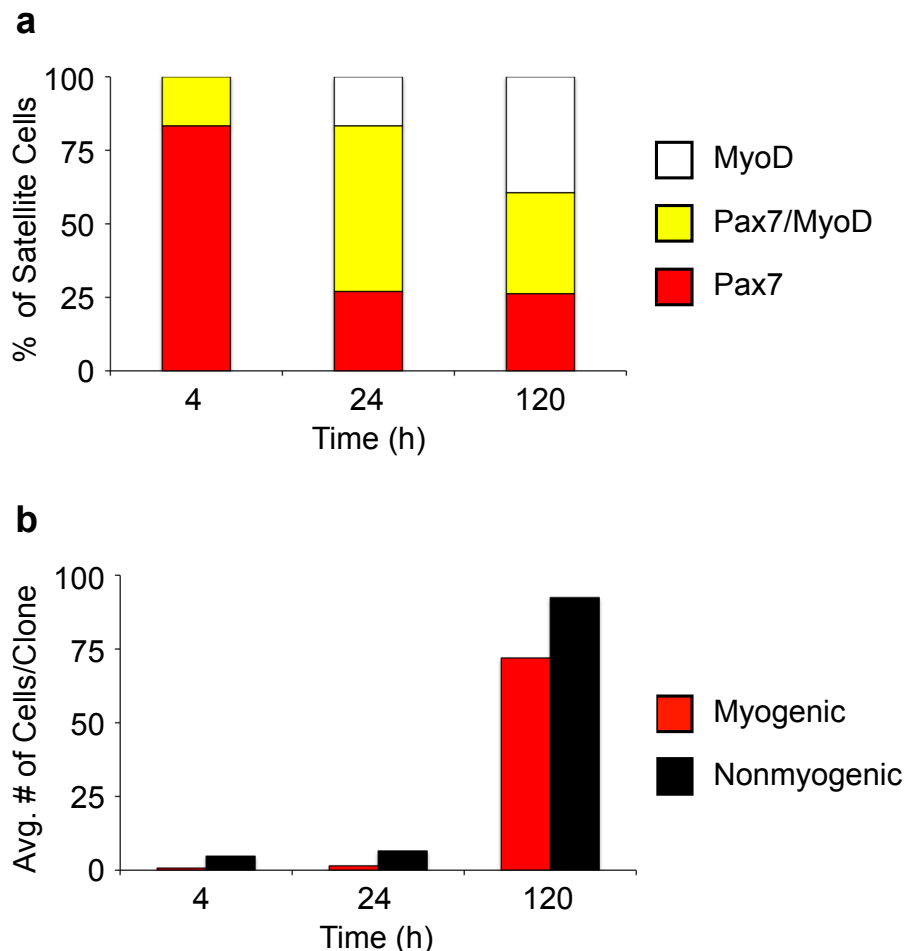


**Figure 3.3: Satellite cells proliferate after adhering to hydrogels.** Satellite cell fate in 2D hydrogels was analyzed to determine if satellite cells self-renew in hydrogel culture. Satellite cells were cultured on 6 wt% hydrogels (2D) containing 300 nM laminin. Hydrogels were fixed at 4h, 24h and 120h, then immunostained and visualized for DAPI, Pax7 and MyoD. **(a)** Pax7 and MyoD immunoreactivity in cells was quantified and plotted as a percentage of the total number of myogenic cells that were Pax7+/MyoD- reserve cells (red), Pax7+/MyoD+ myoblasts (yellow) or Pax7-/MyoD+ committed myocytes (white). Satellite cells adhered to hydrogels (4h) and then began to proliferate (24h) and differentiate (120h) on the hydrogels. **(b)** The average number of myogenic (Pax7+,MyoD+; red) and nonmyogenic (Pax7-/MyoD-; black) cells per hydrogel was calculated and plotted. (Data were from a single experiment).

niche were laminin and collagen whereas fibronectin was common in other stem cell niches. These proteins were known to promote cell adhesion through integrin-binding peptide sequences (Collagen (DGEA peptide) (Staatz et al., 1991), laminin (IKVAV peptide) (Tashiro et al., 1989), and fibronectin (RGDS peptide) (Wright and Meyer, 1985)). I first added the integrin-binding peptides to the hydrogels instead of the full-length proteins to reduce the complexity of signals presented to the satellite cells. Satellite cells were cultured on 2D hydrogels for 6d and were quantified for Pax7/MyoD immunoreactivity. After 24h, similar numbers of cells adhered to all of the hydrogels. By 6d, satellite cells proliferated poorly and exhibited reduced self-renewal (fewer Pax7+/MyoD- cells) on hydrogels containing no peptides (Figure 3.4a), indicating that the base hydrogel was insufficient to promote robust self-renewal. Adding IKVAV peptide to hydrogels increased the percentage of Pax7+/MyoD- reserve cells (3-fold) and Pax7+/MyoD+ myoblasts (3-fold) compared to the unmodified hydrogels. DGEA addition increased the percentage of Pax7+/MyoD- reserve cells 2-fold, increased myogenic proliferation 7-fold, and inhibited the proliferation of nonmyogenic cells (Figure 3.4b). In contrast, RGDS addition did not increase reserve cell generation. These data demonstrated that addition of integrin-binding peptides from ECM proteins present in the niche increased satellite cell self-renewal.

ECM proteins contained other domains, besides the integrin-binding sequences, that could influence satellite cell self-renewal. I repeated the peptide screen with full-length laminin and fibronectin proteins to test whether protein addition increased self-renewal more than peptide addition. I did not screen collagen as hydrogel polymerization could have prevented the formation of collagen's helical structure. Quantifying Pax7/MyoD immunoreactivity revealed that laminin addition to hydrogels increased the proportion of Pax7+/MyoD- reserve cells and

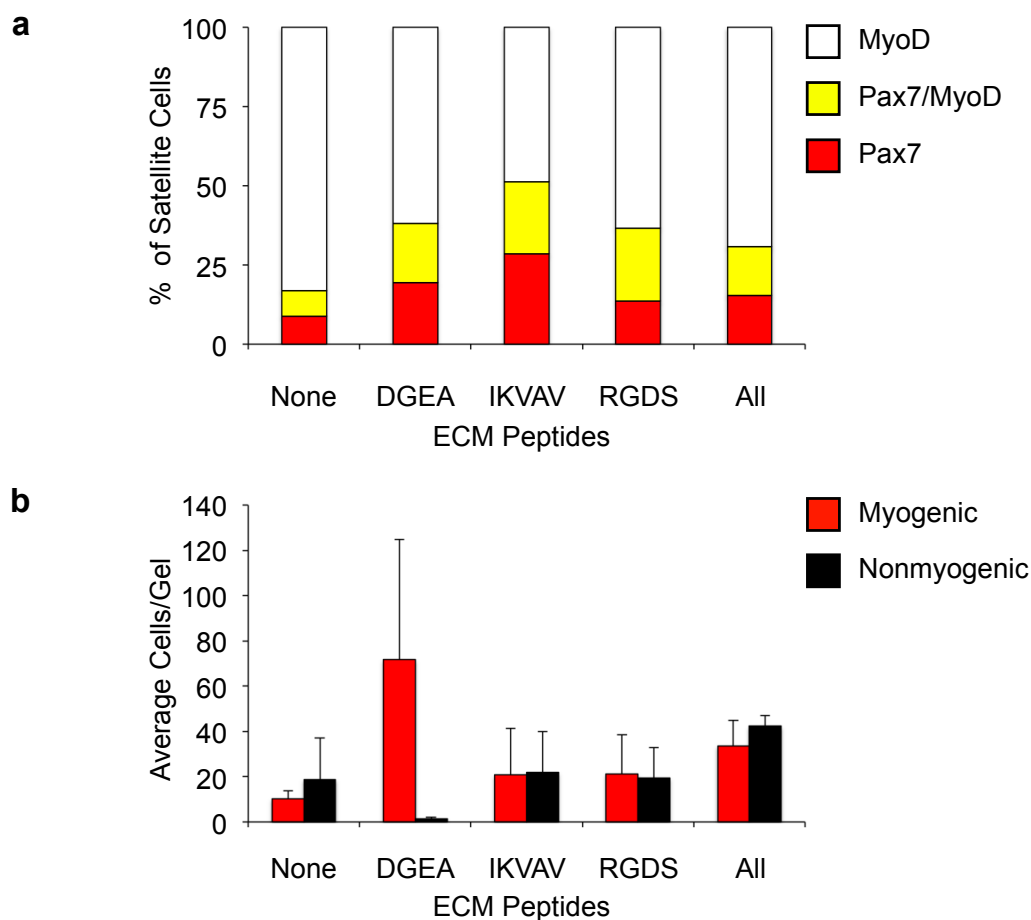


**Figure 3.4: Integrin-binding peptide sequences promote self-renewal in 2D hydrogel culture.** Pendant peptides were incorporated into the hydrogel matrix to determine if these sequences promoted self-renewal in 2D hydrogels. Satellite cells were cultured for 6d on 6 wt% hydrogels (2D) containing DGEA (collagen), IKVAV (laminin) or RGDS (fibronectin) peptides. Hydrogels were fixed, then immunostained and visualized for DAPI, Pax7 and MyoD. **(a)** Pax7 and MyoD immunoreactivity in cells was quantified and plotted as a percentage of the total number of myogenic cells that were Pax7+/MyoD- reserve cells (red), Pax7+/MyoD+ myoblasts (yellow) or Pax7-/MyoD+ committed myocytes (white). The percentage of Pax7+ cells was decreased in hydrogels containing no pendant peptides (None). The percentage of Pax7+/MyoD- cells was increased in IKVAV peptide containing hydrogels, while the percentage of Pax7+/MyoD- cells was decreased in hydrogels containing all three peptides (All). **(b)** The average number of myogenic (Pax7+, MyoD+; red) and nonmyogenic (Pax7-/MyoD-; black) cells per hydrogel was calculated and plotted. (Data represent three independent experiments. Error bars are standard deviation (S.D.)).

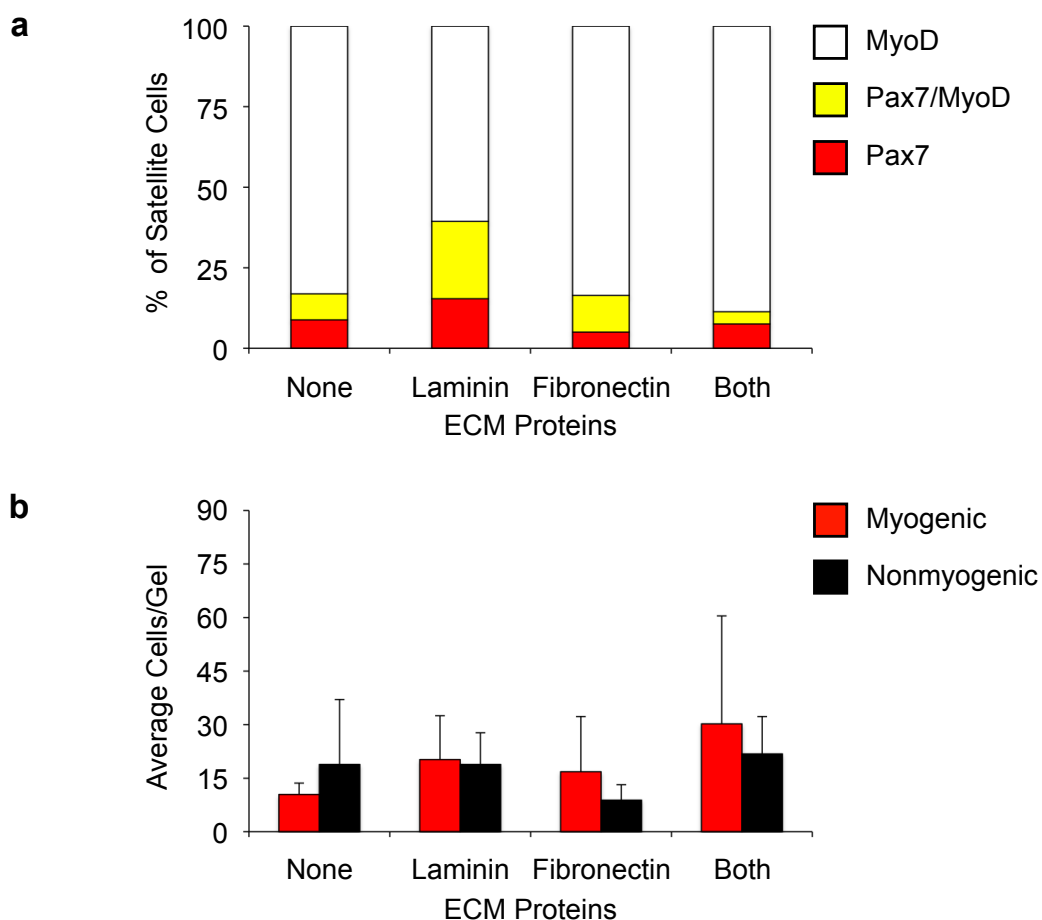


**Figure 3.5: Laminin increases the proportion of self-renewing cells in 2D hydrogel culture.** ECM proteins present in the basal lamina were screened to identify proteins that promoted self-renewal in 2D hydrogels. Satellite cells were cultured for 6d on 6 wt% 4-arm PEG norbornene hydrogels (2D) containing laminin or fibronectin protein. Hydrogels were fixed, then stained and visualized for DAPI, Pax7 and MyoD. **(a)** Pax7 and MyoD immunoreactivity in cells was quantified and plotted as a percentage of the total number of myogenic cells that were Pax7+/MyoD- reserve cells (red), Pax7+/MyoD+ myoblasts (yellow) or Pax7-/MyoD+ committed myocytes (white). The percentage of Pax7+/MyoD- and Pax7+/MyoD+ cells was increased in Laminin containing hydrogels, while hydrogels containing either no protein (None) or fibronectin exhibited a decreased percentage of Pax7+ cells. **(b)** The average number of myogenic (Pax7+,MyoD+; red) and nonmyogenic (Pax7-/MyoD-; black) cells per hydrogel was calculated and plotted (Data represent average of three independent experiments. Error bars are S.D.).

Pax7<sup>+</sup>/MyoD<sup>+</sup> myoblasts 2-3-fold compared to fibronectin addition (Figure 3.5a), but did not increase proliferation (Figure 3.5b). However, laminin increased the percentage of reserve cells less than the IKVAV peptide (Figure 3.4). These data demonstrated that laminin, the most prevalent protein in the basal lamina, promoted self-renewal and that addition of integrin-binding peptides increased self-renewal more than full-length proteins.

### **The concentration and presentation of signals affect satellite cell activity**

The concentration of a signal in the niche can influence satellite cell fate, so I have cultured satellite cells for 6d on hydrogels containing different concentrations of laminin, the ECM protein that most increases self-renewal. Lower concentrations (150 and 300 nM) of laminin increase the proportion of Pax7<sup>+</sup>/MyoD<sup>-</sup> reserve cells 2-fold over cells cultured on a hydrogel containing a higher (600 nM) concentration of laminin (Figure 3.6a). However, addition of 300 nM laminin increases proliferation 3-fold over addition of 150 or 600 nM laminin (Figure 3.6a, b). Thus, the concentration of signal in hydrogels does affect satellite cell activity.

The satellite cell niche contains signals in addition to ECM proteins that direct satellite cell fate, including growth factors like FGF-2. FGF-2 signaling inhibits myogenic differentiation (Clegg et al., 1987), enhances engraftment after transplantation (Hall et al., 2010) and promotes self-renewal in other stem cell populations (Coutu and Galipeau, 2011). I have demonstrated that FGF signaling has a role in satellite cell self-renewal and that FGF may induce asymmetric division (Chapter 2). Perhaps, polar distribution of FGF ligands in the satellite cell niche induces asymmetric division by activating FGFR on only one side of a satellite cell (Cosgrove et al., 2009). If the presentation of FGF ligand in the niche directs the orientation of division, then the

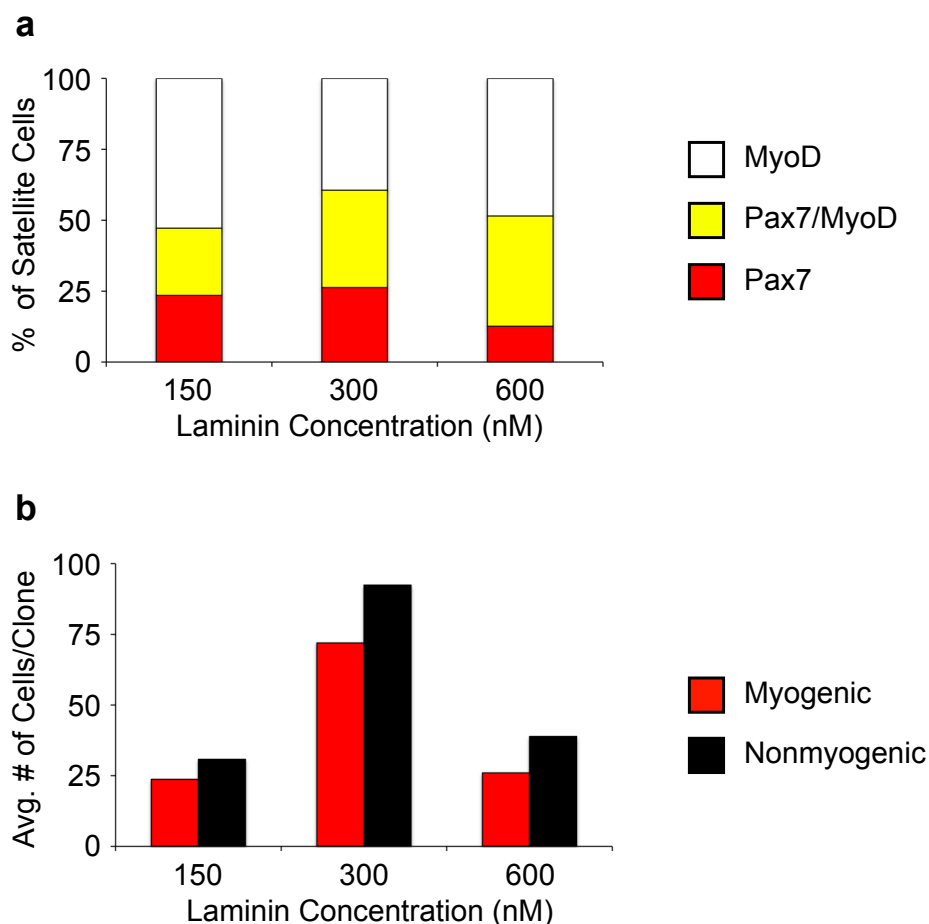


**Figure 3.6: Laminin concentration affects satellite cell self-renewal and proliferation.** As laminin increased self-renewal in hydrogel culture, different laminin concentrations were screened to assess the relationship between laminin concentration and satellite cell fate. Satellite cells were cultured for 120h on 6 wt% 4-arm PEG norbornene hydrogels (2D) containing 150-600 nM laminin. Hydrogels were fixed, then stained and visualized for DAPI, Pax7 and MyoD. **(a)** Pax7 and MyoD immunoreactivity in cells was quantified and plotted as a percentage of the total number of myogenic cells that were Pax7+/MyoD- reserve cells (red), Pax7+/MyoD+ myoblasts (yellow) or Pax7-/MyoD+ committed myocytes (white). Addition of 300 nM laminin to hydrogels increased both the percentage of reserve cells and myoblasts. **(b)** The average number of myogenic (Pax7+,MyoD+; red) and nonmyogenic (Pax7-/MyoD-; black) cells per hydrogel was calculated and plotted (Data were from a single experiment).

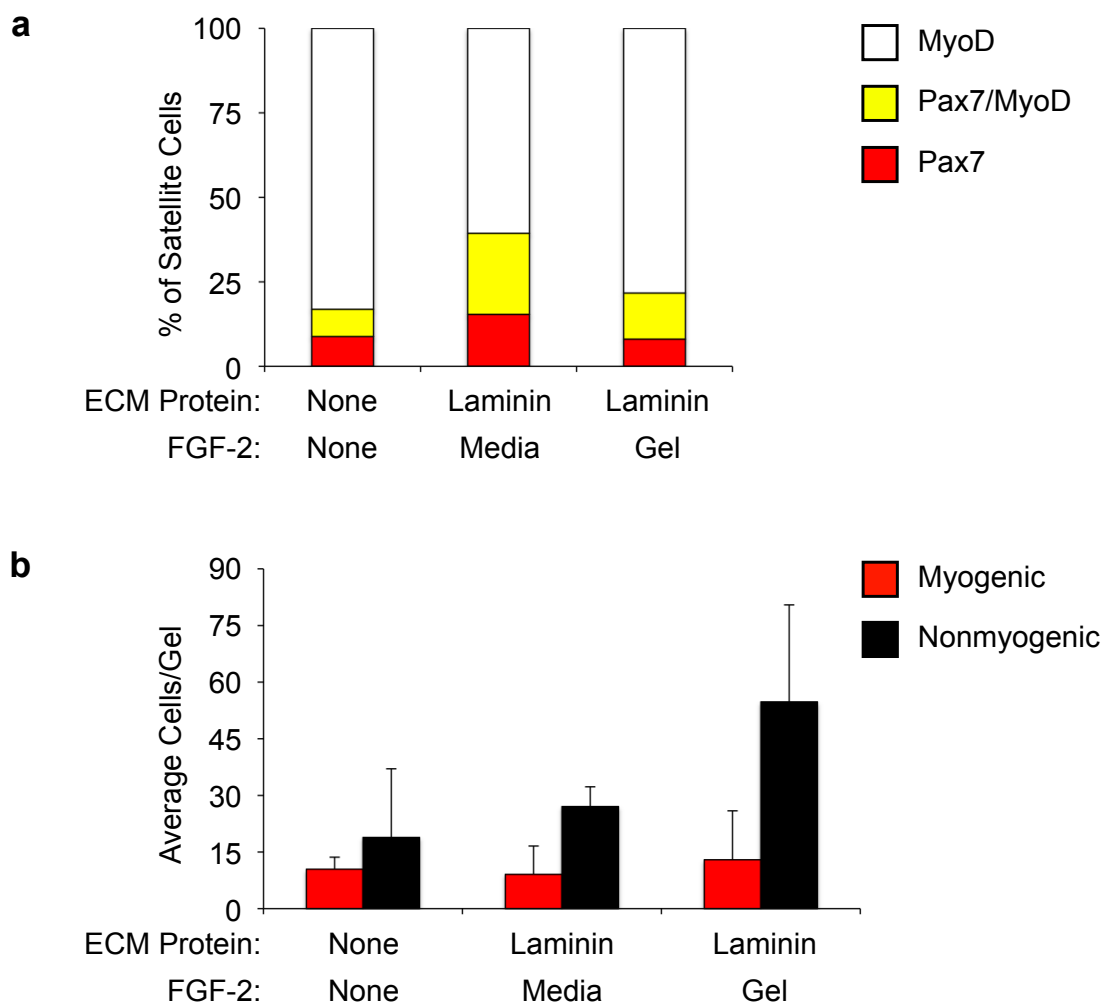


**Figure 3.7: FGF-2 addition to culture media increases self-renewal.** FGF-2 was added to media or entrapped within hydrogels to determine if the method of growth factor delivery affected satellite cell fate. Satellite cells were cultured for 6d on 6 wt% 4-arm PEG norbornene hydrogels (2D) containing no protein, containing laminin with FGF-2 encapsulated in the hydrogel, or containing laminin with FGF-2 added to the growth media. Hydrogels were fixed, immunostained and visualized for DAPI, Pax7 and MyoD. **(a)** Pax7 and MyoD immunoreactivity in cells was quantified and plotted as a percentage of the total number of myogenic cells that were Pax7+/MyoD- reserve cells (red), Pax7+/MyoD+ myoblasts (yellow) or Pax7-/MyoD+ committed myocytes (white). FGF-2 addition to the media increased the Pax7+/MyoD- and Pax7+/MyoD+ populations relative to encapsulated FGF-2. **(b)** The average number of myogenic (Pax7+,MyoD+; red) and nonmyogenic (Pax7-/MyoD-; black) cells per hydrogel was calculated and plotted (Data represent the average of two independent experiments. Error bars are S.D.).

distribution of FGF-2 in hydrogels should influence self-renewal (Figure 3.3). I have cultured satellite cells on hydrogels for 6d with FGF-2 added to the media (non-polar) or entrapped in the hydrogel (polar) and then quantified for Pax7/MyoD immunoreactivity to measure self-renewal. FGF-2 addition to media increases the proportion of reserve cells (2-fold) and myoblasts (2- to 3-fold) compared to other conditions. Surprisingly, entrapping FGF-2 in the hydrogel does not increase the proportion of Pax7+/MyoD- reserve cells (Figure 3.7a) but does increase the proliferation of nonmyogenic cells (Figure 3.7b). These data suggest that polar distribution of FGF-2 ligand does not increase satellite cell self-renewal in hydrogels.

### **Heparin addition in hydrogels has complex effects on satellite cell self-renewal**

Heparan sulfate proteoglycans facilitate growth factor signaling (Jenniskens et al., 2000; Jenniskens et al., 2002; Bink et al., 2003), so addition of heparin (Figure 3.8), which is used in place of heparan sulfate in culture, to hydrogels may enhance growth factor signaling and increase self-renewal. Heparin exists in a range of sizes that exhibit different activities (Salzman et al., 1980; De Cristofaro et al., 1998), so I have screened both low and high molecular weight heparin in hydrogel culture. I have cultured satellite cells on hydrogels containing laminin and heparin or heparin alone and quantified cells for Pax7 and MyoD immunoreactivity to measure self-renewal (Figure 3.9b). Unexpectedly, satellite cells do not attach to high molecular weight (h.w.) heparin hydrogels but do attach to low molecular weight (l.w.) heparin (Figure 3.9b). Satellite cells cultured on l.w. heparin hydrogels exhibit increased Pax7 expression compared to cells cultured on laminin/heparin hydrogels even though proliferation does not change (Figure 3.9b). Overall, heparin addition does not increase self-renewal as much as laminin or IKVAV peptide addition (Figures 3.4, 3.5). However, entrapped heparin may be sequestering growth

factors in the hydrogel which could render growth factors inaccessible to the satellite cells (Yoon et al., 2006; Park et al., 2009; Galderisi et al., 2013).

### **Satellite cells survive encapsulation in hydrogels to form myspheres**

As the distribution of growth factors in hydrogel culture affects satellite cell activity, I have developed 3D hydrogels to further probe the influence of signal distribution in the niche on satellite cell self-renewal (Mauro, 1961; DeForest and Anseth, 2012). Satellite cells can be grown on top of 2D hydrogels (a polar niche) or encapsulated within the hydrogel scaffold in 3D culture (a non-polar niche) (Figure 3.1d). I have first determined that satellite cells survive within 3D hydrogels by culturing encapsulated cells for 1d and staining cells with ethidium homodimer-1, which labels dying cells (red cells; Figure 3.10b). Upon quantifying ethidium homodimer-1 staining, I find that 80% of cells survive encapsulation (Figure 3.10a). When I culture hydrogel-encapsulated satellite cells for 1d - 6d and stain for Pax7/MyoD, I find that encapsulated satellite cells proliferate to form myspheres containing reserve cells (Pax7+/MyoD-) and myoblasts (MyoD+) (Figure 3.2c) whereas contaminating (Pax7-/MyoD-) cells form large branching structures (Figure 3.2d). Real-time imaging reveals that these myspheres represent individual colonies as cells do not migrate through the hydrogel matrix. These results demonstrate that 3D hydrogels maintain a self-renewing satellite cell population. In future studies, 3D hydrogels will be used in combination with 2D culture to probe the effects of polar distribution of ECM proteins, growth factors and heparin in the niche.

### **Heparan sulfate GAGs are important regulators of self-renewal in the satellite cell niche**

As the changes in cell fate after heparin addition to hydrogels suggest (Figure 3.9), heparan sulfate proteoglycans are important regulators of signaling in the satellite cell niche and

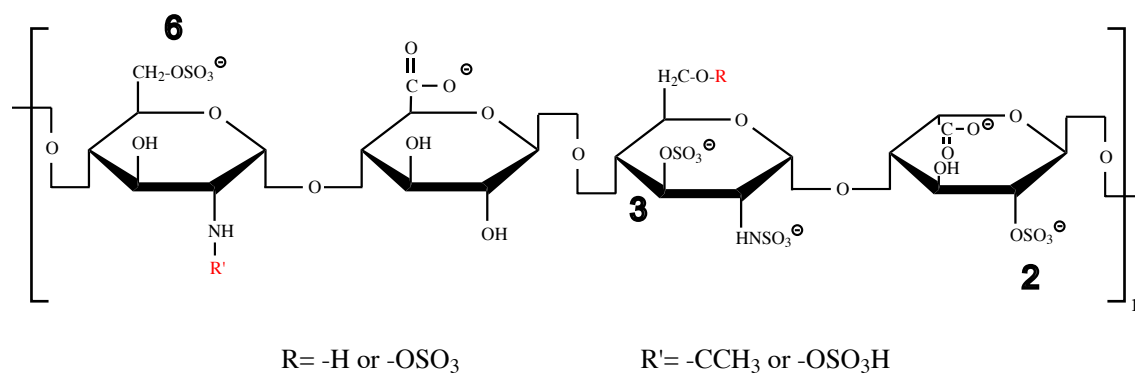


**Figure 3.8: The glycosaminoglycan heparin is composed of variably sulfated, repeating disaccharide units.** Heparin has a closely related structure to heparan sulfate, which is found on proteoglycans present on cell surfaces. Heparin, which is well characterized and commercially available, is used in place of heparan sulfate in the culture experiments described in this chapter as little is known of the composition of heparan sulfate in the satellite cell niche. This structure depicts the saccharides most commonly found in heparin which include L-iduronic acid (2-O-sulfated) and D-glucosamine (6-O-sulfated, N-sulfated). Disaccharide units of both heparin and heparan sulfate are modified by O-sulfation, which creates binding domains for heparin-binding growth factors and other proteins. The types of O-sulfation (2, 3 and 6) are marked in the structure above. 2-O- and 6-O-sulfation facilitate FGF-2/FGFR signaling while 3-O-sulfation is a rare modification that is not known to regulate FGF-2 signaling. **R** and **R**<sup>1</sup> are groups produced by variable enzymatic modification during glycosaminoglycan biosynthesis.

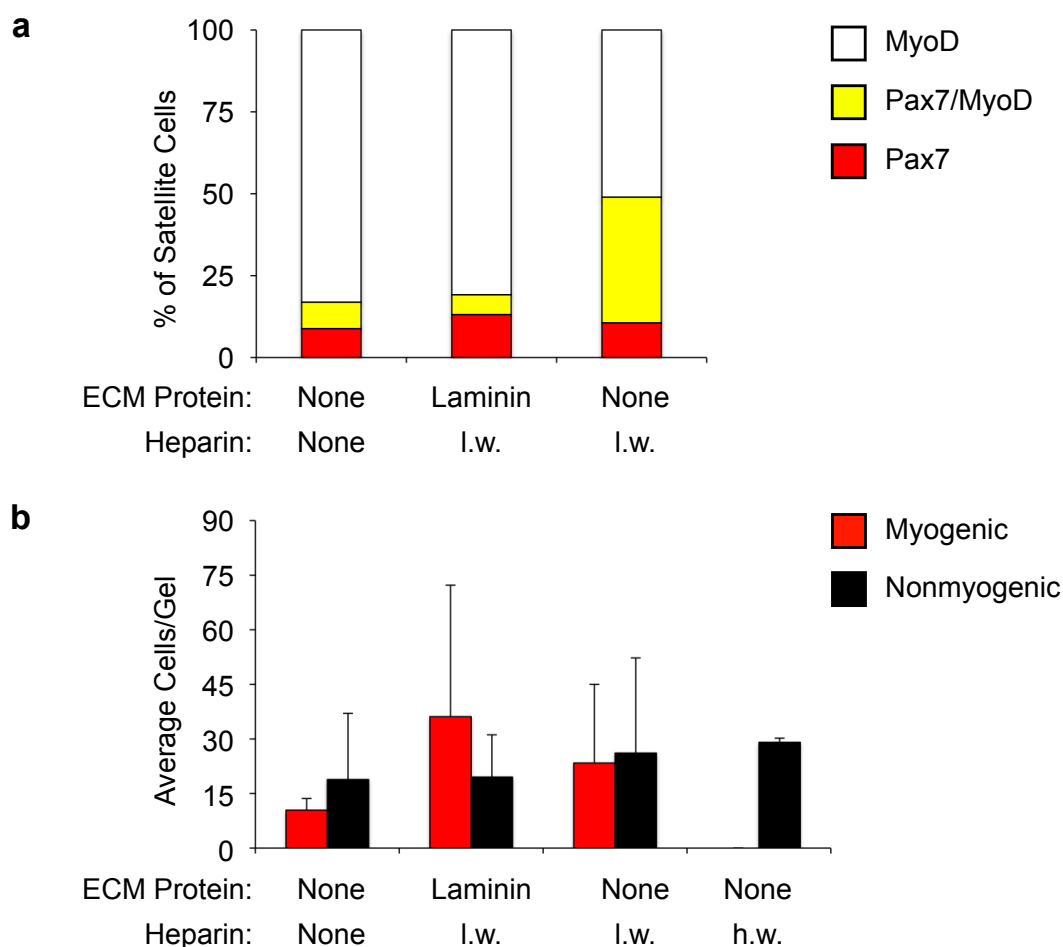


**Figure 3.9: Encapsulating heparin in hydrogels increases proliferation but not self-renewal.**

Heparin was added hydrogel culture to determine if entrapping heparin, which binds growth factors, would increase self-renewal of satellite cells. Satellite cells were cultured for 6d on 6 wt % 4-arm PEG norbornene hydrogels (2D) containing either laminin and low weight (l.w.) heparin, low weight (l.w.) heparin, or high weight (h.w.) heparin. Hydrogels were fixed, stained and visualized for DAPI, Pax7 and MyoD. **(a)** Pax7 and MyoD immunoreactivity in cells was quantified and plotted as a percentage of the total number of myogenic cells that were Pax7+/MyoD- reserve cells (red), Pax7+/MyoD+ myoblasts (yellow) or Pax7-/MyoD+ (white) committed myocytes. The percentage of Pax7+ cells was low in hydrogels containing no heparin or laminin (None). Culturing cells on hydrogels containing laminin and l.w. heparin increased the proportion of Pax7+/MyoD- reserve satellite cells whereas culturing cells on hydrogels containing only l.w. heparin greatly increased the Pax7+/MyoD+ myoblast population. No myogenic cells were found on hydrogels containing h.w. Heparin. **(b)** The average number of myogenic (Pax7+,MyoD+; red) and nonmyogenic (Pax7-/MyoD-; black) cells per hydrogel was calculated and plotted. (Data are the mean of two independent experiments. Error bars are S.D.).

are required for satellite cell self-renewal and activation. Satellite cells activate and self-renew poorly in mice lacking Syndecan-3 or -4, two membrane-bound heparan sulfate proteoglycans expressed by satellite cells (Cornelison et al., 2004; Pisconti et al., 2010). A general loss of heparan sulfate proteoglycans or heparan sulfate chains on satellite cells reduces Pax7 expression and inhibits both FGF and Notch signaling, which drive self-renewal (Rapraeger et al., 1991; Olwin and Rapraeger, 1992; Pisconti et al., 2010). Intriguingly, both FGF-2 and heparan sulfate GAGs localize to satellite cells on myofibers, which suggests that heparan sulfate GAGs may be particularly important to signal transduction in the satellite cell niche (Figure 3.13).

To probe the role of heparan sulfate in the satellite cell niche, I have first determined whether the levels of heparan sulfate proteoglycan transcripts change in satellite cells over an injury time course (Time post-injury: 0h (quiescence), 12h, (activation), 24h and 48h (first cell division)) (Table 3.1). The level of several proteoglycan transcripts are upregulated or downregulated after activation. I indirectly assess whether heparan sulfate composition changes by determining whether transcripts of enzymes acting in the heparan sulfate GAG biosynthesis pathway are changing (Table 3.2). GAGs are synthesized by a complex enzymatic pathway where changes in enzyme expression appear to result in altered GAG chain composition (Esko and Lindahl, 2001). Intriguingly, the expression of several enzymes change through activation (0h-12h) and the first cell division (0h-48h) (Table 3.2). These results suggest that heparan sulfate composition may change with satellite cell activity. As the heparan sulfate sequence establishes growth factor binding sites (Guimond et al., 1993), dynamic heparan sulfate composition may regulate which signaling pathways are activated in satellite cells after muscle injury.

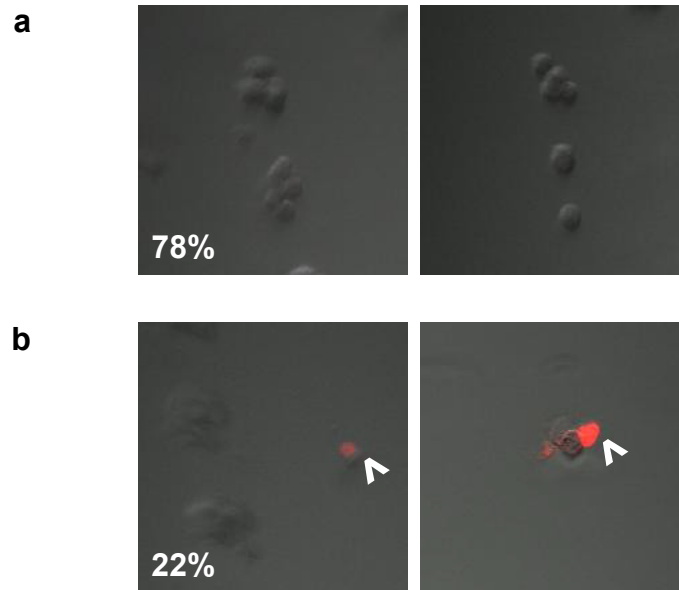


**Figure 3.10: Satellite cells survive encapsulation into 3D hydrogels.** I determined whether satellite cells would survive encapsulation into 3D hydrogels as a 3D niche better represented the *in vivo niche*. For 3D hydrogel culture, satellite cells were resuspended in 7 wt% 4-arm PEG norbornene monomer solution with RDGS peptide, then hydrogels were polymerized and returned to growth media for 1d. Hydrogels were stained with ethidium homodimer-1, a marker of death and cell membrane instability, and scored for ethidium homodimer-1+ (red) cells. **(a)** Most (78%) satellite cells did not take up ethidium homodimer-1 label indicating that these cells survived encapsulation, **(b)** a while proportion of cells (22%) were positive for ethidium homodimer-1 (^, red nuclei) and dying.

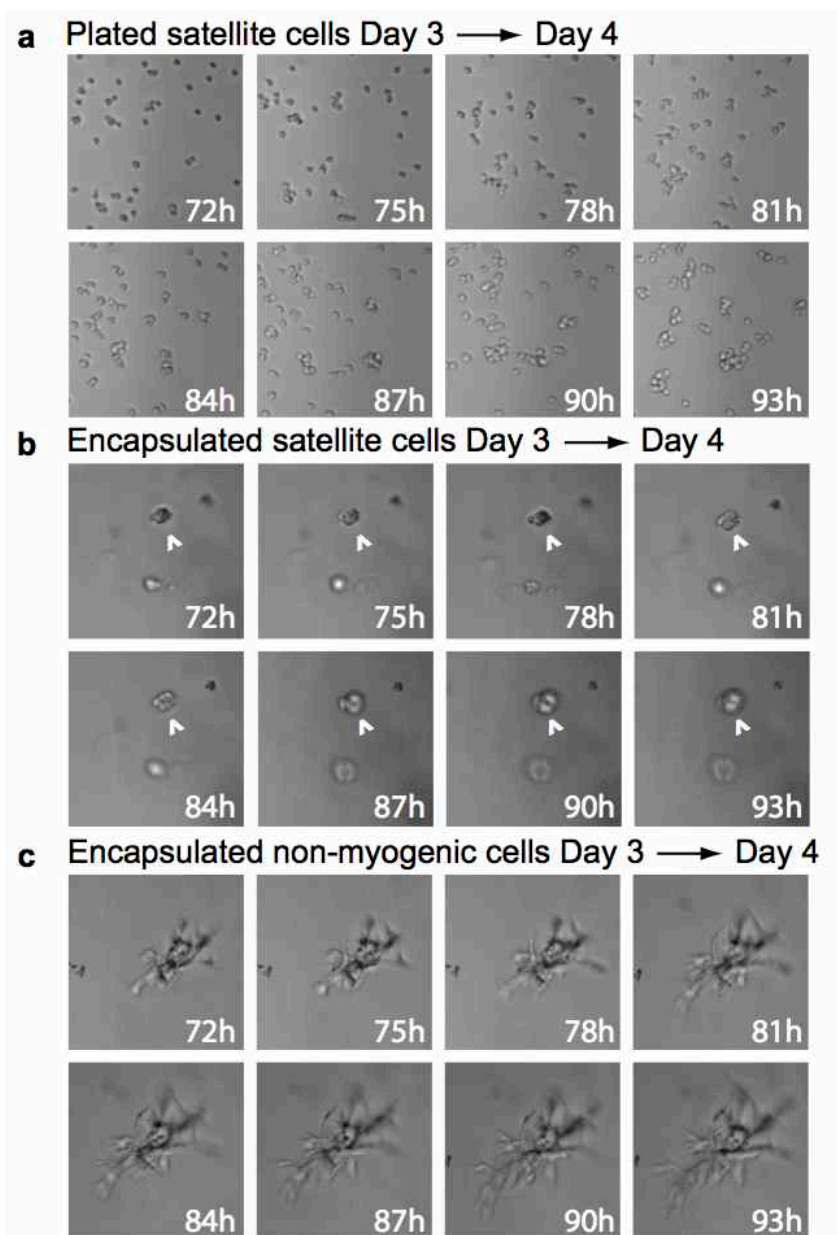


**Figure 3.11: Satellite cells in 3D hydrogels proliferate from small clones to form myosphere-like structures.** 3D hydrogel cultures were observed by live imaging to determine their dynamics of myosphere formation. For 3D hydrogel culture, satellite cells were resuspended in 6 wt% 4-arm PEG norbornene monomer solution with RDGS, then encapsulated by polymerizing hydrogels with UV light and returned to growth media. Some cells were also plated to gelatin-coated plastic plates. From 3d to 4d, cells were imaged (brightfield) hourly to capture cell division and migration in real-time. **(a)** Satellite cells plated to gelatin-coated plastic plates were highly mobile. **(b)** Satellite cells encapsulated within hydrogels proliferated to form spherical clusters (^) but did not migrate through the hydrogel. **(c)** Nonmyogenic cells formed large, branching structures.

### **Heparin sequence length and sulfation pattern influence satellite cell self-renewal**

Heparan sulfate GAG chain length and sulfation pattern may regulate interactions with growth factors and growth factor receptors. GAG chains are composed of repeating hexuronic acid and glucosamine disaccharide units that are modified during biosynthesis by N- and O-sulfation of discrete regions along the oligosaccharide (Gallagher, 2001) (Figure 3.8).

Biochemical assays with fragmented heparin demonstrate that both the type of sulfation and the sequence length of sulfated disaccharides establish different growth factor domains (Delehedde et al., 2002; Mohammadi et al., 2005; Pellegrini et al., 2000). For example, the putative FGF-2 domain requires 2-O-sulfation (binding) and 6-O-sulfation (active signaling) (Guimond et al., 1993; Guglieri et al., 2008). However, genetic experiments *in vivo* suggest that the overall charge of heparin chains rather than sequence specificity determines heparan sulfate activity (Merry et al., 2001; Kamimura et al., 2006), which contradicts data generated *in vitro*. Further complicating the issue, the specific composition and spatio-temporal distribution of heparan sulfate GAGs are unknown in the satellite cell niche and other stem cell niches (Jenniskens et al., 2000; Jenniskens et al., 2002; Bink et al., 2003).

As heparan sulfate activity in the satellite cell niche was poorly understood, I used heparin to further optimize hydrogels as an artificial satellite cell niche. I developed a high-throughput screen for 96-well plate culture to efficiently identify sequences from a heparin library (Turnbull laboratory) that promote FGF signaling and self-renewal in an FGF-sensitive cell line (MM14 cells) (Lim and Hauschka, 1984; Clegg et al., 1987). MM14 cells were known to proliferate in response to heparan sulfate-facilitated FGF-2 stimulation, which inhibits

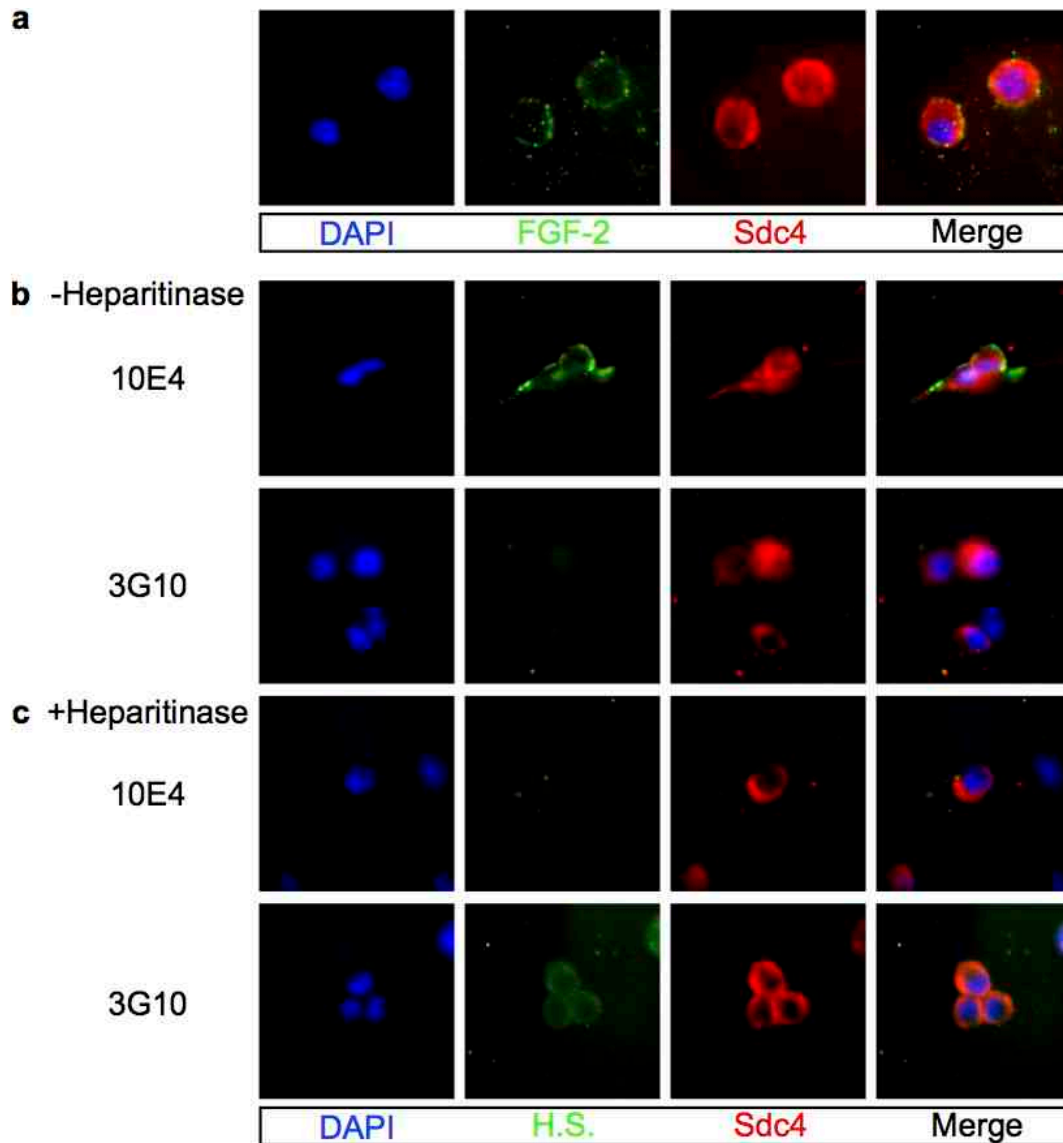


**Figure 3.12: FGF-2 and heparan sulfate are concentrated at myofiber-associated satellite cells.** FGF-2 and heparan sulfate localization were characterized as a preliminary study of heparan sulfate activity in myofiber culture. **(a)** Myofiber-associated satellite cells were cultured in growth media with FGF-2, fixed, stained and visualized for DAPI (blue), FGF-2 (green) and Syndecan-4 (red), which marks satellite cells. FGF-2 staining localized to satellite cells. **(b)** Myofiber-associated satellite cells were stained and visualized for DAPI (blue), Syndecan-4 (red) and heparan sulfate (H.S.) (green) with the antibodies 10E4 (detects a common H.S. domain) or 3G10 (detects an H.S. domain created by heparitinase-treatment). Heparan sulfate immunoreactivity was concentrated around satellite cells. **(c)** To determine that staining was specific to the H.S. epitope, myofibers were treated with heparitinase, and stained and visualized for DAPI (blue), Syndecan-4 (red), 10E4 (green) or 3G10 (green). Heparitinase-treatment extinguished 10E4 immunoreactivity and induced 3G10 immunoreactivity, revealing that heparan sulfate staining localized to satellite cells.

**Table 3.1: Heparan sulfate proteoglycan transcript levels changed throughout satellite cell activation and proliferation.** Microarray analysis of transcripts in satellite cells isolated from skeletal muscle over an injury time course revealed dynamic proteoglycan expression after injury. Comparisons were made between satellite cells isolated from uninjured (quiescent satellite cells) and injured tibialis anterior muscles at 12h (activated cells), 24h (cells begin first round of mitosis), and 48h (proliferating myoblasts) following BaCl<sub>2</sub>-induced injury. Total mRNA was extracted and hybridized on Affymetrix gene chips to perform global gene expression analysis. (The table comprises proteoglycan transcripts that significantly change 2-fold or more between the time points indicated. Red = upregulated transcripts. Blue = downregulated transcripts. n.c. indicates no change in expression. *P* value < 0.01).

Proteoglycan	Symbol	0-12h	0-24h	12-24h	24-48h	0-48h
CD44 antigen	CD44	n.c.	n.c.	7.85	n.c.	n.c.
Syndecan 4	Sdc4	n.c.	n.c.	10.42	n.c.	11.68
Glypican 4	Gpc4	-3.52	-3.56	n.c.	n.c.	-3.66
Glypican 6	Gpc6	n.c.	-2.11	n.c.	n.c.	-2.20
Sparc/osteonectin, cwcv and kazal-like domains proteoglycan 2	Spock2	n.c.	n.c.	-2.26	n.c.	n.c.
Syndecan 1	Sdc1	-4.00	n.c.	n.c.	n.c.	-4.50
Syndecan 2	Sdc2	-9.97	-12.47	n.c.	n.c.	-10.58

**Table 3.2: Transcript levels of heparan sulfate glycosaminoglycan biosynthesis enzymes changed throughout satellite cell activation and proliferation.** Microarray analysis of transcripts in satellite cells isolated from skeletal muscle over an injury time course revealed dynamic expression of GAG biosynthesis enzymes after injury. Comparisons were made between satellite cells isolated from uninjured (quiescent cells) and injured tibialis anterior muscles at 12h (activated cells), 24h (cells begin first round of mitosis), and 48h (proliferating myoblasts) following BaCl<sub>2</sub>-induced injury. Total mRNA was extracted and hybridized on Affymetrix gene chips to perform global gene expression analysis. (The table shows all proteoglycans that significantly changed 2-fold or more between time points as indicated. Red = upregulated transcripts. Yellow = transcript levels were variable over injury time course. Blue = downregulated transcripts. n.c. indicates no change in expression. *P* value < 0.01).

Enzyme	Symbol	0-12h	0-24h	12-24h	24-48h	0-48h
Exotoses (multiple)-like 2	Extl2	n.c.	n.c.	n.c.	10.81	n.c.
Heparan sulfate (glucosamine) 3-O-sulfotransferase 3B1	Hs3st3b1	2.43	2.36	n.c.	n.c.	n.c.
N-deacetylase/N-sulfotransferase (heparan glucosaminyl) 1	Ndst1	-3.01	-3.28	n.c.	n.c.	6.50
Exostoses (multiple)-like 3	Extl3	n.c.	-4.54	n.c.	4.24	n.c.
Exostoses (multiple) 1	Ext1	-4.63	-3.24	n.c.	n.c.	-4.55
Glucuronyl C5-epimerase	Glce	-12.00	-14.12	n.c.	n.c.	-8.94
Heparan sulfate 2-O-sulfotransferase 1	Hs2st1	-2.13	n.c.	n.c.	n.c.	-2.22
3'-phosphoadenosine 5'-phosphosulfate synthase 2	PAPSS2	-6.87	-5.92	n.c.	n.c.	n.c.
Sulfatase 1	Sulf1	-5.10	-5.25	n.c.	n.c.	-12.11
Sulfatase 2	Sulf2	-29.94	n.c.	n.c.	n.c.	n.c.

differentiation in cells (Clegg et al., 1987; Rapraeger et al., 1991; Olwin and Rapraeger, 1992; Schlessinger et al., 2000). Proliferation was measured by BrdU incorporation into the DNA of cycling MM14 cells. I determined that the high-throughput assay could detect small changes in MM14 proliferation by measuring the effect of FGF-2 and heparin concentration on BrdU incorporation. The amount of BrdU incorporated by MM14 cells was proportional to the concentration of FGF-2 and heparin added (Figure 3.13a). Additionally, removal of FGF-2 prevented MM14 cells from incorporating BrdU (Figure 3.13a) and caused MM14 cells to differentiate and form myotubes (^) (Figure 3.13b).

After confirming that the high-throughput assay had detected small changes in MM14 proliferation, I began to screen the heparin library to determine if heparin fragment length affected growth factor signal transduction and satellite cell activity. Endogenous heparan sulfate activity was inhibited by treating MM14 cells with sodium chlorate ( $\text{NaClO}_3$ ) which prevents biosynthesis of the 3'-phosphoadenosine 5'-phosphosulfate (PAPS) sulfate donor, inhibits GAG sulfation, and blocks FGF signaling (Olwin and Rapraeger, 1992; Rapraeger et al., 1991) (Figure 3.13c). Exogenous heparin addition to chlorate-treated cells rescued FGF signaling and BrdU incorporation (Figure 3.13c), which indicated that heparin overcame the inhibition of endogenous heparan sulfate activity. I then cultured chlorate-treated MM14 cells in the presence of FGF-2 and heparin fragments of 2-20 saccharides and measured BrdU incorporation (Figure 3.13d, e). Heparin fragment length had a biphasic effect on MM14 proliferation where 8mer to 12mer (8 saccharides to 12 saccharides; 4 to 6 disaccharide units) heparin fragments best rescued BrdU incorporation compared to other heparin lengths. Previous studies had found 8mer or 10mer fragments were the minimal domain size capable of enhancing FGF-2 signaling in culture

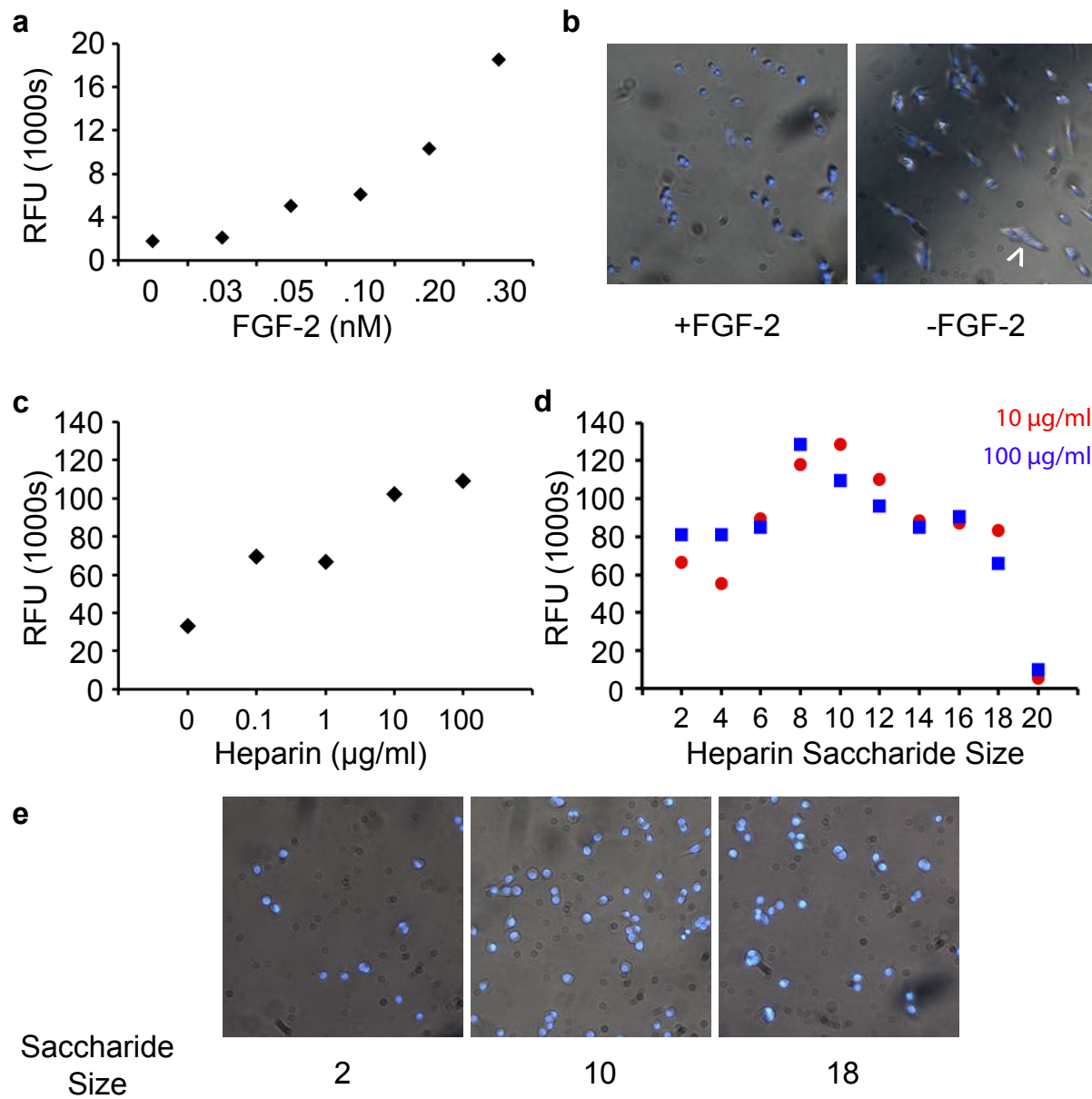


**Figure 3.13: Heparin fragment length regulates FGF signaling in MM14 cells.** A library of fragmented heparin sequences was screened to determine the effect of heparin length on FGF signal transduction. The FGF-sensitive MM14 cell line was previously shown to require FGF-2 addition to inhibit rapid differentiation. **(a)** MM14 cells were passaged, then fed 0 - 0.33 nM FGF-2 and BrdU, a marker of S-phase, to establish that the Calbiochem HTS01 high-throughput assay could detect small changes in MM14 proliferation. BrdU incorporation in proliferating cells was measured by ELISA and plotted in relative fluorescence units (RFU) normalized to background fluorescence, revealing that FGF-2 addition increased BrdU incorporation. **(b)** Cells were also fixed, stained with DAPI (blue) and visualized. Representative images depict merged DAPI and brightfield channels. Cells receiving FGF-2 remained mononuclear while FGF-2-starved cells formed differentiated myotubes (^, a representative, multinucleate myotube). **(c)** To confirm the requirement for heparin in FGF signaling, MM14s were passaged then treated with sodium chlorate (to inhibit endogenous GAG sulfation), FGF-2, and 0-100  $\mu\text{g/ml}$  heparin, then given BrdU. BrdU incorporation was measured by ELISA and plotted in relative fluorescence units. MM14 proliferation declined in the absence of heparin and increased after exogenous heparin addition. **(d)** The experiment was repeated with the library of 2-20 saccharide heparin fragments (2mer - 20mer = 1-10 disaccharide units) added to MM14 cells at 10 (red) or 100 (blue)  $\mu\text{g/ml}$ . 8mer - 12mer heparin addition increased BrdU incorporation. **(e)** Cells were fixed and stained with DAPI (blue). Representative images depict merged DAPI and brightfield channels. Proliferation decreased after addition of 2mer or 18mer heparin relative to the increased proliferation observed after 10mer heparin addition. (RFU varies between experiments due to use of multiple fluorimeters. Datapoints are the average of triplicate wells.)

(Guimond et al., 1993), which confirmed that the high-throughput assay had identified real differences in the activity of heparin sequences.

I hypothesized that heparin fragment length affected self-renewal and screened the library for fragments that promoted Pax7 expression. I cultured MM14 cells with heparin fragments as before then scored MM14 cells for Pax7 immunoreactivity as a measure of self-renewal (Troy et al., 2012) and for myotube formation as a measure of differentiation. 85% of MM14 cells retained Pax7 in the presence of FGF-2 while only 33% of MM14 cells were Pax7+ in the absence of FGF-2 (Figure 3.14a), which established that Pax7 marked undifferentiated cells. Only 15% of chlorate-treated MM14 cells retained Pax7 whereas ~65% of chlorate-treated cells that received exogenous heparin retained Pax7. Addition of 2mer heparin failed to rescue Pax7 levels (36% of cells were Pax7+), but both 10mer heparin and 18mer heparin increased Pax7 levels (~75% of cells were Pax7+) (Figure 3.14a), which suggested that 10mer and 18mer heparin fragments promote self-renewal through FGF signaling. All heparin fragments inhibited terminal differentiation and myotube formation (Figure 3.14b). Thus, heparin length influenced FGF-2 signal transduction to inhibit or promote self-renewal in MM14 cells.

The amount and type of O-sulfation on GAG chains influenced growth factor binding *in vitro*, so I next screened a library of selectively desulfated heparin fragments to identify fragments that promoted FGF-2 signal transduction in MM14 cells. I cultured chlorate-treated MM14 cells with FGF-2 and heparin fragments selectively desulfated of 2- or 6-O-sulfate, then measured BrdU incorporation. Cells receiving 4mer heparin proliferated less overall compared to cells receiving 10mer and 18mer heparin (Figure 3.15a). However, loss of 2-O- or 6-O-sulfation from 4mer heparin fragments further decreased BrdU incorporation. Addition of 6-O-desulfated

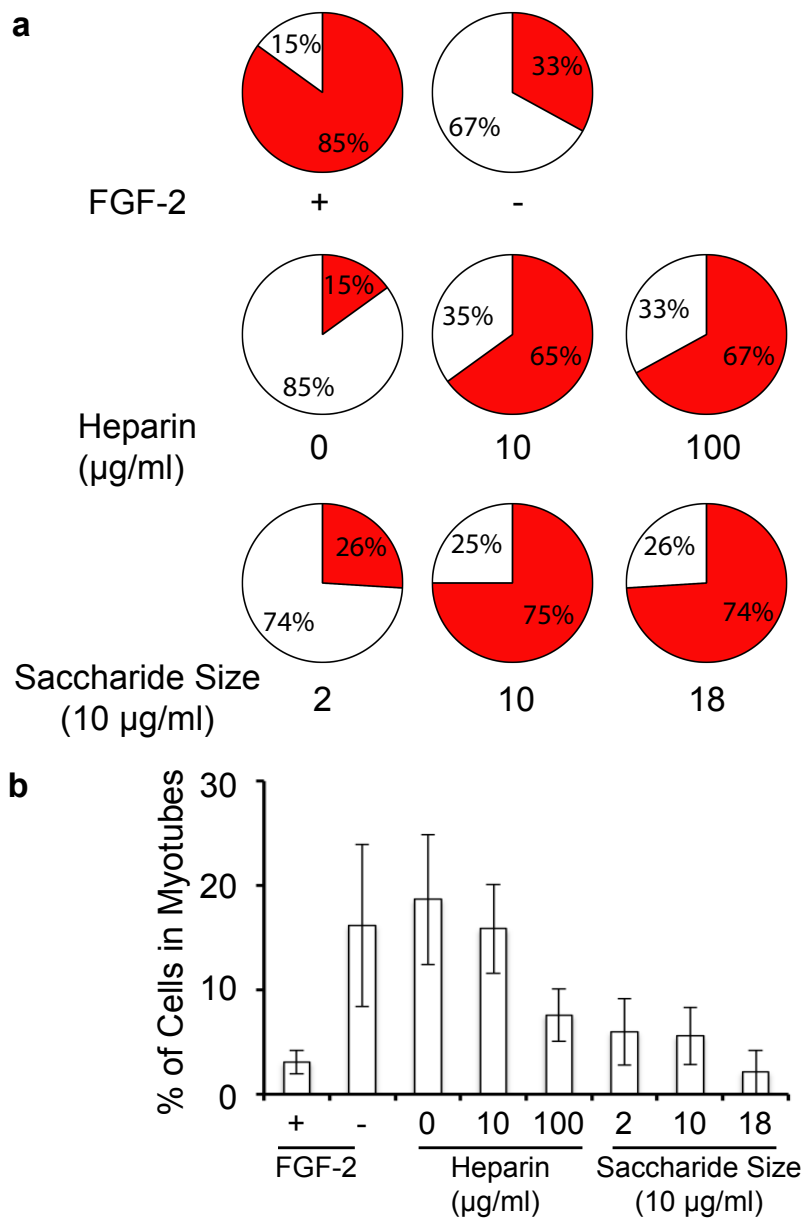


**Figure 3.14: Addition of longer heparin fragments increases self-renewal and decreases differentiation in MM14 cells.** Heparin fragments were screened to determine the effect of heparin length on MM14 cell fate. MM14 cells were passaged, then cultured with sodium chlorate, FGF-2, and 0-100  $\mu\text{g/ml}$  heparin or 2mer - 18mer heparin. Some cells did not receive sodium chlorate but were treated with or without FGF-2 as controls. Cells were fixed, immunostained and visualized for DAPI and Pax7, a marker of self-renewal. **(a)** Pax7 immunoreactivity was plotted as a portion of each pie chart representing the percentage of Pax7+ cells (red) or Pax7- cells (white) compared to the total number of cells. Pie charts are not scaled. FGF-2 addition increased the percentage of Pax7+ cells by 2.5-fold. Both 10 and 100  $\mu\text{g/ml}$  heparin rescued the percentage of Pax7+ chlorate-treated cells to the level of untreated cells receiving FGF-2. Both 10mer and 18mer heparin, but not 2mer heparin, rescued Pax7 expression to the level seen in untreated cells receiving FGF-2. **(b)** MM14 cells that received insufficient FGF signal fused into myotubes. The myonuclei of myotubes were quantified to measure differentiation and plotted as the percentage of nuclei in myotubes compared to the total number of nuclei. Both FGF-2 removal and sodium chlorate treatment without heparin addition promoted myotube formation. Addition of 100  $\mu\text{g/ml}$  heparin but not 10  $\mu\text{g/ml}$  heparin reduced myotube formation. Addition of any length of fragmented heparin reduced myotube formation. (Data shown are the averages of triplicate wells. 2mer - 20mer = 2 - 20 saccharides = 1 - 10 disaccharide units).

or 2/6-O-desulfated 10mer and 18mer heparin fragments decreased BrdU incorporation in MM14 cells, indicating that 6-O-sulfation was required for MM14 proliferation. The requirement for 2-O-sulfation varied with heparin fragment length (Figure 3.15b, c). These results suggested that heparin domain length and sulfation pattern together determined which sequences were FGF-2 domains. Sequences from the heparin library affect satellite cell function in hydrogel culture

The screen identified heparin fragments that promoted FGF signal transduction and self-renewal in myogenic cells, so I next confirmed that heparin fragments were functional in hydrogel cultures. I encapsulated satellite cells in hydrogels with 10mer or 18mer heparin fragments. After 1d, I observed that cell doublets formed in 10mer heparin hydrogels but not in 18mer heparin containing hydrogels (Figure 3.16a, b), indicating that the results of the heparin library screen could be translated to 3D hydrogel culture.

## **DISCUSSION**

My work demonstrates that degradable 4-arm PEG norbornene hydrogels serve as artificial satellite cell niches in culture. Satellite cells survive and proliferate in both 2D and 3D PEG hydrogels. In hydrogels, satellite cells form large myospheres that maintain populations of Pax7<sup>+</sup>/MyoD<sup>-</sup> stem cells and MyoD<sup>+</sup> transit-amplifying cells whereas terminal differentiation and myotube formation are inhibited. In the future, I plan to determine whether these Pax7<sup>+</sup>/MyoD<sup>-</sup> satellite cells have retained stem cell function by measuring donor-derived engraftment after transplantation of satellite cells cultured on 4-arm PEG norbornene hydrogels (Gilbert et al., 2010). If hydrogels function as a true satellite cell niche, hydrogel culture should enhance satellite cell self-renewal as measured by engraftment after transplantation.

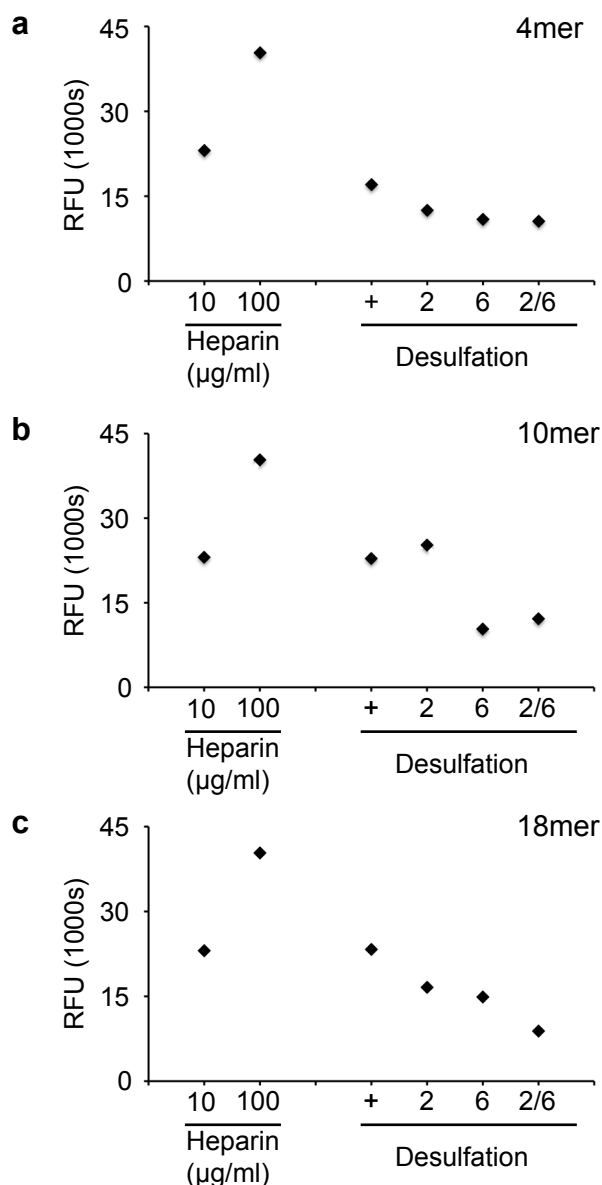


**Figure 3.15: Specific heparin sulfation patterns drive FGF signaling in MM14 cells.** A library of fragmented and selectively desulfated heparin sequences was screened to determine the relationship of heparin length and sulfation pattern on FGF signal transduction. MM14s were passaged and treated with sodium chlorate, FGF-2, and 10-100  $\mu\text{g/ml}$  heparin or selectively desulfated heparin fragments (+, untreated fragments; 2, 2-O-sulfation removed; 6, 6-O-sulfation removed; 2/6, 2/6-O-sulfation removed) and then given BrdU. BrdU incorporation was measured by ELISA and was plotted in relative fluorescence units (RFU). **(a)** BrdU incorporation was lowest overall in 4mer heparin-treated cells relative to cells receiving **(b)** 10mer heparin and **(c)** 18mer heparin. Addition of either 2-O-desulfated heparin or 6-O-desulfated heparin decreased BrdU incorporation. BrdU incorporation was lowest in cells receiving 2/6-O-desulfated heparin. (4mer = 4 saccharides = 2 disaccharide units).

Incorporating components of the niche into hydrogels reveals which structural and biochemical cues promote satellite cell self-renewal. Of the ECM components, I find that adding IKVAV peptide, the integrin-binding sequence in laminin (Tashiro et al., 1989), to the hydrogel scaffold increases the Pax7<sup>+</sup>/MyoD<sup>-</sup> self-renewing cell population (Troy et al., 2012). Surprisingly, laminin protein is less effective at promoting self-renewal in satellite cells, so other domains in laminin may instead promote proliferation or differentiation. After screening components involved in growth factor signaling, I find that both FGF-2 and heparin affect satellite cell activity, but the effect on self-renewal varies with their localization in the hydrogel. I demonstrate that the length and sulfation pattern of heparin fragments affects satellite cell activity and that FGF-dependent self-renewal requires 6-O-sulfated heparin sequences at least 8 saccharides in length. Now that I have identified individual niche components that increase satellite cell self-renewal, I plan to determine if multiple signals act synchronistically to regulate self-renewal. For example, both FGF and Notch signaling have been described to regulate satellite cell self-renewal, so these signals could act together to promote or inhibit asymmetric division.

Hydrogel culture provides a tool to probe whether the polar nature of the myofiber niche underlies the molecular mechanisms of asymmetric division in satellite cells (Mauro, 1961; Knoblich, 2008; Cosgrove et al., 2009). Preliminary data suggest that changing the presentation of signals in hydrogels alters satellite cell activity. Entrapping heparin in 2D hydrogels produces different satellite cell activity than entrapping heparin fragments in 3D hydrogels. Additionally, adding FGF-2 to the media increases the proportion of reserve cells (Pax7<sup>+</sup>/MyoD<sup>-</sup>) and myoblasts (MyoD<sup>+</sup>) compared to entrapping FGF-2 in hydrogels, which expands only the

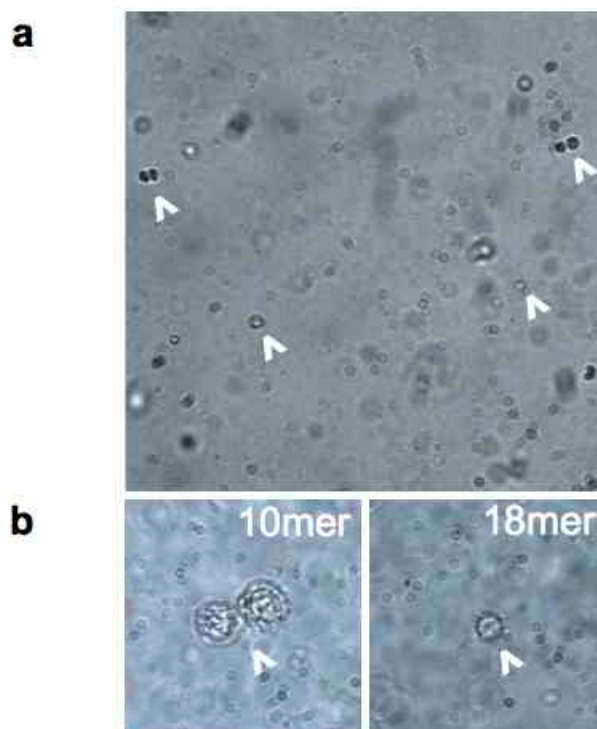


**Figure 3.16: Heparin fragments direct satellite cell activity in 3D hydrogel cultures.** Heparin fragments were entrapped in 3D hydrogels to determine if the results from the MM14 heparin screen translated to satellite cell culture. Satellite cells were encapsulated in 6 wt% 4-arm PEG norbornene hydrogels with RGDS/IKVAV/DGEA and 10  $\mu\text{g/ml}$  10mer or 18mer heparin. Hydrogels were cultured in 18%  $\text{O}_2$  in growth media with FGF-2. **(a)** Representative brightfield images, captured at 1d post-encapsulation, reveal that satellite cells (^) were sparsely dispersed through the hydrogels. **(b)** Cell doublets were observed in hydrogels containing 10mer heparin but not 18mer heparin. Single cells in 18mer-containing hydrogels also appeared smaller in size. (10mer = 10 saccharides = 5 disaccharides; debris and out-of-focus cells are visible in these images).

myoblasts. These results suggest that signal localization in the niche does affect satellite cell self-renewal (Figure 1.2) (Cosgrove et al., 2009). Many signals are known to localize to only one area of the satellite cell niche, which may help regulate asymmetric division. Myofiber membrane-bound Delta-1, a Notch ligand, may interact with Notch-3+ on the apical membrane of satellite cells (Kuang et al., 2009), while heparan sulfate in the basal lamina may sequester FGF ligands to form the FGF-FGFR-Syndecan-4 ternary complex on the basal satellite cell membrane (Steinfeld et al., 1996; Rapraeger et al., 1991; Cosgrove et al., 2009; Troy et al., 2012). Activated FGFR may induce phosphorylation of p38 $\alpha$  $\beta$  MAPK on one side of the satellite cell so that phospho-p38 $\alpha$  $\beta$  segregates with the Par-3 complex to the daughter cell that commits to differentiation (Troy et al., 2012). The Par-3 complex restricts Numb, an inhibitor of Notch, to the opposite daughter cell that becomes a quiescent satellite cell (Knoblich, 2008), which could serve to reinforce the activation of Notch on only one side of the daughter cell. In the future, these putative interactions in the niche may be tested in hydrogel culture to help determine whether polar distribution of FGF and Delta ligands in the niche act in combination to promote asymmetric division.

While 2D and 3D hydrogels are promising tools to study the effects of signal orientation on self-renewal, neither truly recapitulates the satellite cell niche. 2D hydrogels form a polar niche that presents niche components to one side of the satellite cell membrane while the other side is exposed to media. 3D hydrogels surround the satellite cells and present signals evenly across the cell membrane. A better model of the myofiber would be a polar, 3D hydrogel where satellite cells would be sandwiched between two hydrogel layers that could contain different signals. Currently, we are developing such a polar, 3D hydrogel for satellite cell culture to better

determine how signal presentation affects asymmetric division. The flexibility provided by 2D, 3D and polar 3D hydrogels will allow us to study the molecular mechanisms driving self-renewal in satellite cells and may lead to creating hydrogel-based therapies for sarcopenia and other skeletal muscle diseases.

## **METHODS**

### **Animal Studies**

Animal experiments in this study were performed in accordance with protocols approved by the Institutional Animal Care and Use Committee at the University of Colorado. Mice were housed in a pathogen-free facility at the University of Colorado-Boulder. Female C57BL/6 mice (Jackson Laboratories) 3-6 months of age were used for all *ex vivo* experiments.

### **Cell Isolation and Culture**

MM14 cells (Lim and Hauschka, 1984) are grown from frozen cell stocks and passaged twice before use. MM14 cells are grown at 18% O<sub>2</sub> in growth media (Ham's F12-C + 15% horse serum (Hyclone)) with FGF-2 addition every 12h with daily media changes. For proliferation experiments, MM14 cells were passaged and plated at 1,000 cells/well in gelatin-coated, black, clear-bottom 96-well plates to triplicate wells. Passaging removes exogenous FGF-2. Cells were returned to growth media with additional reagents as described for each experiment. To inhibit sulfation of heparan sulfate, 60 nM Sodium chlorate (NaClO<sub>3</sub>) was added upon plating. To measure Bromodeoxyuridine (BrdU) incorporation, the BrdU Cell Proliferation Assay, HTS (Calbiochem HTS01) was used. Cells were cultured for 12h post-passage (one MM14 cell cycle), BrdU was added and cells were cultured for 24h. The assay kit was used to stain incorporated BrdU with anti-BrdU antibody, which was labeled with a secondary antibody

conjugated to horse radish peroxidase. Addition of peroxidase substrate produced a soluble, fluorescent product that was detected by 96-well plate fluorimeters. Additionally, MM14 cells were cultured in different media conditions to determine Pax7 retention and differentiation. For these experiments, cells were passaged and plated in growth media at 1,000 cells/well in triplicate wells. Reagents were added as described for each experiment, with FGF-2 added every 12h and media changed daily. Cells were fixed at 48h in 4% paraformaldehyde, immunostained then visualized.

Satellite cells were prepared as previously described (Pisconti et al., 2010; Troy et al., 2012). In brief, hind-limb skeletal muscles from mice were harvested, minced, digested with collagenase type I (Worthington) for 1h 15min at 37°C and filtered. Satellite cells were either purified from nonmyogenic cells and debris by 1) density centrifugation through a 40%/70% Percoll (GE Life Sciences) gradient or 2) overnight preplating on uncoated plates followed by 1d culture on gelatin-coated plates. Cells were cultured in growth media (F12-C + 15% horse serum)  $\pm$  1.5 nM FGF-2 at 6% O<sub>2</sub> with daily medium changes. For the culture of 3D hydrogels containing 10mer and 18mer heparin, cells were cultured in 18% O<sub>2</sub> (University of Liverpool).

To isolate live myofibers, whole hindlimb skeletal muscle was dissected, taking care to remove gross fat and connective tissue. Muscles were digested in F12-C and collagenase type I for 1.5h. Collagenase activity was quenched by transfer to plates of growth medium. Live myofibers were collected with a fire-polished glass pipette. Myofibers were transferred to 3-5 plates of growth medium to remove debris. Myofibers were then cultured in growth medium with 1.5 nM FGF-2 at 6% O<sub>2</sub> with daily medium changes. For heparitinase digestion, myofibers were fixed in 4% paraformaldehyde then Heparitinase I was used at 5 mU at 37°C for 10 min.

For cell and hydrogel cultures, reagents were added as described in the text.

Unfragmented heparin (sodium salt from porcine intestinal mucosa) was used at 0-100 ug/ml (Sigma-Aldrich). For hydrogel encapsulation high and low molecular weight heparin was used at 10 ug/ml. Heparin fragments and desulfated heparin fragments were provided by Yassir Ahmed in the Turnbull laboratory (University of Liverpool). These were generated, as described (Powell et al., 2010; Puvirajesinghe et al., 2012), by heparinase digestion and fractionation by gel filtration chromatography from heparin sodium salt from porcine intestinal mucosa.

### **Hydrogel Formation and Culture**

Hydrogel studies were performed in collaboration with Anseth lab members April Kloxin and Melissa Pope, who generated peptides, hydrogels and hydrogel materials. They also imaged hydrogels.

For 2D hydrogel experiments, hydrogels were formed by mixing a base monomer solution (6 wt% 4-arm (poly)ethylene glycol (PEG) norbornene with 0.05 wt% initiator (Irgacure 2959), 10 mM MMP-cleavable, dicysteine crosslinking peptide KKCGGPQGIWGQGCKK (Fairbanks et al., 2009) with extracellular matrix protein pendant peptides, extracellular matrix proteins, heparin or FGF-2. The solution was injected into a rubber mold which produces 20-30  $\mu$ l hydrogels and polymerized under a UVP Black-Ray UV Benchtop Lamp 115 V (Fisher UVP95 0045 04) with Sankyo-Denki Blacklight blue bulb centered at 352 nm (5-10 mW/cm<sup>2</sup>) for ~ 3 min. Hydrogels were then washed and placed into uncoated 24-well tissue culture plastic plates with growth media for 1 h. Hydrogels were again washed with growth media. Pre-plated satellite cells were added to hydrogels at ~10,000 cells/well. Hydrogels were maintained in growth media (without FGF-2 except where described in figures) through 6d with daily media

changes. Hydrogels were fixed in 4% paraformaldehyde for 15 min and washed in phosphate-buffered saline.

For 3D hydrogel experiments, hydrogels were formed as described above except satellite cells were added to the PEG solution before polymerization. The peptides RGDS, IKVAV and DGEA (Figure 3-14, 3-15) and RGDS (Figure 3-16) were added to the PEG monomer solution. Percoll-isolated satellite cells were washed several times in growth media then in Dulbecco's phosphate-buffered saline. Cells were collected to a pellet by centrifugation then resuspended to a single cell solution of 750,000 cells/ml in the PEG monomer solution. Hydrogels were polymerized as described, moved to tissue culture plates, then washed several times in growth media. After 1-2h, media was changed to remove any un-polymerized material from the hydrogel. Hydrogels were maintained in growth media with FGF-2 through 6d with daily media changes. Hydrogels were fixed in 4% paraformaldehyde for 15 min and washed in phosphate-buffered saline. For initial experiments, 5-10 wt% PEG hydrogels were tested with satellite cells. However 5 %wt PEG hydrogels degraded too rapidly, and 10 wt% PEG hydrogels inhibited satellite cell proliferation. Lower cell densities were also tested, but encapsulated cells neither died nor proliferated.

Additional reagents were added to the base PEG solution as follows. Monocysteine tether peptides CGDGEAG (Collagen, modified to increase solubility), KKKKCGIKVAV (Laminin, modified to increase solubility) and CRGDS (Fibronectin) (integrin-binding sequences underlined) were added at 2mM and were produced in the Anseth laboratory (synthesized using a peptide synthesizer (Applied Biosystems or Protein Technologies Inc.), purified by HPLC, and molecular weight verified by MALDI-mass spectroscopy). For hydrogels containing multiple peptides, tether peptides were added to a total concentration of 2mM. Fibronectin (BD

Biosciences 354008, from human plasma) and Laminin (BD Biosciences 354232, from mouse tumor cells) were added at 300 nM, except for the Laminin concentration curve experiment where Laminin was added at 150-600 nM. Heparin was added at 10  $\mu$ g/ml. FGF-2 was added at 1.5 nM.

Satellite cell survival post-encapsulation was determined by staining hydrogels with ethidium homodimer-1 (Invitrogen, LIVE/DEAD Cytotoxicity Assay).

### **Immunofluorescence**

All cells and hydrogels were fixed in 4% paraformaldehyde and permeabilized as necessary with 0.1% Triton X-100 (cells) or 1% Triton X-100 (hydrogels). All slides were blocked in 5% bovine serum albumin (BSA) 1h at RT and stained in 3% BSA. Primary antibodies were incubated at 4°C overnight, and secondary antibodies incubated 1h at RT. Nuclei were stained with 4',6-diamidino-2-phenylindole (DAPI). The following primary antibodies were used: chicken Syndecan-4 (1:500), mouse Pax7 (Developmental Hybridoma Bank at Iowa University, 1:5), rabbit MyoD (C-20, Santa Cruz Biotechnologies, sc-304, 1:400), goat Myogenin (N-20, Santa Cruz Bioltechnologies, 1:100), mouse heparan sulfate 10E4 (1:100), mouse heparan sulfate 3G10 (1:100). AlexaFluor 488-, 555-, and 647-conjugated secondary antibodies (Invitrogen) were used at 1:500. The mounting medium for cells and sections was Vectashield Mounting Medium (Vector). Hydrogels were imaged on a confocal LSM 710 microscope (Carl Zeiss) at 20x magnification (water immersion, N.A. 1) or on a real-time (live imaging) microscope with enclosure maintained at 37°C and 6% O<sub>2</sub>. Images were processed then scored with blinding in ImageJ64. As necessary, the brightness and contrast were adjusted linearly for the entire image and adjusted equivalently across the experimental image

set.

### **Microarrays and Analysis**

The tibialis anterior muscles of 3-month-old female B6D2F1/J mice were injured by injection with 50  $\mu$ L 1.2% BaCl<sub>2</sub> in saline at 12h, 24h or 48h before tissue harvest. The uninjured contralateral tibialis anterior was used for the 0h time point. The tibialis anterior muscles were dissected from the hindlimb, minced, and digested in 400 U/mL collagenase in Ham's F-12C at 37°C for 1h. Cells were filtered through 70 $\mu$ m and 40 $\mu$ m cell strainers (BD Falcon) to remove debris. Cells were centrifuged and the cell pellets were incubated at 4°C with 1:100 rabbit anti-Syndecan-3 antibody in F-12C with 15% horse serum followed by an incubation on ice with Cy5 conjugated anti-rabbit-IgG (Molecular Probes). Satellite cells were sorted by Syndecan-3 immunoreactivity on a MoFlo Legacy cell sorter (Dako Cytomation) into RNA lysis buffer (PicoPure RNA Isolation kit, Arcturus).

RNA was isolated from satellite cells using the PicoPure RNA Isolation kit (Arcturus) followed by two rounds of linear T7-based amplification (RiboAmp HA kit: Arcturus). The RNA equivalent of 5000 cells was hybridized to Affymetrix mouse 430v2 GeneChips (MOE430v2) according to manufacturers' instructions. GeneChips were scanned at the University of Colorado at Boulder on an Affymetrix GeneChip Scanner 3000 and spot intensities were recovered in the GeneChip Operating System (Affymetrix).

All analysis was performed using Spotfire Decision Site 2 for Microarray Analysis. Raw CEL data files (from three experiments) were normalized using GC Robust Multi-array Analysis (GCRMA). All transcripts related to proteoglycans and glycosaminoglycans were converted to log<sub>2</sub> and analyzed for significant changes in expression greater than 2-fold between time points.

The significance between time points was determined using multifactor analysis of variance (ANOVA) with a false discovery rate (FDR)  $\leq 0.05$  and Bonferroni adjustment. For genes covered by multiple probesets, the highest significant fold-change is reported.

## **Chapter 4: Discussion**

## INTRODUCTION

Adult stem cell populations are maintained by self-renewal where stem cells interact with their niche to undergo asymmetric or symmetric divisions (Yamanaka et al., 2001). Stem cells typically divide rarely or slowly throughout an organism's lifetime to prevent DNA damage and cellular senescence (Hayflick, 2000; Finkel and Holbrook, 2000). While stem cells are protected from the stresses of prolonged proliferation, stem cell function inevitably declines as organisms age (López-Otín et al., 2013).

Satellite cells are the resident skeletal muscle stem cells that maintain muscle and repair skeletal muscle. Skeletal muscle is dynamic, capable of hypertrophy or hypotrophy depending on use or injury, and skeletal muscle is continuously maintained as well as regenerated after injury (Booth et al., 1982; Smith et al., 2001; Favier et al., 2008; Ambrosio et al., 2009). In normal muscle, satellite cells divide infrequently to maintain skeletal muscle by replacing the terminally differentiated myonuclei (Smith et al., 2001; Oustanina et al., 2004; Dhawan and Rando, 2005). More satellite cells are recruited when necessary to repair skeletal muscle damaged by muscle use and injury (Caldwell et al., 1990; Rantanen et al., 1995; Smith et al., 2001; Ambrosio et al., 2009). Satellite cell divisions produce self-renewing satellite cells (Zammit et al., 2004; Sacco et al., 2008; Hall et al., 2010) and myoblasts, the transit-amplifying muscle precursor cells, that eventually exit the cell cycle and terminally differentiate to repair myofibers (Schultz et al., 1994). Satellite cell numbers and regenerative capacity decline with aging as satellite cells eventually lose the capacity to maintain and repair muscle after injury (Grounds, 1998; Gopinath and Rando, 2008).

In the first part of my thesis, I examine the underlying causes of declining activity in

aging satellite cells and confirm that old satellite cells are less capable of self-renewal. I demonstrate that is a cell-autonomous loss of old satellite cell self-renewal that cannot be counteracted by exposure to a young muscle environment, which contradicts previous research finding that the aged environment underlies the altered activity of old satellite cells. I find that decreased FGF signaling and a loss of asymmetric activation of phospho-p38 $\alpha\beta$  drive the loss of self-renewal in old satellite cells. The decline in asymmetric division in old satellite cells provides further evidence that asymmetric division may be the dominant mechanism of satellite cell maintenance (Kuang et al., 2007; Troy et al., 2012). I establish that FGF signaling promotes satellite cell self-renewal by asymmetric division, although the relationship between FGF signaling and asymmetric activation of p38 $\alpha\beta$  MAPK is not understood.

In the second part of my thesis, I develop 2D and 3D degradable, 4-arm PEG norbornene hydrogels as artificial satellite cell niches in culture to further study how the niche regulates satellite cell self-renewal. This degradable hydrogel platform (developed by the Anseth laboratory) inhibits terminal differentiation and myotube formation in contrast with other types of hydrogels used for muscle cell culture that often increase differentiation. I optimize the composition of this degradable hydrogel platform by addition of niche components described in the muscle literature to increase satellite cell self-renewal in culture. Specifically, I screen ECM proteins, growth factors, and a heparin library for conditions that promote the expansion of the Pax7<sup>+</sup>/MyoD<sup>-</sup> population and observe that laminin or IKVAV peptide addition best maintains satellite cell self-renewal. In the heparin library, I find that both fragment length and sulfation pattern affect FGF-driven satellite cell self-renewal and demonstrate that functional heparin sequences can be incorporated into hydrogels. My research establishes that using hydrogel

culture and heparin libraries reveal mechanisms that drive satellite cell self-renewal. In future experiments, I will develop hydrogels as tools to promote self-renewal for therapeutic assays such as intramuscular transplantation studies.

### **Both cell intrinsic and extrinsic alterations disrupt self-renewal in aged satellite cells**

Satellite cells isolated from old skeletal muscle exhibit impaired satellite cell activity *in vitro* and *in vivo*. I find half as many old satellite cells as young satellite cells on freshly isolated myofibers acquired from hindlimb muscle, which agrees with the reports that satellite cell numbers decline in aging muscle (Snow, 1977; Gibson and Schultz, 1983; Conboy et al., 2003; Sajko et al., 2004; Brack et al., 2005; Shefer et al., 2006; Chakkalakal et al., 2012). The cycling population of satellite cells expands in old muscle as the dividing cells cannot return to quiescence (Chakkalakal et al., 2012), which agrees with my observation that markers of activation are elevated in old satellite cells within 1h of isolation. I observe that proliferation and Pax7 expression decline while differentiation increases in old satellite cells. The decline in Pax7<sup>+</sup>/MyoD<sup>-</sup> cells represents a loss of satellite cell self-renewal as demonstrated by using transplantation assays in parallel with AraC survival and CFDA-SE label retention assays in culture. These assays highlight the importance of translating techniques from other stem cell fields to muscle research as engraftment after transplantation, label retention and AraC survival are better indicators of stem cell activity than simply measuring Pax7<sup>+</sup> and MyoD<sup>+</sup> populations (Troy et al., 2012).

The molecular basis of impaired satellite cell function in aging muscle is unclear. Heterochronic transplantation, into immunosuppressed or diseased mice, and parabiosis experiments suggest that the aged muscle environment impairs satellite cell function rather than

cell-autonomous defects in old satellite cells (Carlson and Faulkner, 1989). However, growing evidence demonstrates that the young environment is not sufficient to rescue old satellite cell activity (Chakkalakal et al., 2012) (Chapter 2). My transplantation assay further challenges old satellite cell self-renewal by transplanting donor cells into immunosufficient, wildtype hosts where old satellite cells compete with 'healthy,' young satellite cells for niche occupancy.

Transplantation to an immunocompetent, healthy host reveals that there are cell-autonomous defects underlying impaired activity in old cells.

### **Dysregulated FGF and p38 signaling drive the loss of self-renewal in old satellite cells**

Asymmetric division appears to maintain the satellite cell population in young satellite cell cultures (Kuang et al., 2007; Troy et al., 2012) while symmetric division that clonally expands the satellite cell population accounts for a limited number of divisions in culture (Le Grand et al., 2009). Polar distribution of the Par-3/phospho-p38 $\alpha\beta$  complex across a dividing satellite cell results in asymmetric division, which produces opposite fates in the daughter cells (Troy et al., 2012). Elevated levels of phospho-p38 $\alpha\beta$  in old satellite cells appear to prevent asymmetric segregation of the Par-3/phospho-p38 $\alpha\beta$  complex, resulting in two phospho-p38 $\alpha\beta$ <sup>+</sup> daughter cells. Phospho-p38 $\alpha\beta$  in both daughter cells induces MyoD translation (Hausburg, Thesis), entry into the cell cycle, and commitment to a myogenic fate. Each time elevated phospho-p38 $\alpha\beta$  prevents asymmetric division in old satellite cell the quiescent population declines. However, I demonstrate that loss of self-renewal in old satellite cells is reversible as partial inhibition of p38 $\alpha\beta$  MAPK reduces phospho-p38 $\alpha\beta$  to rescue asymmetric distribution of phospho-p38 $\alpha\beta$  in the dividing cell. Perhaps, this culture treatment can be developed for use *in vivo* to treat sarcopenia.

FGF signaling is altered in aging muscle and in aging satellite cells. FGF-2 protein and

FGF-2 transcripts in myofibers increase in the myofiber niche of old muscle (Chakkalakal et al., 2012), suggesting that FGF-2-mediated signaling is altered in aging satellite cells. Inhibition of FGF signaling by injection of SU5402-beads or genetic knockout of Sprouty1, an inhibitor of MAPK pathways and FGF signaling (Hacohen et al., 1998), reduces the number of inappropriately cycling satellite cells and increases regeneration in aging muscle (Chakkalakal et al., 2012). Thus, increased FGF signaling appears to prevent satellite cells from returning to quiescence and begins to exhaust the aging satellite cell pool. Yet, both SU5402 and Sprouty1 are promiscuous inhibitors that may target other signaling pathways. SU5402 inhibits the activation of multiple growth factor receptors, including FGFR and vascular endothelial growth factor receptor (VEGFR), which regulates angiogenesis during muscle regeneration (Sun et al., 1999; Abou-Khalil et al., 2010). Sprouty1 may target multiple signaling pathways and may inhibit multiple targets, including targets not involved in receptor tyrosine kinase signaling (Hacohen et al., 1998; Choi et al., 2006). I demonstrate that constitutive activation of FGFR1 rescues self-renewal in old satellite cells, so I propose that increased FGF-2 in the aging niche is a feedback mechanism to overcome deficient FGF signal transduction. Instead of increased FGF signaling preventing quiescence in old cells (Chakkalakal et al., 2012), attenuated FGF signaling underlies the loss of self-renewal in old satellite cells.

Restoring FGFR1 activation in old satellite cells *in vivo* will address whether FGF signaling is an underlying cause of aged satellite cell impairment. We are currently generating and aging mice that will express FGFR1 under the control of a tetracyclin operator in Pax7-expressing cells, which will restrict exogenous FGFR1 activation to the satellite cell population (Murphy et al., 2011). I expect that inducing FGFR1 activation in aging satellite cells will

expand the self-renewing population and improve muscle regeneration.

Atypical p38 $\alpha\beta$  MAPK activity in old satellite cells correlates with attenuated FGF-2/FGFR signaling, which suggests that FGF signaling may regulate asymmetric division. FGF signaling is required for satellite cell self-renewal as constitutive FGFR1 activation increases self-renewal while pharmacological inhibition of FGF signaling and genetic ablation of FGFR1 eliminate self-renewing cells (Troy, Thesis; Hall, Thesis). As FGF signaling increases self-renewal and activates p38 $\alpha\beta$  MAPK phosphorylation, which is required for asymmetric division in satellite cells, FGF signaling also regulates asymmetric segregation of phospho-p38 $\alpha\beta$ .

Members of the FGFR ternary complex may interact with the Par-3/p38 $\alpha\beta$  MAPK complex to promote self-renewal. Syndecan-4, an FGF co-receptor required for satellite cell activation and self-renewal (Cornelison et al., 2004), often segregates with asymmetrically distributed phospho-p38 $\alpha\beta$  in satellite cells (Troy et al., 2012). Asymmetric distribution of Syndecan-4 on the satellite cell membrane could activate FGFR1 only in the region of the Par-3/p38 $\alpha\beta$  MAPK to restrict further p38 $\alpha\beta$  MAPK activation to one membrane. Future studies using the proximity ligation assay (PLA) will reveal if direct interaction between activated FGFR1 or Syndecan-4 and the Par-3/p38 $\alpha\beta$  MAPK complex. Intriguingly, JAM-A, a member of the protein family that anchors the Par complex to the membrane during asymmetric division, has an essential role in FGF-2 induced blood vessel formation (Cooke et al., 2006), which suggests that JAMs could interact with the FGF pathway in other cell types such as satellite cells. A JAM family member may interact with the FGF-Heparan sulfate-FGFR ternary complex to link FGF activation with segregation of the Par-3/p38 $\alpha\beta$  MAPK complex.

A remaining question is whether mechanisms of satellite cell self-renewal identified *in*

*vitro* represent self-renewal *in vivo*. Wnt7a (Le Grand et al., 2009), Notch1 (Kuang et al., 2007) and FGF-2/p38 $\alpha$  $\beta$  MAPK (Troy et al., 2012) signaling drive symmetric (Wnt) and asymmetric divisions (Notch, p38 $\alpha$  $\beta$  MAPK) in myofiber-associated satellite cells. Furthermore, the satellite cell population contains subpopulations (Beauchamp et al., 2000; Kuang et al., 2007; Tanaka et al., 2009) that may act as satellite cell stem cells while the majority of satellite cells produce transit-amplifying daughter cells. Perhaps, all of these mechanisms contribute to self-renewal *in vivo* to meet the needs of dynamic muscle tissue. The severity of muscle injury may regulate the level of Wnts and FGFs released to the niche, which would affect the proportion of satellite cells undergoing asymmetric divisions or symmetric divisions. In resting muscle or after mild myotrauma, asymmetric division may be sufficient to maintain the number of quiescent satellite cells. However, severe injury may require that satellite cells symmetrically divide to expand the satellite cell population and to produce enough myoblasts to rapidly regenerate muscle, so severe muscle injury could release high levels of Wnt7a to prompt the satellite cell pool to undergo such symmetric divisions.

Life-long stem cell maintenance may require plasticity in the fate of individual stem cells to maintain a homeostatic population *in vivo* (Simons and Clevers, 2011). Multiple mechanisms of self-renewal may maintain the satellite cell population in skeletal muscle through variable muscle use and health over the course of a lifetime. In future studies, lineage tracing and population modeling should reveal if asymmetric division and symmetric division occur primarily in different muscle states such as in resting muscle or after exercise, injury and aging. Additionally, lineage tracing may determine whether the satellite cell subpopulations represent a conserved stem cell lineage or whether interactions with the satellite cell niche create a stem cell

subpopulation.

### **Optimizing degradable hydrogels as an artificial satellite cell niche**

Satellite cells reside in a polar niche, formed by the basal lamina and the myofiber plasma membrane, which regulates satellite cell self-renewal (Dhawan and Rando, 2005; Kuang et al., 2007; Le Grand et al., 2009; Hall et al., 2010). Satellite cells in culture undergo self-renewal by both asymmetric (FGF, Notch-Delta) and symmetric (Wnt7a) divisions (Kuang et al., 2007; Le Grand et al., 2009; Troy et al., 2012). The interaction between satellite cells and the myofiber niche may regulate satellite cell self-renewal to produce a planar-oriented division (symmetric) along the myofiber or an apical-basal oriented division (asymmetric) (Conboy and Rando, 2002; Shinin et al., 2006; Kuang et al., 2007; Le Grand et al., 2009; Troy et al., 2012) (Figure 1.2). The availability and presentation of Delta, FGF and Wnt in the niche may determine the plane of division in individual cells. However, the molecular mechanisms that induce asymmetric and symmetric division are difficult to study *in vivo*. I have developed hydrogels as artificial satellite cell niches to study the molecular mechanisms promoting self-renewal in culture.

2D and 3D hydrogels with tunable elastic moduli and controlled incorporation of signaling ligands can mimic stem cell niches to allow study of the environmental regulation of stem cell activity (Discher et al., 2009; Lutolf et al., 2009; Saha et al., 2007; Sands and Mooney, 2007). Poly(ethylene glycol) (PEG)-based hydrogels are particularly ideal for controlling satellite cell-niche interactions. PEG scaffolds are resistant to cell adhesion mediated by protein adsorption but instead allow for controlled presentation of ligands to cells. Tethering ligands to the scaffold more closely mimics the orientation of signals in the niche than adding growth factors to culture media or coating structural proteins to plastic plates (Langsdorf et al., 2007).

PEG hydrogels can mimic the elastic modulus of healthy resting muscle that is optimal for myogenic differentiation in culture (Collinsworth et al., 2002; Engler et al., 2004; Boonen et al., 2009). PEG hydrogel may be photodegradable to allow temporal control of hydrogel stiffness (Kloxin et al., 2009) or may incorporate degradable motifs to allow cells to modify the scaffold, which could recapitulate the progression of structural changes associated with muscle disease and aging in hydrogel-based satellite cell culture. These characteristics of PEG hydrogels make possible a systematic analysis of the role of specific niche components, which could not be achieved in explanted satellite cell or myofiber culture.

The degradable, 4-arm PEG norbornene hydrogels developed by the Anseth laboratory maintain satellite cell self-renewal and prevents differentiation of satellite cell cultures. I have begun to screen biochemical (growth factors, heparin sequences) and structural (ECM proteins) cues present in the putative satellite cell niche to discover which components of the niche promote self-renewal. These glycans and proteins are difficult to screen efficiently using our current 2D and 3D hydrogel design. Coating macromolecules to 96-well plastic plates to increase screening efficiency can not recapitulate the localization of macromolecules in hydrogel culture, which is now known to affect satellite cell fate (Chapter 3). Instead, I plan to develop a 96-well hydrogel platform similar to microwell-patterned hydrogels (Gilbert et al., 2010) for real-time imaging to track the divisions of satellite cells expressing a transgenic reporter. This system will serve as a high-throughput hydrogel screen of self-renewal and would allow tracking of asymmetric and symmetric divisions. Developing a high-throughput hydrogel screen would allow me to efficiently characterize a much larger set of niche components and allow me to study how satellite cells respond to multiple cues in a niche.

I have identified heparin sequences, from a library provided by the Turnbull laboratory, that promote satellite cell self-renewal and which can be incorporated into hydrogel culture. This work does not attempt to model *in vivo* heparan sulfate activity as the short sequences in heparin libraries cannot recapitulate the specificity and complexity of binding sites in the long heparan sulfate chains present in the satellite cell niche (Sasisekharan and Venkataraman, 2000). In decades to come, improved sequencing of *in vivo* heparan sulfates chains (Huang et al., 2013) and phage display-derived heparan sulfate antibody libraries (Jenniskens et al., 2000; Kurup et al., 2007) may reveal how heparan sulfate function and localization in the satellite cell niche. For now, the results of this heparin screen and the many biochemical studies reported in the literature are better used to develop stem cell therapies for regenerative medicine such as hydrogel platforms for satellite cells.

### **Summary**

Satellite cells exhibit an impressive capacity to maintain and regenerate skeletal muscle by generating proliferating myoblasts while repopulating the satellite cell population by self-renewal. Satellite cells reside within an anatomically-defined niche, consisting of the myofiber and other cells, biochemical components released from local and systemic sources, and structural components. The complex interactions between satellite cells and the niche maintain satellite cell self-renewal although the mechanisms that regulate self-renewal remain unclear. Accumulating cellular and molecular damage from aging disrupt the interactions in the satellite cell niche, resulting in impaired satellite cell activity and muscle function. Skeletal muscle deterioration ultimately leads to frailty and increased risk of death.

## References

Abou-Khalil, R., Mounier, R., and Chazaud, B. (2010). Regulation of myogenic stem cell behavior by vessel cells: the "ménage à trois" of satellite cells, periendothelial cells and endothelial cells. *Cell Cycle* 9, 892-96.

Afilalo, J., Karunanathan, S., Eisenberg, M.J., Alexander, K.P., and Bergman, H. (2009). Role of frailty in patients with cardiovascular disease. *The American journal of cardiology* 103, 1616-621.

Allen, R.E., and Boxhorn, L.K. (1989). Regulation of skeletal muscle satellite cell proliferation and differentiation by transforming growth factor-beta, insulin-like growth factor I, and fibroblast growth factor. *J Cell Physiol* 138, 311-15.

Allen, R.E., McAllister, P.K., and Masak, K.C. (1980). Myogenic potential of satellite cells in skeletal muscle of old rats. A brief note. *Mechanisms of ageing and development* 13, 105-09.

Allen, R.E., Sheehan, S.M., Taylor, R.G., Kendall, T.L., and Rice, G.M. (1995). Hepatocyte growth factor activates quiescent skeletal muscle satellite cells in vitro. *J Cell Physiol* 165, 307-312.

Aloisi, M., Mussini, I., and Schiaffino, S. (1973). Activation of muscle nuclei in denervation and hypertrophy. *Basic Research in Myology* , 338-342.

Ambrosio, F., Kadi, F., Lexell, J., Fitzgerald, G.K., Boninger, M.L., and Huard, J. (2009). The effect of muscle loading on skeletal muscle regenerative potential: an update of current research findings relating to aging and neuromuscular pathology. *Am J Phys Med Rehabil* 88, 145-155.

Anderson, J., and Pilipowicz, O. (2002). Activation of muscle satellite cells in single-

fiber cultures. *Nitric Oxide* 7, 36-41.

Baumgartner, R.N., Koehler, K.M., Gallagher, D., Romero, L., Heymsfield, S.B., Ross, R.R., Garry, P.J., and Lindeman, R.D. (1998). Epidemiology of sarcopenia among the elderly in New Mexico. *American journal of epidemiology* 147, 755-763.

Beauchamp, J.R., Heslop, L., Yu, D.S., Tajbakhsh, S., Kelly, R.G., Wernig, A., Buckingham, M.E., Partridge, T.A., and Zammit, P.S. (2000). Expression of CD34 and Myf5 defines the majority of quiescent adult skeletal muscle satellite cells. *J Cell Biol* 151, 1221-234.

Beccafico, S., Puglielli, C., Pietrangelo, T., Bellomo, R., Fanò, G., and Fulle, S. (2007). Age-dependent effects on functional aspects in human satellite cells. *Ann N Y Acad Sci* 1100, 345-352.

Bernfield, M., Götte, M., Park, P.W., Reizes, O., Fitzgerald, M.L., Lincecum, J., and Zako, M. (1999). Functions of cell surface heparan sulfate proteoglycans. *Annual review of biochemistry* 68, 729-777.

Bink, R.J., Habuchi, H., Lele, Z., Dolk, E., Joore, J., Rauch, G.J., Geisler, R., Wilson, S.W., den Hertog, J., et al. (2003). Heparan sulfate 6-o-sulfotransferase is essential for muscle development in zebrafish. *J Biol Chem* 278, 31118-127.

Bintliff, S., and Walker, B.E. (1960). Radioautographic study of skeletal muscle regeneration. *American Journal of Anatomy* 106, 233-245.

Bischoff, R. (1990). Interaction between satellite cells and skeletal muscle fibers. *Development* 109, 943-952.

Bishop, J.R., Schuksz, M., and Esko, J.D. (2007). Heparan sulphate proteoglycans fine-tune mammalian physiology. *Nature* 446, 1030-37.

Bishop, N.A., Lu, T., and Yankner, B.A. (2010). Neural mechanisms of ageing and cognitive decline. *Nature* 464, 529-535.

Bjornson, C.R., Cheung, T.H., Liu, L., Tripathi, P.V., Steeper, K.M., and Rando, T.A. (2012). Notch signaling is necessary to maintain quiescence in adult muscle stem cells. *Stem Cells* 30, 232-242.

Blais, A., Tsikitis, M., Acosta-Alvear, D., Sharan, R., Kluger, Y., and Dynlacht, B.D. (2005). An initial blueprint for myogenic differentiation. *Genes Dev* 19, 553-569.

Boonen, K.J., Rosaria-Chak, K.Y., Baaijens, F.P., van der Schaft, D.W., and Post, M.J. (2009). Essential environmental cues from the satellite cell niche: optimizing proliferation and differentiation. *Am J Physiol Cell Physiol* 296, C1338-345.

Booth, F.W., Nicholson, W.F., and Watson, P.A. (1982). Influence of muscle use on protein synthesis and degradation. *Exercise and sport sciences reviews* 10, 27-48.

Bortoli, S., Renault, V., Eveno, E., Auffray, C., Butler-Browne, G., and Pietu, G. (2003). Gene expression profiling of human satellite cells during muscular aging using cDNA arrays. *Gene* 321, 145-154.

Bortoluzzi, S., Scannapieco, P., Cestaro, A., Danieli, G.A., and Schiaffino, S. (2006). Computational reconstruction of the human skeletal muscle secretome. *Proteins* 62, 776-792.

Brack, A.S., Bildsoe, H., and Hughes, S.M. (2005). Evidence that satellite cell decrement contributes to preferential decline in nuclear number from large fibres during murine age-related muscle atrophy. *J Cell Sci* 118, 4813-821.

Brack, A.S., Conboy, I.M., Conboy, M.J., Shen, J., and Rando, T.A. (2008). A temporal switch from notch to Wnt signaling in muscle stem cells is necessary for normal adult

myogenesis. *Cell Stem Cell* 2, 50-59.

Brack, A.S., Conboy, M.J., Roy, S., Lee, M., Kuo, C.J., Keller, C., and Rando, T.A. (2007). Increased Wnt signaling during aging alters muscle stem cell fate and increases fibrosis. *Science* 317, 807-810.

Brien, P., Pugazhendhi, D., Woodhouse, S., Oxley, D., and Pell, J.M. (2013). P38 $\alpha$  MAPK Regulates Adult Muscle Stem Cell Fate By Restricting Progenitor Proliferation During Postnatal Growth And Repair. *Stem Cells*

Brooks, S.V., and Faulkner, J.A. (1990). Contraction-induced injury: recovery of skeletal muscles in young and old mice. *American Journal of Physiology-Cell Physiology* 258, C436-442.

Bröhl, D., Vasyutina, E., Czajkowski, M.T., Griger, J., Rassek, C., Rahn, H.P., Purfürst, B., Wende, H., and Birchmeier, C. (2012). Colonization of the satellite cell niche by skeletal muscle progenitor cells depends on Notch signals. *Dev Cell* 23, 469-481.

Bryant, S.J., and Anseth, K.S. (2003). Controlling the spatial distribution of ECM components in degradable PEG hydrogels for tissue engineering cartilage. *J Biomed Mater Res A* 64, 70-79.

Buas, M.F., and Kadesch, T. (2010). Regulation of skeletal myogenesis by Notch. *Exp Cell Res* 316, 3028-033.

Caldwell, C.J., Matthey, D.L., and Weller, R.O. (1990). Role of the basement membrane in the regeneration of skeletal muscle. *Neuropathol Appl Neurobiol* 16, 225-238.

Callister, W.D., and Rethwisch, D.G. (2013). *Fundamentals of materials science and engineering* (Wiley).

Campbell, J.S., Wenderoth, M.P., Hauschka, S.D., and Krebs, E.G. (1995). Differential activation of mitogen-activated protein kinase in response to basic fibroblast growth factor in skeletal muscle cells. *Proc Natl Acad Sci U S A* *92*, 870-74.

Carlson, B.M., and Faulkner, J.A. (1989). Muscle transplantation between young and old rats: age of host determines recovery. *American Journal of Physiology-Cell Physiology* *256*, C1262-66.

Carlson, M.E., Hsu, M., and Conboy, I.M. (2008). Imbalance between pSmad3 and Notch induces CDK inhibitors in old muscle stem cells. *Nature* *454*, 528-532.

Cawthon, P.M., Ensrud, K.E., Laughlin, G.A., Cauley, J.A., Dam, T.T., Barrett-Connor, E., Fink, H.A., Hoffman, A.R., Lau, E., et al. (2009). Sex hormones and frailty in older men: the osteoporotic fractures in men (MrOS) study. *J Clin Endocrinol Metab* *94*, 3806-815.

Chakkalakal, J.V., Jones, K.M., Basson, M.A., and Brack, A.S. (2012). The aged niche disrupts muscle stem cell quiescence. *Nature*

Chaves, P.H., Semba, R.D., Leng, S.X., Woodman, R.C., Ferrucci, L., Guralnik, J.M., and Fried, L.P. (2005). Impact of anemia and cardiovascular disease on frailty status of community-dwelling older women: the Women's Health and Aging Studies I and II. *J Gerontol A Biol Sci Med Sci* *60*, 729-735.

Chen, S., Lewallen, M., and Xie, T. (2013). Adhesion in the stem cell niche: biological roles and regulation. *Development* *140*, 255-265.

Chen, S.E., Jin, B., and Li, Y.P. (2007). TNF-alpha regulates myogenesis and muscle regeneration by activating p38 MAPK. *Am J Physiol Cell Physiol* *292*, C1660-671.

Choi, H., Cho, S.-Y., Schwartz, R.H., and Choi, K. (2006). Dual effects of Sprouty1 on

TCR signaling depending on the differentiation state of the T cell. *The Journal of Immunology* *176*, 6034-045.

Christov, C., Chrétien, F., Abou-Khalil, R., Bassez, G., Vallet, G., Authier, F.J., Bassaglia, Y., Shinin, V., Tajbakhsh, S., et al. (2007). Muscle satellite cells and endothelial cells: close neighbors and privileged partners. *Mol Biol Cell* *18*, 1397-1409.

Christov, C., Chrétien, F., Abou-Khalil, R., Bassez, G., Vallet, G., Authier, F.-J., Bassaglia, Y., Shinin, V., Tajbakhsh, S., et al. (2007). Muscle satellite cells and endothelial cells: close neighbors and privileged partners. *Mol Biol Cell* *18*, 1397-1409.

Clegg, C.H., Linkhart, T.A., Olwin, B.B., and Hauschka, S.D. (1987). Growth factor control of skeletal muscle differentiation: commitment to terminal differentiation occurs in G1 phase and is repressed by fibroblast growth factor. *J Cell Biol* *105*, 949-956.

Clegg, C.H., Linkhart, T.A., Olwin, B.B., and Hauschka, S.D. (1987). Growth factor control of skeletal muscle differentiation: commitment to terminal differentiation occurs in G1 phase and is repressed by fibroblast growth factor. *J Cell Biol* *105*, 949-956.

Cohen, M.W., Hoffstrom, B.G., and DeSimone, D.W. (2000). Active zones on motor nerve terminals contain alpha 3beta 1 integrin. *J Neurosci* *20*, 4912-921.

Collins, C.A., Zammit, P.S., Ruiz, A.P., Morgan, J.E., and Partridge, T.A. (2007). A population of myogenic stem cells that survives skeletal muscle aging. *Stem Cells* *25*, 885-894.

Collinsworth, A.M., Zhang, S., Kraus, W.E., and Truskey, G.A. (2002). Apparent elastic modulus and hysteresis of skeletal muscle cells throughout differentiation. *Am J Physiol Cell Physiol* *283*, C1219-227.

Conboy, I.M., and Rando, T.A. (2002). The regulation of Notch signaling controls

satellite cell activation and cell fate determination in postnatal myogenesis. *Dev Cell* 3, 397-409.

Conboy, I.M., Conboy, M.J., Smythe, G.M., and Rando, T.A. (2003). Notch-mediated restoration of regenerative potential to aged muscle. *Science* 302, 1575-77.

Conboy, I.M., Conboy, M.J., Wagers, A.J., Girma, E.R., Weissman, I.L., and Rando, T.A. (2005). Rejuvenation of aged progenitor cells by exposure to a young systemic environment. *Nature* 433, 760-64.

Conti, L., Pollard, S.M., Gorba, T., Reitano, E., Toselli, M., Biella, G., Sun, Y., Sanzone, S., Ying, Q.L., et al. (2005). Niche-independent symmetrical self-renewal of a mammalian tissue stem cell. *PLoS Biol* 3, e283.

Cooke, V.G., Naik, M.U., and Naik, U.P. (2006). Fibroblast growth factor-2 failed to induce angiogenesis in junctional adhesion molecule-A-deficient mice. *Arterioscler Thromb Vasc Biol* 26, 2005-011.

Coombe, D.R., and Kett, W.C. (2005). Heparan sulfate-protein interactions: therapeutic potential through structure-function insights. *Cell Mol Life Sci* 62, 410-424.

Cooper, R.N., Tajbakhsh, S., Mouly, V., Cossu, G., Buckingham, M., and Butler-Browne, G.S. (1999). In vivo satellite cell activation via Myf5 and MyoD in regenerating mouse skeletal muscle. *J Cell Sci* 112 (Pt 17), 2895-2901.

Cornelison, D.D., Filla, M.S., Stanley, H.M., Rapraeger, A.C., and Olwin, B.B. (2001). Syndecan-3 and syndecan-4 specifically mark skeletal muscle satellite cells and are implicated in satellite cell maintenance and muscle regeneration. *Dev Biol* 239, 79-94.

Cornelison, D.D., Wilcox-Adelman, S.A., Goetinck, P.F., Rauvala, H., Rapraeger, A.C., and Olwin, B.B. (2004). Essential and separable roles for Syndecan-3 and Syndecan-4 in skeletal

muscle development and regeneration. *Genes Dev* 18, 2231-36.

Cornelison, D.D.W., and Wold, B.J. (1997). Single-cell analysis of regulatory gene expression in quiescent and activated mouse skeletal muscle satellite cells. *Dev Biol* 191, 270-283.

Cosgrove, B.D., Sacco, A., Gilbert, P.M., and Blau, H.M. (2009). A home away from home: challenges and opportunities in engineering in vitro muscle satellite cell niches. *Differentiation* 78, 185-194.

Cosgrove, B.D., Sacco, A., Gilbert, P.M., and Blau, H.M. (2009). A home away from home: challenges and opportunities in engineering in vitro muscle satellite cell niches. *Differentiation* 78, 185-194.

Cousin, W., Ho, M.L., Desai, R., Tham, A., Chen, R.Y., Kung, S., Elabd, C., and Conboy, I.M. (2013). Regenerative Capacity of Old Muscle Stem Cells Declines without Significant Accumulation of DNA Damage. *PLoS One* 8, e63528.

Coutu, D.L., and Galipeau, J. (2011). Roles of FGF signaling in stem cell self-renewal, senescence and aging. *Aging (Albany NY)* 3, 920-933.

Crist, C.G., Montarras, D., and Buckingham, M. (2012). Muscle satellite cells are primed for myogenesis but maintain quiescence with sequestration of Myf5 mRNA targeted by microRNA-31 in mRNP granules. *Cell Stem Cell* 11, 118-126.

De Cristofaro, R., De Candia, E., and Landolfi, R. (1998). Effect of high- and low-molecular-weight heparins on thrombin-thrombomodulin interaction and protein C activation. *Circulation* 98, 1297-1301.

Cunningham, C., Wilcockson, D.C., Champion, S., Lunnon, K., and Perry, V.H. (2005).

Central and systemic endotoxin challenges exacerbate the local inflammatory response and increase neuronal death during chronic neurodegeneration. *J Neurosci* 25, 9275-284.

Daley, W.P., Peters, S.B., and Larsen, M. (2008). Extracellular matrix dynamics in development and regenerative medicine. *J Cell Sci* 121, 255-264.

Day, K., Shefer, G., Shearer, A., and Yablonka-Reuveni, Z. (2010). The depletion of skeletal muscle satellite cells with age is concomitant with reduced capacity of single progenitors to produce reserve progeny. *Dev Biol* 340, 330-343.

Decary, S., Mouly, V., Hamida, C.B., Sautet, A., Barbet, J.P., and Butler-Browne, G.S. (1997). Replicative potential and telomere length in human skeletal muscle: implications for satellite cell-mediated gene therapy. *Hum Gene Ther* 8, 1429-438.

DeForest, C.A., and Anseth, K.S. (2012). Advances in bioactive hydrogels to probe and direct cell fate. *Annu Rev Chem Biomol Eng* 3, 421-444.

Delehedde, M., Lyon, M., Gallagher, J.T., Rudland, P.S., and Fernig, D.G. (2002). Fibroblast growth factor-2 binds to small heparin-derived oligosaccharides and stimulates a sustained phosphorylation of p42/44 mitogen-activated protein kinase and proliferation of rat mammary fibroblasts. *Biochem J* 366, 235-244.

Dhawan, J., and Rando, T.A. (2005). Stem cells in postnatal myogenesis: molecular mechanisms of satellite cell quiescence, activation and replenishment. *Trends Cell Biol* 15, 666-673.

Ding, K., Yang, Z., Zhang, Y.L., and Xu, J.Z. (2013). Injectable thermosensitive chitosan/ $\beta$ -glycerophosphate/collagen hydrogel maintains the plasticity of skeletal muscle satellite cells and supports their in vivo viability. *Cell Biol Int*

Ding, X.W., Wu, J.H., and Jiang, C.P. (2010). ABCG2: a potential marker of stem cells and novel target in stem cell and cancer therapy. *Life Sci* 86, 631-37.

Discher, D.E., Mooney, D.J., and Zandstra, P.W. (2009). Growth factors, matrices, and forces combine and control stem cells. *Science* 324, 1673-77.

Durcova-Hills, G., Adams, I.R., Barton, S.C., Surani, M.A., and McLaren, A. (2006). The role of exogenous fibroblast growth factor-2 on the reprogramming of primordial germ cells into pluripotent stem cells. *Stem Cells* 24, 1441-49.

Ebnet, K., Suzuki, A., Horikoshi, Y., Hirose, T., Meyer Zu Brickwedde, M.K., Ohno, S., and Vestweber, D. (2001). The cell polarity protein ASIP/PAR-3 directly associates with junctional adhesion molecule (JAM). *EMBO J* 20, 3738-748.

Edgar, B.A. (2012). Intestinal stem cells: no longer immortal but ever so clever. *EMBO J* 31, 2441-43.

Engler, A.J., Griffin, M.A., Sen, S., Bönnemann, C.G., Sweeney, H.L., and Discher, D.E. (2004). Myotubes differentiate optimally on substrates with tissue-like stiffness: pathological implications for soft or stiff microenvironments. *J Cell Biol* 166, 877-887.

Engler, A.J., Griffin, M.A., Sen, S., Bönnemann, C.G., Sweeney, H.L., and Discher, D.E. (2004). Myotubes differentiate optimally on substrates with tissue-like stiffness: pathological implications for soft or stiff microenvironments. *J Cell Biol* 166, 877-887.

Esko, J.D., and Lindahl, U. (2001). Molecular diversity of heparan sulfate. *Journal of Clinical Investigation* 108, 169-173.

Esko, J.D., and Selleck, S.B. (2002). ORDER OUT OF CHAOS: Assembly of Ligand Binding Sites in Heparan Sulfate. *Annu Rev Biochem* 71, 435-471.

Esko, J.D., and Selleck, S.B. (2002). ORDER OUT OF CHAOS: Assembly of Ligand Binding Sites in Heparan Sulfate. *Annu Rev Biochem* 71, 435-471.

Eswarakumar, V.P., Lax, I., and Schlessinger, J. (2005). Cellular signaling by fibroblast growth factor receptors. *Cytokine Growth Factor Rev* 16, 139-149.

Evans, W.J., and Campbell, W.W. (1993). Sarcopenia and age-related changes in body composition and functional capacity. *The Journal of nutrition* 123, 465-68.

Evans, W.J., and Lexell, J. (1995). Human aging, muscle mass, and fiber type composition. *The Journals of Gerontology Series A: Biological Sciences and Medical Sciences* 50, 11.

Farina, N.H., Hausburg, M., Dalla Betta, N., Pulliam, C., Srivastava, D., Cornelison, D.D., and Olwin, B.B. (2012). A role for RNA post-transcriptional regulation in satellite cell activation. *Skelet Muscle* 2, 21.

Favier, F.B., Benoit, H., and Freyssenet, D. (2008). Cellular and molecular events controlling skeletal muscle mass in response to altered use. *Pflugers Arch* 456, 587-600.

Finkel, T., and Holbrook, N.J. (2000). Oxidants, oxidative stress and the biology of ageing. *Nature* 408, 239-247.

Fried, L.P., Tangen, C.M., Walston, J., Newman, A.B., Hirsch, C., Gottdiener, J., Seeman, T., Tracy, R., Kop, W.J., and Burke, G. (2001). Frailty in older adults evidence for a phenotype. *The Journals of Gerontology Series A: Biological Sciences and Medical Sciences* 56, M146-157.

Fuchs, E., Tumber, T., and Guasch, G. (2004). Socializing with the neighbors: stem cells and their niche. *Cell* 116, 769-778.

Fuchs, E., Tumber, T., and Guasch, G. (2004). Socializing with the neighbors: stem cells

and their niche. *Cell* 116, 769-778.

Galderisi, U., Peluso, G., Di Bernardo, G., Calarco, A., D'Apolito, M., Petillo, O., Cipollaro, M., Fusco, F.R., and Melone, M.A. (2013). Efficient cultivation of neural stem cells with controlled delivery of FGF-2. *Stem Cell Res* 10, 85-94.

Gallagher, J.T. (2001). Heparan sulfate: growth control with a restricted sequence menu. *J Clin Invest* 108, 357-361.

Gelse, K., Pöschl, E., and Aigner, T. (2003). Collagensó structure, function, and biosynthesis. *Advanced drug delivery reviews* 55, 1531-546.

Giancotti, F.G., and Ruoslahti, E. (1999). Integrin signaling. *Science* 285, 1028-033.

Gibson, M.C., and Schultz, E. (1983). Age-related differences in absolute numbers of skeletal muscle satellite cells. *Muscle Nerve* 6, 574-580.

Gilbert, P.M., Havenstrite, K.L., Magnusson, K.E., Sacco, A., Leonardi, N.A., Kraft, P., Nguyen, N.K., Thrun, S., Lutolf, M.P., and Blau, H.M. (2010). Substrate Elasticity Regulates Skeletal Muscle Stem Cell Self-Renewal in Culture. *Science*

Goldspink, G., Fernandes, K., Williams, P.E., and Wells, D.J. (1994). Age-related changes in collagen gene expression in the muscles of mdx dystrophic and normal mice. *Neuromuscul Disord* 4, 183-191.

Gopinath, S.D., and Rando, T.A. (2008). Stem cell review series: aging of the skeletal muscle stem cell niche. *Aging Cell* 7, 590-98.

Grounds, M.D. (1998). Age-associated Changes in the Response of Skeletal Muscle Cells to Exercise and Regeneration. *Annals of the New York Academy of Sciences* 854, 78-91.

Grounds, M.D., Sorokin, L., and White, J. (2005). Strength at the extracellular matrix-

muscle interface. *Scand J Med Sci Sports* 15, 381-391.

Guglieri, S., Hricovi ni, M., Raman, R., Polito, L., Torri, G., Casu, B., Sasisekharan, R., and Guerrini, M. (2008). Minimum FGF2 Binding Structural Requirements of Heparin and Heparan Sulfate Oligosaccharides As Determined by NMR Spectroscopy. *Biochemistry* 47, 13862-69.

Guimond, S., Maccarana, M., Olwin, B.B., Lindahl, U., and Rapraeger, A.C. (1993). Activating and inhibitory heparin sequences for FGF-2 (basic FGF). Distinct requirements for FGF-1, FGF-2, and FGF-4. *J Biol Chem* 268, 23906-914.

Guimond, S., Maccarana, M., Olwin, B.B., Lindahl, U., and Rapraeger, A.C. (1993). Activating and inhibitory heparin sequences for FGF-2 (basic FGF). Distinct requirements for FGF-1, FGF-2, and FGF-4. *J Biol Chem* 268, 23906-914.

Hacohen, N., Kramer, S., Sutherland, D., Hiromi, Y., and Krasnow, M.A. (1998). sprouty encodes a novel antagonist of FGF signaling that patterns apical branching of the *Drosophila* airways. *Cell* 92, 253-263.

Hall, J.K., Banks, G.B., Chamberlain, J.S., and Olwin, B.B. (2010). Prevention of muscle aging by myofiber-associated satellite cell transplantation. *Sci Transl Med* 2, 57ra83.

Hannon, K., Kudla, A.J., McAvoy, M.J., Clase, K.L., and Olwin, B.B. (1996). Differentially expressed fibroblast growth factors regulate skeletal muscle development through autocrine and paracrine mechanisms. *J Cell Biol* 132, 1151-59.

Hawke, T.J., and Garry, D.J. (2001). Myogenic satellite cells: physiology to molecular biology. *J Appl Physiol* 91, 534-551.

Hayflick, L. (2000). The future of ageing. *Nature* 408, 267-69.

Hill, E., Boontheekul, T., and Mooney, D.J. (2006). Regulating activation of transplanted cells controls tissue regeneration. *Proc Natl Acad Sci U S A* *103*, 2494-99.

Holmes, C., and Stanford, W.L. (2007). Concise review: stem cell antigen-1: expression, function, and enigma. *Stem Cells* *25*, 1339-347.

Huang, R., Liu, J., and Sharp, J.S. (2013). An Approach for Separation and Complete Structural Sequencing of Heparin/Heparan Sulfate-like Oligosaccharides. *Anal Chem*

Huang, S., Jia, S., Liu, G., Fang, D., and Zhang, D. (2012). Osteogenic differentiation of muscle satellite cells induced by platelet-rich plasma encapsulated in three-dimensional alginate scaffold. *Oral Surg Oral Med Oral Pathol Oral Radiol* *114*, S32-S40.

Hubbard, R.E., O'Mahony, M.S., and Woodhouse, K.W. (2009). Characterising frailty in the clinical setting--a comparison of different approaches. *Age Ageing* *38*, 115-19.

Ingber, D.E. (2006). Cellular mechanotransduction: putting all the pieces together again. *FASEB J* *20*, 811-827.

Iwata, Y., Ozaki, N., Hirata, H., Sugiura, Y., Horii, E., Nakao, E., Tatebe, M., Yazaki, N., Hattori, T., et al. (2006). Fibroblast growth factor-2 enhances functional recovery of reinnervated muscle. *Muscle Nerve* *34*, 623-630.

J. DiMario, N. Buffinger, S. Yamada, and R.C. Strohman (1989). Fibroblast growth factor in the extracellular matrix of dystrophic (mdx) mouse muscle. *Science* *244*, 688-690.

Janssen, I., Shepard, D.S., Katzmarzyk, P.T., and Roubenoff, R. (2004). The healthcare costs of sarcopenia in the United States. *J Am Geriatr Soc* *52*, 80-85.

Jenniskens, G.J., Hafmans, T., Veerkamp, J.H., and Van Kuppevelt, T.H. (2002). Spatiotemporal distribution of heparan sulfate epitopes during myogenesis and synaptogenesis: a

study in developing mouse intercostal muscle. *Developmental dynamics* 225, 70-79.

Jenniskens, G.J., Oosterhof, A., Brandwijk, R., Veerkamp, J.H., and van Kuppevelt, T.H. (2000). Heparan sulfate heterogeneity in skeletal muscle basal lamina: demonstration by phage display-derived antibodies. *J Neurosci* 20, 4099-4111.

Jenniskens, G.J., Oosterhof, A., Brandwijk, R., Veerkamp, J.H., and van Kuppevelt, T.H. (2000). Heparan sulfate heterogeneity in skeletal muscle basal lamina: demonstration by phage display-derived antibodies. *J Neurosci* 20, 4099-4111.

Jenniskens, G.J., Veerkamp, J.H., and van Kuppevelt, T.H. (2006). Heparan sulfates in skeletal muscle development and physiology. *J Cell Physiol* 206, 283-294.

Johnson, S.E., and Allen, R.E. (1995). Activation of skeletal muscle satellite cells and the role of fibroblast growth factor receptors. *Exp Cell Res* 219, 449-453.

Jones, N.C., Tyner, K.J., Nibarger, L., Stanley, H.M., Cornelison, D.D., Fedorov, Y.V., and Olwin, B.B. (2005). The p38  $\alpha/\beta$  MAPK functions as a molecular switch to activate the quiescent satellite cell. *J Cell Biol* 169, 105-116.

Kamimura, K., Koyama, T., Habuchi, H., Ueda, R., Masu, M., Kimata, K., and Nakato, H. (2006). Specific and flexible roles of heparan sulfate modifications in *Drosophila* FGF signaling. *J Cell Biol* 174, 773-78.

Karakelides, H., and Nair, K.S. (2005). Sarcopenia of aging and its metabolic impact. *Current topics in developmental biology* 68, 123.

Kastner, S., Elias, M.C., Rivera, A.J., and Yablonka-Reuveni, Z. (2000). Gene expression patterns of the fibroblast growth factors and their receptors during myogenesis of rat satellite cells. *J Histochem Cytochem* 48, 1079-096.

Kelly, A.M. (1978). Perisynaptic satellite cells in the developing and mature rat soleus muscle. *Anat Rec* 190, 891-903.

Kim, S.H., Turnbull, J., and Guimond, S. (2011). Extracellular matrix and cell signalling: the dynamic cooperation of integrin, proteoglycan and growth factor receptor. *J Endocrinol* 209, 139-151.

Kirkwood, T.B. (2005). Understanding the odd science of aging. *Cell* 120, 437-447.

Kjaer, M., Magnusson, P., Krogsgaard, M., Boysen Møller, J., Olesen, J., Heinemeier, K., Hansen, M., Haraldsson, B., Koskinen, S., et al. (2006). Extracellular matrix adaptation of tendon and skeletal muscle to exercise. *J Anat* 208, 445-450.

Kloxin, A.M., Kasko, A.M., Salinas, C.N., and Anseth, K.S. (2009). Photodegradable hydrogels for dynamic tuning of physical and chemical properties. *Science* 324, 59-63.

Knoblich, J.A. (2008). Mechanisms of asymmetric stem cell division. *Cell* 132, 583-597.

Kondoh, K., Sunadome, K., and Nishida, E. (2007). Notch signaling suppresses p38 MAPK activity via induction of MKP-1 in myogenesis. *J Biol Chem* 282, 3058-065.

Konigsberg, I. (1960). The differentiation of cross-striated myofibrils in short term cell culture. *Exp. Cell Res.* 21, 414-420.

Konigsberg, I.R. (1961). Cellular differentiation in colonies derived from single cells platings of freshly isolated chick embryo muscle cells. *Proc Nat Acad Sci USA* 47, 1868-872.

Kragstrup, T.W., Kjaer, M., and Mackey, A.L. (2011). Structural, biochemical, cellular, and functional changes in skeletal muscle extracellular matrix with aging. *Scand J Med Sci Sports* 21, 749-757.

Kraushaar, D.C., Dalton, S., and Wang, L. (2013). Heparan sulfate: a key regulator of

embryonic stem cell fate. *Biol Chem* 394, 741-751.

Kuang, S., Gillespie, M.A., and Rudnicki, M.A. (2008). Niche regulation of muscle satellite cell self-renewal and differentiation. *Cell Stem Cell* 2, 22-31.

Kuang, S., Kuroda, K., Le Grand, F., and Rudnicki, M.A. (2007). Asymmetric self-renewal and commitment of satellite stem cells in muscle. *Cell* 129, 999-1010.

Kuang, W., Tan, J., Duan, Y., Duan, J., Wang, W., Jin, F., Jin, Z., Yuan, X., and Liu, Y. (2009). Cyclic stretch induced miR-146a upregulation delays C2C12 myogenic differentiation through inhibition of Numb. *Biochem Biophys Res Commun* 378, 259-263.

Kurup, S., Wijnhoven, T.J., Jenniskens, G.J., Kimata, K., Habuchi, H., Li, J.P., Lindahl, U., van Kuppevelt, T.H., and Spillmann, D. (2007). Characterization of anti-heparan sulfate phage display antibodies AO4B08 and HS4E4. *J Biol Chem* 282, 21032-042.

Lamberts, S.W. (2002). The endocrinology of aging and the brain. *Archives of neurology* 59, 1709.

Landi, F., Cruz-Jentoft, A.J., Liperoti, R., Russo, A., Giovannini, S., Tosato, M., Capoluongo, E., Bernabei, R., and Onder, G. (2013). Sarcopenia and mortality risk in frail older persons aged 80 years and older: results from the SIRENTE study. *Age Ageing* 42, 203-09.

Langsdorf, A., Do, A.T., Kusche-Gullberg, M., Emerson, C.P., and Ai, X. (2007). Sulfs are regulators of growth factor signaling for satellite cell differentiation and muscle regeneration. *Dev Biol* 311, 464-477.

de la Serna, I.L., Ohkawa, Y., Berkes, C.A., Bergstrom, D.A., Dacwag, C.S., Tapscott, S.J., and Imbalzano, A.N. (2005). MyoD targets chromatin remodeling complexes to the myogenin locus prior to forming a stable DNA-bound complex. *Mol Cell Biol* 25, 3997-4009.

Lassar, A., Thayer, M., Overell, R., and Weintraub, H. (1989). Transformation by activated ras or fos prevents myogenesis by inhibiting expression of MyoD1. *Cell* 58, 659-667.

Lees, S.J., Zwetsloot, K.A., and Booth, F.W. (2009). Muscle precursor cells isolated from aged rats exhibit an increased tumor necrosis factor- $\alpha$  response. *Aging Cell* 8, 26-35.

Le Grand, F., Jones, A.E., Seale, V., Scimè, A., and Rudnicki, M.A. (2009). Wnt7a activates the planar cell polarity pathway to drive the symmetric expansion of satellite stem cells. *Cell Stem Cell* 4, 535-547.

Le Grand, F., Jones, A.E., Seale, V., Scimè, A., and Rudnicki, M.A. (2009). Wnt7a activates the planar cell polarity pathway to drive the symmetric expansion of satellite stem cells. *Cell Stem Cell* 4, 535-547.

Leng, S.X., Cappola, A.R., Andersen, R.E., Blackman, M.R., Koenig, K., Blair, M., and Walston, J.D. (2004). Serum levels of insulin-like growth factor-I (IGF-I) and dehydroepiandrosterone sulfate (DHEA-S), and their relationships with serum interleukin-6, in the geriatric syndrome of frailty. *Aging Clin Exp Res* 16, 153-57.

Lepper, C., Partridge, T.A., and Fan, C.M. (2011). An absolute requirement for Pax7-positive satellite cells in acute injury-induced skeletal muscle regeneration. *Development* 138, 3639-646.

Lewandowski, J.P., Sheehan, K.B., Bennett, P.E., and Boswell, R.E. (2010). Mago Nashi, Tsunagi/Y14, and Ranshi form a complex that influences oocyte differentiation in *Drosophila melanogaster*. *Dev Biol* 339, 307-319.

Li, Y.P. (2003). TNF- $\alpha$  is a mitogen in skeletal muscle. *Am J Physiol Cell Physiol* 285, C370-76.

Lim, R.W., and Hauschka, S.D. (1984). A rapid decrease in epidermal growth factor-binding capacity accompanies the terminal differentiation of mouse myoblasts in vitro. *J Cell Biol* 98, 739-747.

López-Otín, C., Blasco, M.A., Partridge, L., Serrano, M., and Kroemer, G. (2013). The Hallmarks of Aging. *Cell* 153, 1194-1217.

Lutolf, M.P., Gilbert, P.M., and Blau, H.M. (2009). Designing materials to direct stem-cell fate. *Nature* 462, 433-441.

Machida, S., and Booth, F.W. (2004). Increased nuclear proteins in muscle satellite cells in aged animals as compared to young growing animals. *Exp Gerontol* 39, 1521-25.

Marshall, P.A., Williams, P.E., and Goldspink, G. (1989). Accumulation of collagen and altered fiber-type ratios as indicators of abnormal muscle gene expression in the mdx dystrophic mouse. *Muscle Nerve* 12, 528-537.

Mauro, A. (1961). Satellite cell of skeletal muscle fibers. *The Journal of biophysical and biochemical cytology* 9, 493-95.

McIntire, K.L., and Hoffman, A.R. (2011). The endocrine system and sarcopenia: potential therapeutic benefits. *Curr Aging Sci* 4, 298-305.

Megeney, L.A., Kablar, B., Garrett, K., Anderson, J.E., and Rudnicki, M.A. (1996). MyoD is required for myogenic stem cell function in adult skeletal muscle. *Genes Dev* 10, 1173-183.

Megeney, L.A., Kablar, B., Garrett, K., Anderson, J.E., and Rudnicki, M.A. (1996). MyoD is required for myogenic stem cell function in adult skeletal muscle. *Genes Dev* 10, 1173-183.

Merry, C.L., Bullock, S.L., Swan, D.C., Backen, A.C., Lyon, M., Beddington, R.S., Wilson, V.A., and Gallagher, J.T. (2001). The molecular phenotype of heparan sulfate in the Hs2st<sup>-/-</sup> mutant mouse. *J Biol Chem* 276, 35429-434.

Metter, E.J., Conwit, R., Tobin, J., and Fozard, J.L. (1997). Age-associated loss of power and strength in the upper extremities in women and men. *J Gerontol A Biol Sci Med Sci* 52, B267-276.

Mezzogiorno, A., Coletta, M., Zani, B.M., Cossu, G., and Molinaro, M. (1993). Paracrine stimulation of senescent satellite cell proliferation by factors released by muscle or myotubes from young mice. *Mech Ageing Dev* 70, 35-44.

Miller, R.A. (1996). The aging immune system: primer and prospectus. *Science* 273, 70-74.

Mohammadi, M., McMahon, G., Sun, L., Tang, C., Hirth, P., Yeh, B., Hubbard, S., and Schlessinger, J. (1997). Structures of the tyrosine kinase domain of fibroblast growth factor receptor in complex with inhibitors. *Science* 276, 955-960.

Mohammadi, Olsen, and Ibrahimi (2005). Structural basis for fibroblast growth factor receptor activation. *Cytokine & growth factor reviews* 16, 107-137.

Montarras, D., Morgan, J., Collins, C., Relaix, F., Zaffran, S., Cumano, A., Partridge, T., and Buckingham, M. (2005). Direct isolation of satellite cells for skeletal muscle regeneration. *Science* 309, 2064-67.

Montarras, D., Pinset, C., Chelly, J., Kahn, A., and Gros, F. (1989). Expression of MyoD1 coincides with terminal differentiation in determined but inducible muscle cells. *EMBO J* 8, 2203-07.

Mourikis, P., Sambasivan, R., Castel, D., Rocheteau, P., Bizzarro, V., and Tajbakhsh, S. (2012). A critical requirement for notch signaling in maintenance of the quiescent skeletal muscle stem cell state. *Stem Cells* 30, 243-252.

Murphy, M.M., Lawson, J.A., Mathew, S.J., Hutcheson, D.A., and Kardon, G. (2011). Satellite cells, connective tissue fibroblasts and their interactions are crucial for muscle regeneration. *Development* 138, 3625-637.

O'Connor, M.S., Carlson, M.E., and Conboy, I.M. (2009). Differentiation rather than aging of muscle stem cells abolishes their telomerase activity. *Biotechnol Prog* 25, 1130-37.

Olguin, H.C., and Olwin, B.B. (2004). Pax-7 up-regulation inhibits myogenesis and cell cycle progression in satellite cells: a potential mechanism for self-renewal. *Dev Biol* 275, 375-388.

Olguin, H.C., Yang, Z., Tapscott, S.J., and Olwin, B.B. (2007). Reciprocal inhibition between Pax7 and muscle regulatory factors modulates myogenic cell fate determination. *J Cell Biol* 177, 769-779.

Oliver, W.T., Rosenberger, J., Lopez, R., Gomez, A., Cummings, K.K., and Fiorotto, M.L. (2005). The local expression and abundance of insulin-like growth factor (IGF) binding proteins in skeletal muscle are regulated by age and gender but not local IGF-I in vivo. *Endocrinology* 146, 5455-462.

Olwin, B.B., and Hauschka, S.D. (1986). Identification of the fibroblast growth factor receptor of Swiss 3T3 cells and mouse skeletal muscle myoblasts. *Biochemistry* 25, 3487-492.

Olwin, B.B., and Rapraeger, A. (1992). Repression of myogenic differentiation by aFGF, bFGF, and K-FGF is dependent on cellular heparan sulfate. *J Cell Biol* 118, 631-39.

Olwin, B.B., Arthur, K., Hannon, K., Hein, P., McFall, A., Riley, B., Szebenyi, G., Zhou, Z., Zuber, M.E., and Rapraeger, A.C. (1994). Role of FGFs in skeletal muscle and limb development. *Mol Reprod Dev* 39, 90-100; discussion 100-1.

Oustanina, S., Hause, G., and Braun, T. (2004). Pax7 directs postnatal renewal and propagation of myogenic satellite cells but not their specification. *EMBO J* 23, 3430-39.

Park, K., Cho, K.J., Kim, J.J., Kim, I.H., and Han, D.K. (2009). Functional PLGA scaffolds for chondrogenesis of bone-marrow-derived mesenchymal stem cells. *Macromol Biosci* 9, 221-29.

Pellegrini, L., Burke, D.F., von Delft, F., Mulloy, B., and Blundell, T.L. (2000). Crystal structure of fibroblast growth factor receptor ectodomain bound to ligand and heparin. *Nature* 407, 1029-034.

Pietrangelo, T., Puglielli, C., Mancinelli, R., Beccafico, S., Fanò, G., and Fulle, S. (2009). Molecular basis of the myogenic profile of aged human skeletal muscle satellite cells during differentiation. *Exp Gerontol* 44, 523-531.

Pisconti, A., Cornelison, D.D., Olguín, H.C., Antwine, T.L., and Olwin, B.B. (2010). Syndecan-3 and Notch cooperate in regulating adult myogenesis. *J Cell Biol* 190, 427-441.

Prody, C.A., and Merlie, J.P. (1991). A developmental and tissue-specific enhancer in the mouse skeletal muscle acetylcholine receptor alpha-subunit gene regulated by myogenic factors. *J Biol Chem* 266, 22588-596.

Puvirajesinghe, T.M., Ahmed, Y.A., Powell, A.K., Fernig, D.G., Guimond, S.E., and Turnbull, J.E. (2012). Array-based functional screening of heparin glycans. *Chem Biol* 19, 553-58.

Rantanen, J., Hurme, T., Lukka, R., Heino, J., and Kalimo, H. (1995). Satellite cell proliferation and the expression of myogenin and desmin in regenerating skeletal muscle: evidence for two different populations of satellite cells. *Lab Invest* 72, 341-47.

Rantanen, J., Hurme, T., Lukka, R., Heino, J., and Kalimo, H. (1995). Satellite cell proliferation and the expression of myogenin and desmin in regenerating skeletal muscle: evidence for two different populations of satellite cells. *Lab Invest* 72, 341-47.

Rapraeger, A.C., Krufka, A., and Olwin, B.B. (1991). Requirement of heparan sulfate for bFGF-mediated fibroblast growth and myoblast differentiation. *Science* 252, 1705-08.

Ratajczak, M.Z., Majka, M., Kucia, M., Drukala, J., Pietrkowski, Z., Peiper, S., and Janowska-Wieczorek, A. (2003). Expression of functional CXCR4 by muscle satellite cells and secretion of SDF-1 by muscle-derived fibroblasts is associated with the presence of both muscle progenitors in bone marrow and hematopoietic stem/progenitor cells in muscles. *Stem Cells* 21, 363-371.

Relaix, F., and Zammit, P.S. (2012). Satellite cells are essential for skeletal muscle regeneration: the cell on the edge returns centre stage. *Development* 139, 2845-856.

[NO STYLE for: Wei 2012].

Reznik, M. (1969). Thymidine-3H uptake by satellite cells of regenerating skeletal muscle. *J Cell Biol* 40, 568-571.

Roth, S.M., Martel, G.F., Ivey, F.M., Lemmer, J.T., Metter, E.J., Hurley, B.F., and Rogers, M.A. (2000). Skeletal muscle satellite cell populations in healthy young and older men and women. *The Anatomical Record* 260, 351-58.

Roubenoff, R. (2000). Sarcopenia: A major modifiable cause of frailty in the elderly:

Sarcopenia in aging. *The journal of nutrition, health & aging* 4, 140-42.

Rudd, T.R., Gaudesi, D., Skidmore, M.A., Ferro, M., Guerrini, M., Mulloy, B., Torri, G., and Yates, E.A. (2011). Construction and use of a library of bona fide heparins employing <sup>1</sup>H NMR and multivariate analysis. *Analyst* 136, 1380-89.

Sacco, A., Doyonnas, R., Kraft, P., Vitorovic, S., and Blau, H.M. (2008). Self-renewal and expansion of single transplanted muscle stem cells. *Nature* 456, 502-06.

Saha, A., Manna, S., and Nandi, A.K. (2007). A mechanistic approach on the self-organization of the two-component thermoreversible hydrogel of riboflavin and melamine. *Langmuir* 23, 13126-135.

Sajko, S., Kubinova, L., Cvetko, E., Kreft, M., Wernig, A., and Erzen, I. (2004). Frequency of M-cadherin-stained satellite cells declines in human muscles during aging. *J Histochem Cytochem* 52, 179-185.

Salzman, E.W., Rosenberg, R.D., Smith, M.H., Lindon, J.N., and Favreau, L. (1980). Effect of heparin and heparin fractions on platelet aggregation. *Journal of Clinical Investigation* 65, 64.

Sambasivan, R., Yao, R., Kissenpfennig, A., Van Wittenberghe, L., Paldi, A., Gayraud-Morel, B., Guenou, H., Malissen, B., Tajbakhsh, S., and Galy, A. (2011). Pax7-expressing satellite cells are indispensable for adult skeletal muscle regeneration. *Development* 138, 3647-656.

Sands, R.W., and Mooney, D.J. (2007). Polymers to direct cell fate by controlling the microenvironment. *Curr Opin Biotechnol* 18, 448-453.

Sanes, J.R. (2003). The basement membrane/basal lamina of skeletal muscle. *Journal of*

Biological Chemistry 278, 12601-04.

Sanes, J.R., Rubenstein, J.L., and Nicolas, J.F. (1986). Use of a recombinant retrovirus to study post-implantation cell lineage in mouse embryos. *Embo J* 5, 3133-142.

Sarig, R., Baruchi, Z., Fuchs, O., Nudel, U., and Yaffe, D. (2006). Regeneration and transdifferentiation potential of muscle-derived stem cells propagated as myospheres. *Stem Cells* 24, 1769-778.

Sasisekharan, R., and Venkataraman, G. (2000). Heparin and heparan sulfate: biosynthesis, structure and function. *Current opinion in chemical biology* 4, 626-631.

Scadden, D.T. (2006). The stem-cell niche as an entity of action. *Nature* 441, 1075-79.

Schiaffino, S., and Partridge, T. (2008). Skeletal muscle repair and regeneration (Springer Science+ Business Media).

Schlessinger, J., Plotnikov, A.N., Ibrahimi, O.A., Eliseenkova, A.V., Yeh, B.K., Yapon, A., Linhardt, R.J., and Mohammadi, M. (2000). Crystal structure of a ternary FGF-FGFR-heparin complex reveals a dual role for heparin in FGFR binding and dimerization. *Mol Cell* 6, 743-50..

Schultz, E. (1984). A quantitative study of satellite cells in regenerated soleus and extensor digitorum longus muscles. *Anat Rec* 208, 501-06.

Schultz, E., and Lipton, B.H. (1982). Skeletal muscle satellite cells: changes in proliferation potential as a function of age. *Mech Ageing Dev* 20, 377-383.

Schultz, E., Darr, K.C., and Macius, A. (1994). Acute effects of hindlimb unweighting on satellite cells of growing skeletal muscle. *J Appl Physiol* 76, 266-270.

Seale, P., Ishibashi, J., Scime, A., and Rudnicki, M.A. (2004). Pax7 Is Necessary and

Sufficient for the Myogenic Specification of CD45(+):Sca1(+) Stem Cells from Injured Muscle. *PLoS Biol* 2, E130.

Seale, P., Sabourin, L.A., Girgis-Gabardo, A., Mansouri, A., Gruss, P., and Rudnicki, M.A. (2000). Pax7 is required for the specification of myogenic satellite cells. *Cell* 102, 777-786.

Sheehan, S.M., and Allen, R.E. (1999). Skeletal muscle satellite cell proliferation in response to members of the fibroblast growth factor family and hepatocyte growth factor. *J Cell Physiol* 181, 499-506.

Shefer, G., Van de Mark, D.P., Richardson, J.B., and Yablonka-Reuveni, Z. (2006). Satellite-cell pool size does matter: defining the myogenic potency of aging skeletal muscle. *Dev Biol* 294, 50-66.

Sherwood, R.I., Christensen, J.L., Conboy, I.M., Conboy, M.J., Rando, T.A., Weissman, I.L., and Wagers, A.J. (2004). Isolation of adult mouse myogenic progenitors: functional heterogeneity of cells within and engrafting skeletal muscle. *Cell* 119, 543-554.

Shinin, V., Gayraud-Morel, B., Gomès, D., and Tajbakhsh, S. (2006). Asymmetric division and cosegregation of template DNA strands in adult muscle satellite cells. *Nat Cell Biol* 8, 677-682.

Simons, B.D., and Clevers, H. (2011). Strategies for homeostatic stem cell self-renewal in adult tissues. *Cell* 145, 851-862.

Slaughter, B.V., Khurshid, S.S., Fisher, O.Z., Khademhosseini, A., and Peppas, N.A. (2009). Hydrogels in regenerative medicine. *Advanced Materials* 21, 3307-329.

Smith, C.A., Lau, K.M., Rahmani, Z., Dho, S.E., Brothers, G., She, Y.M., Berry, D.M., Bonneil, E., Thibault, P., et al. (2007). aPKC-mediated phosphorylation regulates asymmetric

membrane localization of the cell fate determinant Numb. *EMBO J* 26, 468-480.

Smith, H.K., Maxwell, L., Rodgers, C.D., McKee, N.H., and Plyley, M.J. (2001). Exercise-enhanced satellite cell proliferation and new myonuclear accretion in rat skeletal muscle. *J Appl Physiol* 90, 1407-414.

Snippert, H.J., Flier, L.G.V.D., Sato, T., Es, J.H.V., Born, M.V.D., Kroon-Veenboer, C., Barker, N., Klein, A.M., Rheenen, J.V., et al. (2010). Intestinal Crypt Homeostasis Results from Neutral Competition between Symmetrically Dividing Lgr5 Stem Cells. *Cell* 143, 134 - 144.

Snow, M.H. (1977). The effects of aging on satellite cells in skeletal muscles of mice and rats. *Cell Tissue Res* 185, 399-408.

Song, X., Mitnitski, A., and Rockwood, K. (2010). Prevalence and 10-year outcomes of frailty in older adults in relation to deficit accumulation. *J Am Geriatr Soc* 58, 681-87.

Sorokin, L.M., Maley, M.A., Moch, H., von der Mark, H., von der Mark, K., Cadalbert, L., Karosi, S., Davies, M.J., McGeachie, J.K., and Grounds, M.D. (2000). Laminin alpha4 and integrin alpha6 are upregulated in regenerating dy/dy skeletal muscle: comparative expression of laminin and integrin isoforms in muscles regenerating after crush injury. *Exp Cell Res* 256, 500-514.

Staatz, W.D., Fok, K.F., Zutter, M.M., Adams, S.P., Rodriguez, B.A., and Santoro, S.A. (1991). Identification of a tetrapeptide recognition sequence for the alpha 2 beta 1 integrin in collagen. *Journal of Biological Chemistry* 266, 7363-67.

Steinfeld, R., Van Den Berghe, H., and David, G. (1996). Stimulation of fibroblast growth factor receptor-1 occupancy and signaling by cell surface-associated syndecans and glypican. *J Cell Biol* 133, 405-416.

Streit, W.J. (2006). Microglial senescence: does the brain's immune system have an expiration date? *Trends Neurosci* 29, 506-510.

Sun, L., Tran, N., Liang, C., Tang, F., Rice, A., Schreck, R., Waltz, K., Shawver, L.K., McMahon, G., and Tang, C. (1999). Design, synthesis, and evaluations of substituted 3-[(3-or 4-carboxyethylpyrrol-2-yl) methylidene] indolin-2-ones as inhibitors of VEGF, FGF, and PDGF receptor tyrosine kinases. *Journal of medicinal chemistry* 42, 5120-130.

Suzuki, A., and Ohno, S. (2006). The PAR-aPKC system: lessons in polarity. *J Cell Sci* 119, 979-987.

Tanaka, K.K., Hall, J.K., Troy, A.A., Cornelison, D.D., Majka, S.M., and Olwin, B.B. (2009). Syndecan-4-Expressing Muscle Progenitor Cells in the SP Engraft as Satellite Cells during Muscle Regeneration. *Cell Stem Cell* 4, 217-225.

Tapscott, S.J. (2005). The circuitry of a master switch: MyoD and the regulation of skeletal muscle gene transcription. *Development* 132, 2685-695.

Tapscott, S.J., Davis, R.L., Thayer, M.J., Cheng, P.F., Weintraub, H., and Lassar, A.B. (1988). MyoD1: a nuclear phosphoprotein requiring a Myc homology region to convert fibroblasts to myoblasts. *Science* 242, 405-411.

Tapscott, S.J., Davis, R.L., Thayer, M.J., Cheng, P.F., Weintraub, H., and Lassar, A.B. (1988). MyoD1: a nuclear phosphoprotein requiring a Myc homology region to convert fibroblasts to myoblasts. *Science* 242, 405-411.

Tashiro, K., Sephel, G.C., Weeks, B., Sasaki, M., Martin, G.R., Kleinman, H.K., and Yamada, Y. (1989). A synthetic peptide containing the IKVAV sequence from the A chain of laminin mediates cell attachment, migration, and neurite outgrowth. *J Biol Chem* 264,

16174-182.

Tatsumi, R., Anderson, J.E., Nevoret, C.J., Halevy, O., and Allen, R.E. (1998). HGF/SF is present in normal adult skeletal muscle and is capable of activating satellite cells. *Dev Biol* *194*, 114-128.

Tatsumi, R., Hattori, A., Ikeuchi, Y., Anderson, J.E., and Allen, R.E. (2002). Release of hepatocyte growth factor from mechanically stretched skeletal muscle satellite cells and role of pH and nitric oxide. *Mol Biol Cell* *13*, 2909-918.

Tatsumi, R., Yamada, M., Katsuki, Y., Okamoto, S., Ishizaki, J., Mizunoya, W., Ikeuchi, Y., Hattori, A., Shimokawa, H., and Allen, R.E. (2006). Low-pH preparation of skeletal muscle satellite cells can be used to study activation in vitro. *Int J Biochem Cell Biol* *38*, 1678-685.

Tibbitt, M.W., and Anseth, K.S. (2009). Hydrogels as extracellular matrix mimics for 3D cell culture. *Biotechnol Bioeng* *103*, 655-663.

Tkachenko, E., Lutgens, E., Stan, R.V., and Simons, M. (2004). Fibroblast growth factor 2 endocytosis in endothelial cells proceed via syndecan-4-dependent activation of Rac1 and a Cdc42-dependent macropinocytic pathway. *J Cell Sci* *117*, 3189-199.

Troy, A., Cadwallader, A.B., Fedorov, Y., Tyner, K., Tanaka, K.K., and Olwin, B.B. (2012). Coordination of Satellite Cell Activation and Self-Renewal by Par-Complex-Dependent Asymmetric Activation of p38 $\alpha$ / $\beta$  MAPK. *Cell Stem Cell* *11*, 541-553.

Urciuolo, A., Quarta, M., Morbidoni, V., Gattazzo, F., Molon, S., Grumati, P., Montemurro, F., Tedesco, F.S., Blaauw, B., and Cossu, G. (2013). Collagen VI regulates satellite cell self-renewal and muscle regeneration. *Nat Commun* *4*

Walston, J., Hadley, E.C., Ferrucci, L., Guralnik, J.M., Newman, A.B., Studenski, S.A.,

Ershler, W.B., Harris, T., and Fried, L.P. (2006). Research agenda for frailty in older adults: toward a better understanding of physiology and etiology: summary from the American Geriatrics Society/National Institute on Aging Research Conference on Frailty in Older Adults. *J Am Geriatr Soc* 54, 991-1001.

Walston, J.D. (2012). Sarcopenia in older adults. *Current Opinion in Rheumatology* 24, 623-27.

Watanabe, K., Oohira, A., Uramoto, I., and Totsuka, T. (1986). Age-related changes in the content and composition of glycosaminoglycans isolated from the mouse skeletal muscle: normal and dystrophic conditions. *J Biochem* 100, 167-173.

Weber, L.M., Hayda, K.N., and Anseth, K.S. (2008). Cell-matrix interactions improve beta-cell survival and insulin secretion in three-dimensional culture. *Tissue Eng Part A* 14, 1959-968.

Wen, Y., Bi, P., Liu, W., Asakura, A., Keller, C., and Kuang, S. (2012). Constitutive notch activation upregulates pax7 and promotes the self-renewal of skeletal muscle satellite cells. *Mol Cell Biol* 32, 2300-311.

Whitney, M.L., Otto, K.G., Blau, C.A., Reinecke, H., and Murry, C.E. (2001). Control of myoblast proliferation with a synthetic ligand. *J Biol Chem* 276, 41191-96.

Whitney, M.L., Otto, K.G., Blau, C.A., Reinecke, H., and Murry, C.E. (2001). Control of myoblast proliferation with a synthetic ligand. *J Biol Chem* 276, 41191-96.

Wright, S.D., and Meyer, B.C. (1985). Fibronectin receptor of human macrophages recognizes the sequence Arg-Gly-Asp-Ser. *J Exp Med* 162, 762-67.

Yamanaka, T., Horikoshi, Y., Suzuki, A., Sugiyama, Y., Kitamura, K., Maniwa, R., Nagai,

Y., Yamashita, A., Hirose, T., et al. (2001). PAR-6 regulates aPKC activity in a novel way and mediates cell-cell contact-induced formation of the epithelial junctional complex. *Genes Cells* 6, 721-731.

Yoon, J.J., Chung, H.J., Lee, H.J., and Park, T.G. (2006). Heparin-immobilized biodegradable scaffolds for local and sustained release of angiogenic growth factor. *J Biomed Mater Res A* 79, 934-942.

Yoshida, N., Yoshida, S., Koishi, K., Masuda, K., and Nabeshima, Y. (1998). Cell heterogeneity upon myogenic differentiation: down-regulation of MyoD and Myf-5 generates 'reserve cells'. *J Cell Sci* 111 (Pt 6), 769-779.

Young, H.E., Carrino, D.A., and Caplan, A.I. (1990). Change in synthesis of sulfated glycoconjugates during muscle development, maturation and aging in embryonic to senescent CBF-1 mouse. *Mech Ageing Dev* 53, 179-193.

Young, H.E., Carrino, D.A., and Caplan, A.I. (1990). Change in synthesis of sulfated glycoconjugates during muscle development, maturation and aging in embryonic to senescent CBF-1 mouse. *Mech Ageing Dev* 53, 179-193.

Zacks, S.I., and Sheff, M.F. (1982). Age-related impeded regeneration of mouse minced anterior tibial muscle. *Muscle Nerve* 5, 152-161.

Zammit, P.S., Carvajal, J.J., Golding, J.P., Morgan, J.E., Summerbell, D., Zolnerciks, J., Partridge, T.A., Rigby, P.W., and Beauchamp, J.R. (2004). Myf5 expression in satellite cells and spindles in adult muscle is controlled by separate genetic elements. *Dev Biol* 273, 454-465.

Zammit, P.S., Heslop, L., Hudon, V., Rosenblatt, J.D., Tajbakhsh, S., Buckingham, M.E., Beauchamp, J.R., and Partridge, T.A. (2002). Kinetics of myoblast proliferation show that

resident satellite cells are competent to fully regenerate skeletal muscle fibers. *Exp Cell Res* 281, 39-49.

Zammit, P.S., Relaix, F., Nagata, Y., Ruiz, A.P., Collins, C.A., Partridge, T.A., and Beauchamp, J.R. (2006). Pax7 and myogenic progression in skeletal muscle satellite cells. *J Cell Sci* 119, 1824-832.

Zhu, C.H., Mouly, V., Cooper, R.N., Mamchaoui, K., Bigot, A., Shay, J.W., Di Santo, J.P., Butler-Browne, G.S., and Wright, W.E. (2007). Cellular senescence in human myoblasts is overcome by human telomerase reverse transcriptase and cyclin-dependent kinase 4: consequences in aging muscle and therapeutic strategies for muscular dystrophies. *Aging Cell* 6, 515-523.

Zou, Y., Zhang, R.Z., Sabatelli, P., Chu, M.L., and Bönnemann, C.G. (2008). Muscle interstitial fibroblasts are the main source of collagen VI synthesis in skeletal muscle: implications for congenital muscular dystrophy types Ullrich and Bethlem. *J Neuropathol Exp Neurol* 67, 144-154.

## **Appendix 1**

**RELATED TO FIGURE 2.1. Percentage of explanted Syndecan-4+ satellite cells at 5d culture expressing myogenic transcription factors\***

Age:	Young (mean)	s.e.m.	Old (mean)	s.e.m.	p-value
Pax7	15	2	14	3	n.s.
Pax7/ MyoD	28	4	15	3	0.04
MyoD	57	3	71	6	0.02

\*Mean  $\pm$  s.e.m. n.s. = no significance. n=3 independent experiments. *P* values by one-way ANOVA with Tukey's test.

**RELATED TO FIGURE 2.2. Percentage of 24h myofiber-associated satellite cells expressing myogenic transcription factors\***

Age:	Young (mean)	s.e.m.	Old (mean)	s.e.m.	p-value
Pax7	2	1	1	0.1	n.s.
Pax7/ MyoD	84	3	31	6	0.001
MyoD	13	4	19	3	n.s.
Myog.	0	0	2	0.04	0.00001
Myog./ MyoD	0	0	0	0	
MyoD	87	4	50	2	0.0006

\*Mean  $\pm$  s.e.m. n.s. = no significance. n=3 independent experiments. *P* values by unpaired, two-way Student's t-test.

**RELATED TO FIGURE 2.2. Percentage of 96h myofiber-associated satellite cells expressing myogenic transcription factors\***

Age:	Young (mean)	s.e.m.	Old (mean)	s.e.m.	p-value
Pax7	15	2	10	1	0.05
Pax7/ MyoD	33	1	32	14	n.s.
MyoD	39	4	26	8	n.s.
Myog.	9	1	24	5	0.03
Myog./ MyoD	54	2	30	14	0.02
MyoD	20	1	10	5	0.02

\*Mean  $\pm$  s.e.m. n.s. = no significance. n=3 independent experiments. *P* values by unpaired, two-way Student's t-test.

**RELATED TO FIGURE 2.5. Percentage of 96h, +FGF-2 myofiber-associated satellite cells expressing myogenic transcription factors\***

Age:	Young (mean)	s.e.m.	Old (mean)	s.e.m.	p-value
Pax7	18	7	15	6	n.s.
Pax7/ MyoD	62	3	37	8	0.04
MyoD	14	3	25	7	n.s.
Sdc4 Alone	6	0.4	23	6	n.s.
Myog.	2.22	0.13	13.27	2.84	0.0009
Myog./ MyoD	40.7	4.64	26.11	6.55	n.s.
MyoD	45.32	6.75	27.33	4.51	n.s.
Sdc4 Alone	11.73	2.23	33.29	5.93	0.04

\*Mean  $\pm$  s.e.m. n.s. = no significance. n=3 independent experiments. *P* values by unpaired, two-way Student's t-test.

## **Appendix 2**

**RELATED TO FIGURE 2.7. Normalized expression values for probesets included in the Par3/p38 $\alpha$  $\beta$  MAPK asymmetry complex.**

	<b>Young</b>	<b>Old</b>
<b>Ccm2</b>	0.35	-1.04
<b>Ccm2</b>	-0.10	0.00
<b>Ccm2</b>	0.00	-0.31
<b>Cdc42</b>	-0.17	0.36
<b>Cdc42</b>	0.11	-0.18
<b>Cdc42</b>	-0.30	0.19
<b>Cdc42</b>	-0.44	0.31
<b>Map2k3</b>	0.05	-0.34
<b>Map2k3</b>	0.10	-0.00
<b>Map2k4</b>	0.00	-0.69
<b>Map2k4</b>	0.71	-0.72
<b>Map2k6</b>	1.78	-1.01
<b>Map3k10</b>	-0.04	0.10
<b>Map3k10</b>	0.00	0.18
<b>Map3k10</b>	-0.43	0.16
<b>Map3k11</b>	-0.32	0.00
<b>Map3k3</b>	0.41	-0.78
<b>Map3k3</b>	-0.80	0.56
<b>Map3k3</b>	-0.44	0.29
<b>Map3k4</b>	0.25	0.00
<b>Map3k4</b>	1.34	-0.87
<b>Map3k4</b>	-0.00	-0.48
<b>Map3k4</b>	0.52	-1.65
<b>Mapk14</b>	0.62	-0.99
<b>Mapk14</b>	-0.09	0.02
<b>Mapk14</b>	-0.50	0.13
<b>Mapk14</b>	0.58	-0.45

**RELATED TO FIGURE 2.8. Normalized expression values for probesets included in GO: 0030308 Negative Regulation of Cell Growth.**

	Young	Old		Young	Old		Young	Old
<b>Acvr1b</b>	-0.02	0.13	<b>Ccdc85b</b>	0.39	-0.45	<b>Dnajc2</b>	-0.00	-0.44
<b>Acvr1b</b>	-0.16	0.33	<b>Cda</b>	-0.22	0.36	<b>Dnajc2</b>	-0.49	0.14
<b>Acvr1l</b>	0.90	0.00	<b>Cdhr2</b>	0.09	-0.39	<b>Dnajc2</b>	1.10	-0.30
<b>Acvr1l</b>	0.18	0.00	<b>Cdkn1a</b>	0.20	-0.63	<b>Dnajc2</b>	0.05	0.00
<b>Adipor1</b>	0.27	-0.21	<b>Cdkn1a</b>	0.00	-0.09	<b>Eaf2</b>	0.10	-0.02
<b>Adipor1</b>	1.57	-1.76	<b>Cdkn2a</b>	0.67	0.00	<b>Ei24</b>	0.89	-0.91
<b>Adipor1</b>	0.84	-1.46	<b>Cdkn2aip</b>	0.22	0.00	<b>Fgf2</b>	-0.12	0.06
<b>Adipor2</b>	0.21	-0.20	<b>Cdkn2aip</b>	0.27	-0.19	<b>Foxk1</b>	-0.08	0.00
<b>Adipor2</b>	0.00	-0.02	<b>Cdkn2c</b>	0.09	0.00	<b>Foxk1</b>	0.00	-0.00
<b>Agt</b>	0.14	-0.17	<b>Cdkn2c</b>	0.00	0.01	<b>Foxk1</b>	1.65	-1.08
<b>Ahsg</b>	-0.24	0.14	<b>Cgref1</b>	-0.50	0.65	<b>Gdf2</b>	0.04	-0.20
<b>Apbb1</b>	0.28	-0.24	<b>Cgref1</b>	-0.20	-0.00	<b>Gdf9</b>	-0.19	0.22
<b>Apbb1</b>	0.06	-0.24	<b>Cgrrf1</b>	0.23	-0.10	<b>Gng4</b>	-0.33	0.23
<b>Apbb2</b>	1.00	-1.19	<b>Cgrrf1</b>	0.00	0.16	<b>Gng4</b>	-0.16	0.22
<b>Apbb2</b>	-0.04	0.00	<b>Cgrrf1</b>	0.52	-0.39	<b>Gng4</b>	0.13	-0.00
<b>Apbb2</b>	0.60	-1.30	<b>Cgrrf1</b>	-0.20	0.00	<b>Grem1</b>	-0.09	0.24
<b>Arhgap4</b>	0.72	0.00	<b>Cryab</b>	0.82	-2.53	<b>Hspa1a</b>	-0.18	0.23
<b>Arhgap4</b>	-0.17	0.17	<b>Cryab</b>	0.88	-1.14	<b>Hspa1b</b>	0.00	-0.28
<b>Arhgap4</b>	-0.00	0.37	<b>Cryab</b>	-0.09	0.11	<b>Hspa1b</b>	0.00	-0.19
<b>Bbc3</b>	-0.54	0.60	<b>Cth</b>	0.00	-0.03	<b>Hspa1b</b>	-0.00	0.04
<b>Bcl2</b>	-0.80	1.36	<b>Cyp27b1</b>	-0.22	0.25	<b>Ifi204</b>	0.10	-0.40
<b>Bcl2</b>	0.00	0.67	<b>Dab2</b>	1.66	-1.57	<b>Ifi204</b>	0.03	-0.05
<b>Bcl2</b>	0.15	-1.13	<b>Dab2</b>	0.29	-0.26	<b>Ifi204</b>	-0.32	0.29
<b>Bcl2</b>	0.00	-0.02	<b>Dab2</b>	0.33	-0.48	<b>Il7</b>	-0.06	0.00
<b>Bcl2</b>	-0.71	0.44	<b>Dab2</b>	0.48	-0.84	<b>Il7</b>	0.71	-0.04
<b>Bcl6</b>	0.04	-0.57	<b>Dab2ip</b>	-0.00	-0.33	<b>Inhba</b>	-0.24	0.73
<b>Bcl6</b>	-0.60	0.55	<b>Dab2ip</b>	-0.53	1.34	<b>Inhba</b>	-0.05	0.48
<b>Bdkrb1</b>	-0.12	0.21	<b>Dcbld2</b>	0.67	-0.01	<b>Mndal</b>	0.19	-0.90
<b>Bmp10</b>	0.26	-0.17	<b>Dcbld2</b>	-0.00	0.10	<b>Mndal</b>	0.01	-0.49
<b>Bmpr2</b>	0.03	-0.03	<b>Dcbld2</b>	-0.61	0.00	<b>Mull1</b>	-0.19	0.60
<b>Bmpr2</b>	0.00	-0.06	<b>Dcun1d3</b>	-0.71	0.77	<b>Mull1</b>	1.39	-0.98
<b>Bmpr2</b>	-0.42	0.28	<b>Dcun1d3</b>	-0.93	1.15	<b>Myl2</b>	1.03	-1.55
<b>Caprin2</b>	-0.28	0.76	<b>Dnajb2</b>	1.21	-1.21	<b>Ndufa13</b>	0.60	-1.09

	<b>Young</b>	<b>Old</b>		<b>Young</b>	<b>Old</b>
<b>Ndufs3</b>	0.75	-0.65	<b>Psrc1</b>	-0.23	0.17
<b>Nf2</b>	-0.40	-0.00	<b>Rbbp7</b>	-0.08	0.62
<b>Nf2</b>	0.28	-1.68	<b>Rbbp7</b>	0.00	0.28
<b>Nf2</b>	1.40	-0.89	<b>Rerg</b>	0.22	0.00
<b>Nf2</b>	-0.41	0.44	<b>Rnf6</b>	1.68	-1.11
<b>Nme6</b>	0.67	-0.07	<b>Rnf6</b>	0.72	-0.65
<b>Nppa</b>	0.00	0.04	<b>Rrad</b>	0.08	-0.28
<b>Nppb</b>	-0.27	0.20	<b>Rtn4</b>	0.14	-0.21
<b>Nrp1</b>	-0.93	0.49	<b>Rtn4</b>	0.19	-0.22
<b>Nrp1</b>	-0.04	0.06	<b>Rtn4</b>	-0.65	0.70
<b>Nrp1</b>	-0.28	0.26	<b>Rtn4</b>	-0.60	0.49
<b>Nrp1</b>	-0.11	0.24	<b>Rtn4</b>	-0.73	0.38
<b>Ntn1</b>	-0.18	0.45	<b>Ryk</b>	0.60	-0.80
<b>Ntn1</b>	-0.12	0.14	<b>Ryk</b>	0.00	-0.03
<b>Osgin1</b>	-0.27	0.00	<b>Ryk</b>	-0.16	-0.00
<b>Plscr3</b>	0.26	-0.22	<b>Sema3a</b>	-0.15	0.33
<b>Plscr3</b>	0.19	-0.06	<b>Sema3a</b>	-0.14	0.41
<b>Plxna3</b>	0.32	-0.25	<b>Sema3a</b>	0.00	0.16
<b>Plxna3</b>	0.03	0.00	<b>Sema3f</b>	0.00	-0.26
<b>Pml</b>	-1.00	0.68	<b>Sema3f</b>	-0.17	0.25
<b>Pml</b>	0.13	-0.14	<b>Sema3f</b>	-0.48	0.32
<b>Pml</b>	0.00	0.18	<b>Sema4f</b>	0.00	0.72
<b>Ppard</b>	0.00	0.18	<b>Sema4f</b>	0.00	0.41
<b>Ppard</b>	-0.77	0.00	<b>Serpine2</b>	-0.06	0.00
<b>Pparg</b>	-0.39	0.00	<b>Sertad1</b>	-0.53	0.20
<b>Ppt1</b>	-0.00	0.44	<b>Sertad2</b>	-0.27	0.26
<b>Ppt1</b>	-0.69	0.85	<b>Sertad2</b>	1.21	-0.08
<b>Ppt1</b>	-0.00	-0.13	<b>Sertad3</b>	-0.00	0.09
<b>Ppt1</b>	0.00	-0.05	<b>Sertad3</b>	-0.36	0.26
<b>Ppt1</b>	0.58	-0.90	<b>Slit1</b>	0.00	-0.39
<b>Prdm4</b>	0.53	-1.65	<b>Slit2</b>	-0.29	0.24
<b>Psrc1</b>	0.00	0.15	<b>Slit2</b>	0.16	0.00
<b>Psrc1</b>	-0.05	0.00	<b>Slit2</b>	-0.17	0.37

	<b>Young</b>	<b>Old</b>		<b>Young</b>	<b>Old</b>
<b>Slit3</b>	-0.15	0.45	<b>Ulk1</b>	-0.03	0.00
<b>Slit3</b>	0.38	-0.00	<b>Ulk1</b>	0.43	-1.60
<b>Smad3</b>	0.29	-0.98	<b>Ulk2</b>	0.77	-0.53
<b>Smad3</b>	0.00	-0.51	<b>Ulk2</b>	1.05	-1.34
<b>Smad3</b>	0.23	-0.80	<b>Ulk2</b>	0.00	0.19
<b>Smad4</b>	0.29	0.00	<b>Ulk2</b>	-0.00	0.00
<b>Smad4</b>	0.00	0.62	<b>Wnt11</b>	-0.28	0.49
<b>Smad4</b>	0.01	-0.37	<b>Wnt3</b>	-0.51	0.00
<b>Sox17</b>	0.28	-0.09	<b>Wnt3a</b>	-0.14	0.17
<b>Sox17</b>	0.00	0.76	<b>Wnt5a</b>	-0.26	0.24
<b>Spp1</b>	-0.17	0.32	<b>Wnt5a</b>	0.32	-0.21
<b>Tgfb1</b>	0.31	0.00	<b>Wnt5a</b>	0.10	-0.16
<b>Tgfb1</b>	-0.04	0.17	<b>Wnt5a</b>	-0.10	0.10
<b>Tgif1</b>	-0.67	0.00	<b>Wt1</b>	0.33	0.00
<b>Tnk1</b>	0.00	0.49	<b>Zmat3</b>	0.32	-0.01
<b>Tnk1</b>	0.00	0.62			
<b>Tnk1</b>	-0.21	0.39			
<b>Tro</b>	-0.25	0.30			
<b>Tro</b>	-0.06	0.00			
<b>Trp53</b>	0.00	0.00			
<b>Trp53</b>	-0.33	0.00			
<b>Trp53</b>	0.06	0.00			
<b>Trp53</b>	-1.27	1.81			
<b>Trp53</b>	-0.14	0.00			
<b>Trp53</b>	-0.16	0.05			
<b>Trp53</b>	-0.09	0.21			
<b>Trp63</b>	-0.19	0.00			
<b>Trp63</b>	0.07	0.00			
<b>Trp63</b>	0.35	-0.21			
<b>Trp63</b>	-0.22	0.56			
<b>Trp73</b>	-0.23	0.69			
<b>Trp73</b>	-0.33	0.20			
<b>Tspyl2</b>	0.24	-0.19			

**RELATED TO FIGURE 2.8. Normalized expression values for probesets included in GO:  
0010454 Negative Regulation of Cell Fate Commitment.**

	<b>Young</b>	<b>Old</b>
<b>Ctnnb1</b>	-0.24	0.04
<b>Ctnnb1</b>	0.00	0.30
<b>Ctnnb1</b>	-0.34	0.28
<b>Gfi1</b>	-0.30	2.17
<b>Inpp5a</b>	0.73	-1.01
<b>Jup</b>	0.75	-0.63
<b>Mesp1</b>	0.19	-0.01
<b>Nanog</b>	-0.17	0.55
<b>Nkx6-2</b>	0.00	-0.60
<b>Sfrp2</b>	1.19	0.00
<b>Spdef</b>	-0.20	0.51
<b>Wnt3a</b>	-0.14	0.17
<b>Wnt8b</b>	0.21	-0.32
<b>Wnt8b</b>	0.34	0.00
<b>Wnt8b</b>	1.51	-0.97

**RELATED TO FIGURE 2.8. Normalized expression values for probesets included in GO: 0051148 Negative Regulation of Muscle Cell Differentiation.**

	<b>Young</b>	<b>Old</b>
<b>Bmp4</b>	-0.32	0.46
<b>Ereg</b>	-0.31	0.38
<b>Ezh2</b>	0.45	-0.24
<b>Foxo4</b>	0.22	-0.00
<b>Foxo4</b>	1.10	-1.71
<b>Gm7040</b>	0.05	0.00
<b>Hdac4</b>	1.01	-0.26
<b>Hdac4</b>	0.00	-0.24
<b>Hdac4</b>	0.66	0.00
<b>Itgb1bp3</b>	0.53	-0.43
<b>Mbnl3</b>	0.00	0.17
<b>Mbnl3</b>	-0.17	0.00
<b>Mbnl3</b>	0.46	-0.68
<b>Nkx2-5</b>	-0.00	-0.00
<b>Notch1</b>	0.23	-0.37
<b>Notch1</b>	0.43	0.00
<b>Prdm6</b>	-0.12	0.18
<b>Prl2c2</b>	-0.16	0.32
<b>Rcan1</b>	0.49	-0.09
<b>Rcan1</b>	-0.21	0.47
<b>Shh</b>	-0.24	0.02
<b>Shh</b>	0.19	-0.04
<b>Sox8</b>	-0.32	0.70
<b>Sox9</b>	-0.03	0.15
<b>Sox9</b>	0.00	1.66
<b>Sox9</b>	0.19	0.00
<b>Tbx3</b>	-0.35	0.21
<b>Tbx3</b>	-0.16	0.80
<b>Tbx3</b>	-0.02	0.13
<b>Tbx3</b>	0.06	-0.00
<b>Tbx3</b>	-0.16	0.00
<b>Zfhx3</b>	-0.54	0.19
<b>Zfhx3</b>	0.80	-1.58
<b>Zfhx3</b>	0.51	-1.03
<b>Zfhx3</b>	0.08	-1.11
<b>Zfhx3</b>	0.00	-0.68
<b>Zfhx3</b>	-1.07	0.94

**RELATED TO FIGURE 2.9. Normalized expression values for probesets included in GO:**

**0040037 Negative Regulation of FGFR Signaling Pathway.**

	<b>Young</b>	<b>Old</b>
<b>Fgfr1</b>	-0.61	0.09
<b>Fgfr1</b>	-0.07	0.05
<b>Ngfr</b>	-0.03	0.16
<b>Ngfr</b>	-0.17	0.09
<b>Ngfr</b>	-0.01	0.04
<b>Spry1</b>	0.26	0.00
<b>Spry2</b>	-0.09	0.00
<b>Spry2</b>	-0.69	0.75
<b>Thbs1</b>	-0.98	1.12
<b>Thbs1</b>	-0.67	1.30
<b>Thbs1</b>	-0.52	0.48
<b>Wnt4</b>	-0.40	0.00
<b>Wnt4</b>	-0.32	1.02
<b>Wnt5a</b>	-0.26	0.24
<b>Wnt5a</b>	0.32	-0.21
<b>Wnt5a</b>	0.10	-0.16
<b>Wnt5a</b>	-0.10	0.10

**RELATED TO FIGURE 2.9. Normalized expression values for probesets included in GO:  
0004707 MAP Kinase Activity.**

	<b>Young</b>	<b>Old</b>
<b>Mapk1</b>	-0.28	0.26
<b>Mapk1</b>	0.62	-1.17
<b>Mapk1</b>	0.56	-0.58
<b>Mapk3</b>	0.00	-0.03
<b>Mapk4</b>	0.17	-0.02
<b>Mapk6</b>	0.09	-0.19
<b>Mapk6</b>	-0.39	0.26
<b>Mapk6</b>	0.64	-0.87
<b>Mapk6</b>	0.11	-0.03
<b>Mapk7</b>	0.19	-0.32
<b>Mapk8</b>	1.19	-1.22
<b>Mapk8</b>	-0.18	0.44
<b>Mapk8</b>	-0.29	0.34
<b>Mapk8</b>	1.01	-0.18
<b>Mapk8</b>	0.11	-0.01
<b>Mapk9</b>	1.04	-0.48
<b>Mapk9</b>	0.00	-1.00
<b>Mapk9</b>	1.44	-1.13
<b>Mapk10</b>	-0.02	0.16
<b>Mapk10</b>	0.00	0.10
<b>Mapk10</b>	0.00	-0.01
<b>Mapk11</b>	0.02	0.00
<b>Mapk11</b>	0.21	-0.27
<b>Mapk12</b>	1.31	-0.99
<b>Mapk12</b>	0.94	-0.67
<b>Mapk13</b>	-0.13	0.08
<b>Mapk14</b>	0.62	-0.99
<b>Mapk14</b>	-0.09	0.02
<b>Mapk14</b>	-0.50	0.13
<b>Mapk14</b>	0.58	-0.45
<b>Mapk14</b>	0.00	0.20
<b>Mapk14</b>	1.80	-0.24
<b>Mapk15</b>	-0.62	0.33
<b>Nik</b>	0.24	-0.21
<b>Nik</b>	-0.13	0.27
<b>Nik</b>	0.61	-1.18

**RELATED TO FIGURE 2.9. Normalized expression values for probesets included in GO: 0019827 Stem Cell Maintenance.**

	Young	Old		Young	Old		Young	Old
<b>Apc</b>	0.00	-1.52	<b>Igf1</b>	0.05	-0.14	<b>Vangl2</b>	-0.33	0.18
<b>Apc</b>	0.00	-1.25	<b>Kit</b>	0.09	-0.09	<b>Vangl2</b>	-0.04	0.32
<b>Apc</b>	0.39	-0.11	<b>Kit</b>	-0.51	0.43	<b>Vangl2</b>	0.00	0.07
<b>Apc</b>	0.00	0.21	<b>Klf4</b>	0.18	-0.31	<b>Wnt7a</b>	-0.36	0.54
<b>Ascl2</b>	0.05	-0.10	<b>Klf4</b>	0.32	-0.48	<b>Wnt7a</b>	0.20	0.00
<b>Ascl2</b>	0.02	0.00	<b>Lif</b>	-0.09	-0.00	<b>Wnt7a</b>	-0.00	0.08
<b>Ascl2</b>	0.09	-0.03	<b>Lif</b>	0.36	-0.20	<b>Zcchc11</b>	-0.56	0.44
<b>Bmpr1a</b>	0.41	-2.16	<b>Lig4</b>	-0.30	0.19	<b>Zcchc11</b>	0.40	-0.00
<b>Bmpr1a</b>	0.22	-1.30	<b>Lin28</b>	0.51	-0.07	<b>Zcchc11</b>	0.22	-0.30
<b>Bmpr1a</b>	0.05	-0.55	<b>Lin28a</b>	-0.14	0.00	<b>Zcchc11</b>	-0.29	1.09
<b>Bmpr1a</b>	0.36	-0.16	<b>Lrp5</b>	-0.09	0.00	<b>Zcchc11</b>	0.27	-0.35
<b>Bmpr1a</b>	0.21	-0.22	<b>Myst3</b>	0.00	-0.33	<b>Zfp358</b>	-0.22	0.57
<b>Bmpr1a</b>	-0.11	0.15	<b>Myst3</b>	0.15	-0.12	<b>Zfp358</b>	1.69	-0.48
<b>Cdx2</b>	0.08	-0.18	<b>Myst3</b>	0.00	-0.11			
<b>Cdx2</b>	-0.34	0.39	<b>Nanog</b>	-0.17	0.55			
<b>Crebbp</b>	2.27	-0.35	<b>Nodal</b>	0.00	0.16			
<b>Crebbp</b>	-0.00	0.29	<b>Nodal</b>	-0.20	0.16			
<b>Crebbp</b>	0.00	0.09	<b>Nog</b>	-0.09	0.25			
<b>Crebbp</b>	0.00	-0.05	<b>Piwil2</b>	-0.66	0.55			
<b>Dicer1</b>	0.72	-0.95	<b>Pla2g2a</b>	-0.10	0.01			
<b>Dicer1</b>	1.20	-1.25	<b>Pou5f1</b>	0.00	0.25			
<b>Esrrb</b>	-0.46	0.07	<b>Rif1</b>	0.01	-0.11			
<b>Esrrb</b>	-0.35	0.45	<b>Rif1</b>	0.00	-0.18			
<b>Esrrb</b>	-0.32	0.00	<b>Rif1</b>	-0.46	0.46			
<b>Fgf10</b>	-0.10	0.41	<b>Rif1</b>	0.00	1.95			
<b>Fgf4</b>	0.00	-0.00	<b>Rif1</b>	0.46	-0.00			
<b>Fgf4</b>	0.00	-0.15	<b>Sfrp1</b>	0.22	-0.00			
<b>Fgf4</b>	-0.60	0.34	<b>Sfrp1</b>	-0.15	0.26			
<b>Fgf4</b>	-0.17	0.39	<b>Sfrp1</b>	-0.28	0.00			
<b>Fgfr1</b>	0.23	0.00	<b>Sfrp1</b>	0.33	-0.37			
<b>Fgfr1</b>	-0.06	0.51	<b>Sfrp1</b>	0.00	0.43			
<b>Fgfr1</b>	-0.75	0.36	<b>Sox2</b>	-0.01	0.16			
<b>Fzd7</b>	0.04	0.00	<b>Tcf7l2</b>	-0.01	0.08			
<b>Fzd7</b>	0.87	-1.44	<b>Tcf7l2</b>	0.44	0.00			
<b>Igf1</b>	0.00	0.85	<b>Tcf7l2</b>	0.00	0.26			
<b>Igf1</b>	0.35	-0.93	<b>Tcf7l2</b>	-0.86	0.37			
<b>Igf1</b>	0.02	-0.24	<b>Tcl1</b>	-0.20	0.14			